ARKIV FÖR FYSIK Band 12 nr 19

Communicated 5 June 1957 by The Svedberg and Manne Siegbahn

Nuclear energy levels and multipole transitions in the lead region

Part I

By I. Bergström and G. Andersson

With 30 figures in the text

Contents

Page
Abstract 416
1. Introduction 416
  1.1. Scope and purpose of the study 416
  1.2. General experimental background 418
    1.21. Beta- and gamma-ray spectrometry 418
    1.22. Information from alpha-decay 419
    1.23. Particle reactions 419
    1.24. Half-life measurements 420
2. Single-particle levels 421
  2.1. Shell model predictions 421
  2.2. Neutron levels 422
    2.21. Introductory remarks 422
    2.22. Assignment of levels 422
    2.23. Validity of assignments 426
    2.24. Level separations $i_{13/2}$–$f_{5/2}$ 426
    2.25. Level separations $f_{5/2}$–$p_{3/2}$–$p_{1/2}$ 430
  2.3. Proton levels 431
    2.31. Introductory remarks 431
    2.32. Assignment of levels 432
    2.33. Level separations $h_{11/2}$–$d_{5/2}$ 435
    2.34. Level separations $d_{5/2}$–$d_{3/2}$–$s_{1/2}$ 436
3. Complex levels 436
  3.1. Theoretical and experimental background 436
  3.2. Level systematics 441
    3.21. Introductory remarks 441
    3.22. First excited states in even-even nuclei 441
    3.23. Excited states in even Pb isotopes 443
    3.24. Levels in odd-odd nuclei 444
    3.25. "Anomalous" levels in Hg^{199} and Hg^{201} 446
4. Multipole transitions 447
  4.1. Distribution of transitions from metastable states 447
  4.2. Transition probabilities 451
    4.21. Treatment of data 451

Page
4.22. Discussion of regularities 458
4.23. Multipole mixing 463
4.3. Internal conversion ratios 465
4.31. Introductory remarks 465
4.32. Treatment of data 469
4.33. Discussion 475

ABSTRACT

A compilation has been made of experimental data concerning energy levels of nuclei in the Z-region 77–84. The data include spin, parity and lifetime of the levels as well as energy and conversion ratios of the multipole transitions involved in their de-excitation. K/L and $(L_{\mathrm{I}}+L_{\mathrm{II}})/L_{\mathrm{III}}$ conversion ratios are found to agree reasonably well with the values obtained from Rose's tables. Regularities in level separations are pointed out and the appearance of certain levels is discussed on the basis of single-particle shell model predictions. A comparison is made between experimentally determined γ-transition probabilities for $E2$, $E3$, $E4$, $E5$, and $M4$ transitions and those calculated from single-particle theory. A marked influence of the magic numbers $Z = 82$ and $N = 126$ shows up both in level separations and in transition probabilities. Special attention is payed to the present theoretical and experimental knowledge of levels in nuclei in the immediate neighbourhood of the double magic Pb^{208}.

1. Introduction

1.1. *Scope and purpose of the study*

Nuclei with proton and neutron numbers near the closed shells 82 and 126, respectively, are often referred to as belonging to the (nuclear) lead region. The significance of this region from a nuclear spectroscopic point of view is intimately connected with the double shell closure appearing in Pb^{208}.

The nuclei $^{-1}_{\ 0}\mathrm{Pb}^{207}$, $^{+1}_{\ 0}\mathrm{Pb}^{209}$, $^{\ 0}_{-1}\mathrm{Tl}^{207}$, and $^{\ 0}_{+1}\mathrm{Bi}^{209}$, which all have one nucleon more or less than the "hard core" of Pb^{208} as indicated by the superscripts (ΔN) and subscripts (ΔZ) preceding the symbols, should exhibit a sequence of low-lying energy states in particularly good agreement with the single-particle levels of the strong spin-orbit coupling shell model.[1] Of these four nuclei, Pb^{207} is the most well known and the correspondence between experimentally established levels and those predicted by the shell theory is very striking.

The importance of the one-particle nuclei for the theoretical treatment of levels in neighbouring nuclei may be compared with that of the hydrogen levels in solving atomic problems. In fact, calculations on the basis of experimentally established level energies in Pb^{207} have been performed, leading in some cases to even quantitative agreement with experiments. With the present methods of calculation, however, it seems to be of a limited value to compare theory and experiment when the sum of holes and nucleons outside the core exceeds four. This defines a very restricted "lead 208 region" which will be discussed in some detail in section 3.1 of this paper.

On the other hand, single-particle features may be traced further away from the double shell closure, notably towards lower Z and N values. Thus we have considered it reasonable to include all known experimental material on levels in lead, thallium, and mercury in our survey. The lead region in this broader sense is especially interesting from the point of view of isomerism. The typical single-particle states $i_{13/2}$ and $h_{11/2}$, for instance, may be expected to show up in odd mass isotopes of lead and mercury and of thallium, respectively, and should also give rise to high spin levels in the even mass isotopes.

---

[1] For clarity it may be remarked that the term single-particle level will be used for energy states of odd mass nuclei where the spin is determined solely by the single unpaired nucleon, irrespective of the total number of excessive nucleons or holes.

An extensive and fruitful search for isomeric transitions in this region has been performed by various groups in Sweden. The present authors have been intimately associated with these investigations. The need for a summary of the experimental knowledge obtained so far forms the basic reason for undertaking this review work.

Obviously the lower Z-limit to the lead region is quite arbitrary. As is well known, nuclear energy levels in the rare earth region and in the uranium region show collective features. Platinum is a typical boundary case. Vibrational levels are identified in the even-even isotopes, while three $i_{13/2} \rightarrow f_{5/2}$ transitions are known in the odd platinum isotopes. Similarly there is evidence of $h_{11/2}$ levels in iridium. Thus when systematic trends are discussed we have often included also cases in elements such as gold, platinum, and iridium which are believed to be significant for comparisons with the single-particle shell model. It may be remarked that in some respects the present paper constitutes a continuation and extension of Mihelich's and de-Shalit's work on regularities in Hg, Au, and Pt [6M54].

Besides the behaviour of level spacings, which is the main subject of chapters 2 and 3, we have in addition reviewed the gamma-transition probabilities and internal conversion ratios for $E2$ and higher multipole orders (chapter 4). Transition probabilities are known to offer the most direct way of confronting experimental findings with theory. In the region concerned a comparison with the expected probabilities of single-particle transitions is certainly of special interest.

In several ways the nuclear spectroscopist is dependent on internal conversion data for the interpretation of experimental results. We have, therefore, considered it of practical importance to test the validity of the available tables of theoretical conversion coefficients. This is done by comparing the calculated and measured conversion ratios K/L and $(L_{\mathrm{I}} + L_{\mathrm{II}})/L_{\mathrm{III}}$. As further discussed in section 4.3 there is even a slight possibility that nuclear properties may show up in such a comparison. Of course a direct study of the conversion coefficients and not only of their ratios would be of considerable interest but unfortunately the experimental material is not very extensive. We believe, however, that accurate measurements of conversion coefficients will receive increased attention in the near future.

To summarize, the experimental data compiled include energies, conversion ratios, and multipolarities of transitions between nuclear energy levels together with level properties such as spin, parity, and lifetime. Though we have been mainly concerned with single-particle levels the work has meant a general survey and revision of level schemes in the lead region. These will be published separately as Part II of this paper.

It should be stressed that the only or primary purpose of our work has not been to seek explanations of the various trends and regularities revealed. We have as much aimed at a critical examination of existing experimental data in order to make clear which assignments and values are certain or reasonable and in which cases improved measurements are needed. For this reason a few remarks on the experimental methods underlying the information used may be appropriate.

1.2. *General experimental background*

1.21. *Beta- and gamma-ray spectrometry*

Most of the information comes from the study of beta decay (β^-, β^+, and electron capture) and the decay of isomeric states. Though in many cases a large number of levels are observed, it must be kept in mind when comparing experiment and theory that due to beta and gamma selection rules all possible levels are not populated in the decays.

The assignments of levels emerge from observation of changes in energy, angular momentum, and parity. Such information may be obtained by studying the emission of gamma-rays, conversion electrons, or electron pairs when the nucleus goes from one state to another. Gamma-ray intensities and energies may be measured in a crystal spectrometer with the technique developed by DuMond and his collaborators [5D55]. Unfortunately this method requires sample strengths of the order of 1C and has therefore a limited applicability.

The rapid development of high transmission beta spectrometers has provided a powerful tool for measuring gamma-ray energies and intensities as well as electron energies and intensities. Especially the two-directional focusing spectrometers have proved to be very useful. A great part of the investigations reviewed in this paper has been made in such spectrometers. Their main advantage is that sources many hundred times weaker than those required in the crystal spectrometer can be used for the same accuracy. It has been doubted whether one can rely upon electron intensities measured in iron-yoke double focusing spectrometers. Bergkvist [4B57] has recently shown that these instruments give correct intensities within 1 % even if the window curve of the spectrometer may vary considerably because of different premagnetization.

Gamma-ray intensities can in principle be determined in an electron spectrometer by measuring the intensities of photo electrons from external conversion. A difficulty has been the poor knowledge of the energy and angular dependence of the photo electron cross section. This was recently studied in the case of uranium by Hultberg *et al.* [10H55, 3N57a], who could use their results to determine the intensities of 20 gamma-rays in Pb^{206}.

The high accuracy in energy measurements which may be achieved both with gamma and electron spectrometers is indispensible in studying complicated level schemes. If the first excited state is known (which is often the case, for instance from alpha-decay or Coulomb excitation) other levels may be obtained by constructing all possible energy sums and differences. Many of the gamma-rays observed in lead and bismuth isotopes, for instance, are known with an energy accuracy of about $5:10^4$. This makes possible the construction of a reasonable though not necessarily correct level scheme which can be used as a guide in coincidence measurements. It is evident that a higher energy accuracy decreases the number of accidental sum ups and thus quicker leads to an acceptable level order.

A high precision in energy determinations is of considerable importance also in studying gamma-transition probabilities (cf. 4.2). The matrix elements of $M4$ transitions in lead, for instance, are so constant that an energy accuracy of about $1:10^3$ proved necessary in looking for any significant differences.

1.22. *Information from alpha-decay*

Isotopes of elements down to thallium are members of well-known alpha-decay chains. In many cases fine structure studies of the alpha-rays have been made, giving information about excited levels in the daughter nuclei. The level spacings are obtained as differences between alpha-branches with energies in the MeV region. Thus, even if magnetic spectrometers are used in the alpha-measurements, the relative energy accuracy for the low-lying states concerned must necessarily be low compared with that of electron spectrometry. The reliability of alpha-decay systematics, however, makes this type of information very valuable. In particular the energy of the first excited state in several nuclei is unambiguously suggested. For more exact determinations of the energy spacings between levels populated in alpha-decay the methods discussed in the preceding section may of course be used as complements, and alpha-gamma coincidence measurements have proved to be a useful technique.

It is not within the scope of this paper to review the present situation of alpha systematics; the reader is referred to recent articles by Perlman and Rasmussen [3P56] and Fröman [5F57]. As far as the lead region is concerned, however, it is quite apparent that much work remains to be done, especially on the neutron-deficient side. In some cases the short half-lives may have prevented a closer study of the decays. This difficulty seems to be largely overcome by the promising technique introduced by Tove [1T57a], involving pulsed cyclotron irradiation, energy analysis in the cyclotron magnet, and simultaneous lifetime determination in a multi-channel time analyser.

1.23. *Particle reactions*

The study of charged particles or neutrons emitted in simple nuclear reactions is a way of acquiring knowledge about excited states of nuclei. For practical reasons such experiments are limited to the stability region. Thus in the actual case the stable isotopes of Hg, Tl, Pb, and Bi can be used as target materials in investigations of levels in the region around Pb^{208} (cf. Fig. 8 p. 438), which from a theoretical point of view is particularly interesting (cf. 3.1).

Because of the Coulomb barrier, charged particles used as projectiles must have a considerable energy. This means that extremely good resolution is required of the energy analysing equipment in order to determine low-lying energy levels from the energies of charged particles emitted in nuclear reactions. Harvey has studied (d,p) and (d,t) reactions in the isotopes of lead and bismuth [9H53]. In a typical case the protons from Pb^{206} (d,p) reactions had energies in the region 12–16 MeV. Harvey analysed the protons and tritons in a triple coincidence ionization chamber arrangement. The resolution of this equipment was a few per cent, which was insufficient to resolve many proton and triton groups. The (d,p) reaction should essentially be a stripping reaction. If an even-even nucleus is used as target material the neutron should enter the nucleus in a single particle state. The Pb^{206} (d,p) reaction beautifully illustrates that this is the case. Harvey also found evidence that in a pick-up process, for instance in a Pb^{208} (d,t) reaction, the resulting neutron hole can be described with a single particle state. If an odd-odd or odd-even nucleus is used as target material a much more complicated situation arises. The number of possible levels and thus of charged particle groups is much larger. In order to obtain significant results in such cases a high resolution magnet must be used.

Recently McEllistrem *et al.* [14M57] reported results obtained in Pb^{206} (d,p) reactions, where the proton energies were analysed in a double-focusing magnet.

Inelastic scattering of charged particles and neutrons may also give information of excited states. The $2+$ state in Pb^{206} for example has been reached by Coulomb excitation [3B56a]. Levels in Bi^{209} have been observed in a Bi^{209} $(n,n'\gamma)$ reaction [6D56]. The gamma-rays emitted from excited states were studied with scintillation counter technique.

It is more difficult to study the energies of inelastically scattered neutrons and in this way to obtain information of excited levels. This, however, has been done in the Bi^{209} case by Cranberg and Levin [9C56], who used a pulsed-beam time-of-flight method for the determination of the neutron energies.

1.24. *Half-life measurements*

The importance of accurate half-life determinations is most obvious when dealing with gamma-transition probabilities, where the lifetimes of excited levels enter directly into the calculations. There are in principle two different ways of learning the lifetime of an excited level. Either the rate of emission of particles or quanta can be directly measured or the lifetime can be inferred from a determination of the energy width or the excitation probability of the level. The former way includes also delayed coincidence techniques, putting a lower half-life limit of 10^{-10}–10^{-11} s to its region of application [5B55]. The indirect methods comprise resonance fluorescence [13M55] and Coulomb excitation [6A56] and make possible the measurement of half-lives down to the order of 10^{-13} s. In these experiments the "pure" gamma-lifetimes are primarily obtained and do not depend on internal conversion corrections.

It must be emphasized, however, that the half-lives play a most significant role also in the study of intensity ratios between electron or gamma lines whenever the time of measurement is not small relative to the half-life. To give an actual example, the internal conversion lines of the 222.5 keV $E3$ transition following the electron capture decay of 42 min Pb^{197m} were investigated in an iron-free double-focusing spectrometer [3A57a]. A 5 % uncertainty in the Pb^{197m} half-life was found to give contributions of 3 % and 5 % to the errors in the K/L_{II} and K/L_{III} ratios, respectively, and was in fact the dominating source of error.

The relative accuracy that can be achieved in half-life measurements is rarely better than 1 %. Already this modest figure demands considerable care to be reached. It is a well-known fact that contaminations from similar half-lives are very difficult to discover, even if the measurements are prolonged over several periods, and may lead to erroneous results in spite of small statistical errors. Preferably an energy selecting device of good stability and resolving power should be used to follow the disintegration of one single representative line in the decay. (This of course refers to the direct methods.) Even such precautions are not always sufficient, however. Recently, for instance, the 2.4 hr half-life of Tl^{196} measured at fixed conditions in a double-focusing beta-spectrometer turned out to be wrong because of an exactly coinciding electron line (resolution about 0.4 %) in the decay of 2.7 hr Tl^{197}. With a mass separated sample the Tl^{196} half-life was found to be 1.8 hr [3A57b]. Thus it is concluded that deviations from the expected behaviour of transition probabilities and conversion ratios may in many cases depend on unsatisfactory half-life determinations.

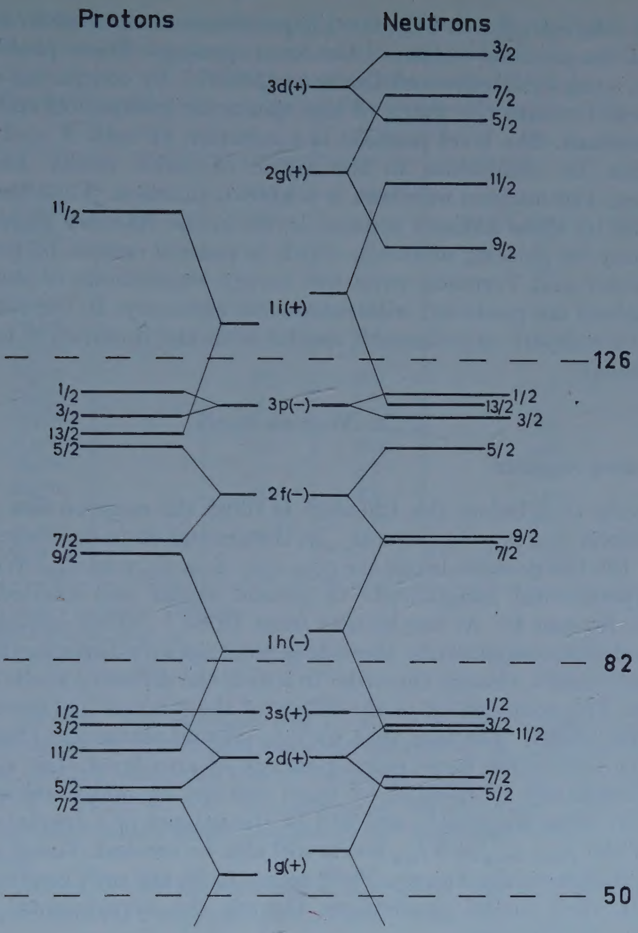

Fig. 1. Single-particle levels for protons and neutrons (N and $Z > 50$). The figure has been redrawn from Fig. 1 appearing in the paper by Klinkenberg [3K52].

2. Single-particle levels

2.1. *Shell model predictions*

It has already been emphasized that the main interest in the systematics of levels in the lead region is due to the fact that the number of protons and neutrons is close to the magic numbers $Z = 82$ and $N = 126$. For this reason low-lying levels in the even-odd or odd-even nuclei should be well represented by the single-particle levels suggested by the Mayer–Jensen shell model. Fig. 1 shows a somewhat revised reproduction of the level sequence of Klinkenberg [3K52], which is essentially based on the spins of stable nuclei. In regions where levels are very close the order of the levels may not be correctly predicted. This approximate scheme, which has been frequently used, does not take into account the level dependence on the nuclear radius and gives no estimate of the absolute values of the level spacings. These problems have been considered in a work by Bleuler and Terreaux [15B57]. By comparing experiment and theory they could obtain the shape of the spin-orbit interaction and determine the interaction constant. The level position is a function of both N and Z. The Z or N dependence can be eliminated in the region of stable nuclei, because here the relation between the nucleon numbers is a known function. Thus the level schemes which are given by these authors concern levels in the stability region. Outside this region there may be crossing of levels, which in general cannot be predicted. In the scheme of Bleuler and Terreaux even the energy separations of the levels close to the magic numbers are predicted with reasonable certainty. In the following sections we are going to compare experimental results with the qualitative level predictions of the shell model.

2.2. *Neutron levels*

2.21. *Introductory remarks*

Fig. 1 suggests that before the 126 shell is filled the neutron has a possibility to populate the shells $f_{5/2}$, $p_{3/2}$, $i_{13/2}$ and $p_{1/2}$ in the ground state or in excited states. For N larger than 126 the possible levels are $g_{9/2}$, $i_{11/2}$, $d_{5/2}$, $g_{7/2}$ and $d_{3/2}$. We are first going to discuss experimental assignments of ground states and excited states in odd isotopes of Pb, Hg and Pt. As can be seen from Table 1, which contains the "experimental" ground state assignments, there does not exist any deviation from the predictions of the shell model, though the order in which the different shells are filled seems to be irregular. The competition of the filling of these levels has been discussed in a paper by Zeldes [1Z56]. The fact that no $i_{13/2}$ ground states are observed has been suggested to be due to the large pairing energy of an i-level. The $i_{13/2}$ level should therefore preferentially be filled in by pairs and not by odd particles. Excited $i_{13/2}$ states, however, occur frequently and will be the subject of a special discussion. The systematics of the $p_{1/2}$, $p_{3/2}$ and $f_{5/2}$ levels will also be treated. For N larger than 126 very little is experimentally known. Pb^{209} seems to be the only nucleus which can be compared with shell model predictions, though the experimental information is incomplete even in this case.

2.22. *Assignment of levels*

Table 2 summarizes the energies of excited states the assignments of which are to be discussed in this section.

Table 1. Ground state assignments of odd mass isotopes of Pb, Hg and Pt (cf. 2.22).

Z \ N	113	115	117	119	121	123	125	127
82		5/2 − ?	5/2 − ?	5/2 −	5/2 −	5/2 −	1/2 −	9/2 + ?
80	3/2 −	3/2 −	1/2 −	1/2 −	3/2 −	5/2 −, 3/2 −	1/2 − ?	
78		5/2 − ?	1/2 −	5/2 −				

Table 2. Energies of single-particle states in Pb, Hg and Pt isotopes.

Nucleus	Energy (keV) above ground state			
	$p_{1/2}$	$p_{3/2}$	$f_{5/2}$	$i_{13/2}$
Pb^{207}	0	894	569	1633
Pb^{205}	500?	282	0	840,[a] 980,[b] 1100[c]
Pb^{203}			0	825
Pb^{201}			0	629
Pb^{199}			0?	424
Pb^{197}			0?	234
Pb^{195}	0?	0?	0?	≈100?
Hg^{205}	0?			
Hg^{203}		0?	0?	
Hg^{201}		0		
Hg^{199}	0	208	158	526
Hg^{197}	0	152	134	299
Hg^{195}		0	37	160
Hg^{193}		0	39	140
Pt^{197}			0?	337
Pt^{195}	0	29	126	255
Pt^{193}		0?	0?	136?

[a] From Pb^{206} (d,t) reactions [9H53].
[b] From interpolation in Fig. 2.
[c] From the calculations of Pryce (cf. Fig. 5).

$^{+1}_{0}\mathrm{Pb}^{209}$.—An "allowed" beta transition ($\log ft = 5.5$) takes place between the ground states of 3.22 hr Pb^{209} and the stable Bi^{209} [3D57], for which the spin 9/2 ($h_{9/2}$) has been spectroscopically measured [3K52]. For this reason the spin of the ground state of Pb^{209} may be expected to be $7/2-$, $9/2-$ or $11/2-$. However, $9/2+$ is suggested by the shell model. This may be one of the many cases in the heavy region where ft-values do not distinguish between first forbidden and allowed transitions.

There are two sources of information about excited states. Harvey [9H53] observed in Pb^{208} (d,p) reactions levels at 0.75, 1.56, 2.03, and 2.54 MeV. These levels were given the assignments $g_{9/2}$ (0.6),[1] $i_{11/2}$ (0.1), $d_{5/2}$ (1.8), $g_{7/2}$ (1.1) and $d_{3/2}$ (2.4), based on proton intensities and shell model predictions. Within parenthesis are given the experimental intensities of the observed proton groups. The probability that the capture neutron populates the single-particle levels of the shell model should decrease with increasing angular momentum of the level. As can be seen from Harvey's results the proton intensities have a plausible relation to the assigned angular momenta. However, from these results alone it is not possible to obtain unambiguous assignments.

In the beta decay of Tl^{209} three excited states in Pb^{209} have been observed [1S56]. Two levels at 1560 and 2010 keV are most probably identical with the levels found by Harvey. The third level has an energy of 2130 keV and was assigned $p_{1/2}$ because it is reached by beta decay from Tl^{209} ($s_{1/2}$ according to shell theory). It is de-excited by a 3 mμs $E1$ transition to the 2010 keV level. The 1560 keV and 2010 keV levels were tentatively given the assignments $d_{5/2}$ or $g_{7/2}$ and $d_{3/2}$, respectively. Further experiments are needed in order to establish the assignments of the observed levels in Pb^{209}.

$^{-1}_{0}\mathrm{Pb}^{207}$.—The ground state spin 1/2 of this stable nucleus has been spectroscopically determined [3K52]. Excited states are observed in electron capture and alpha decay as well as in particle reactions. The electron capture decay of Bi^{207} has been carefully studied by Alburger and Sunyar [1A55]. The reader is referred to their paper for a detailed discussion of level assignments. Below 2.35 MeV the following levels have been observed: 2.35, $f_{7/2}$ (EC, α, dt); 1.633, $i_{13/2}$ (EC, dt); 0.894, $p_{3/2}$ (EC, α, dp, dt); 0.569, $f_{5/2}$ (EC, α, dp, dt) and 0, $p_{1/2}$ (EC, α, dp, dt). It is very satisfactory to note how the different types of experiments complement and check each other in this very important case. Not only do the energies agree but also the proton and triton intensities are in good agreement with the l-values suggested from the study of the electron capture decay of Bi^{207}. In addition the agreement with the level predictions of the shell model is very good. Bleuler and Terreaux [15B57] have pointed out that even the level spacings are in relatively good agreement with their calculations. A larger number of excited states above 2.4 MeV has been observed in (d,p) reactions [9H53, 14M57].

---

[1] Ground state.

$^{-3}_{0}\mathrm{Pb}^{205}$.—The ground state spin of Pb^{205} has not been measured. The half-life 5×10^{7} y is too long to allow the production of this nuclide in sufficiently large amounts. On the other hand the half-life is so short that Pb^{205} is not observed in nature. The arguments for a ground state spin $5/2-$ are discussed in the papers by Pryce [5P56] and Schmorak *et al.* [3S56]. In Pb^{206} (d,t) reactions Harvey observed four levels at 0 MeV (1.4), 0.27 MeV (1.0), 0.84 MeV (0.3) and 1.79 MeV (0.3). The triton intensities (given within parenthesis) suggest the assignments $f_{5/2}$, $p_{3/2}$ and $i_{13/2}$ for the first three levels. The 282 keV level observed by Schmorak *et al.* is probably identical with the 0.27 MeV level observed by Harvey. Its position in the level scheme is consistent with a $3/2-$ assignment. There are also indications of a $3/2-$ or $1/2-$ level at 550 or 493 keV [3S56].

$^{-5}_{0}\mathrm{Pb}^{203}$.—In the isomeric decay of Pb^{203} only an $M4$ γ-ray of energy 825 keV has been observed [5S56]. If other γ-rays are present, they must have energies less than 40 keV. An assignment of $i_{13/2}$ (no experimental proof) to the isomeric state leads to an $f_{5/2}$ ground state. Other low-lying single-particle levels may be populated from the decay of Bi^{203}. So far none of these states have been observed [1F56, 3N57].

From experiments on the electron capture decay of the ground state of Pb^{203} the assignment $p_{3/2}$ or $f_{5/2}$ has been suggested for this state [6P54, 1W54].

$^{-7}_{0}\mathrm{Pb}^{201}$.—An $M4$ γ-ray of energy 629 keV is emitted from an isomeric state which is assumed (no experimental proof) to be the $i_{13/2}$ state [5S56]. Since no further γ-rays have been found, the ground state should be $f_{5/2}$. In the decay of Pb^{201} two positron components, whose energy difference is 0.35 MeV, have been observed [4B57]. It is not yet clear if the positron emission goes to the ground state $(1/2+)$ and the first excited state $(3/2+)$ or to the first excited and second excited $(5/2+)$ states in Tl^{201}. An answer to this question would perhaps give information of the ground state spin of Pb^{201}. No investigations have so far been performed from which knowledge of additional excited states can be deduced.

$^{-9}_{0}\mathrm{Pb}^{199}$.—The energy of the $M4$ γ-ray is 424 keV and it has been concluded that any other γ-rays present in the isomeric decay should have an energy below 40 keV [5S56, 3A57]. The isomeric γ-ray is assumed (no direct experimental proof) to be emitted between $i_{13/2}$ and $f_{5/2}$ (ground state). Positrons are probably emitted in the decay of Pb^{199}. A study of these may give useful information on the ground state spin.

$^{-11}_{0}\mathrm{Pb}^{197}$.—An $M4$ γ-ray of energy 234 keV is assumed (no direct experimental proof) to be emitted between $i_{13/2}$ and the $f_{5/2}$ ground state [3A57]. Other γ-rays belonging to the isomeric decay have not been observed above ≈ 40 keV. It seems puzzling that the ground states of Pb^{199} and Pb^{197} should be $5/2-$ states. This would not be possible if the $f_{5/2}$ level were filled in a regular way. Because of the importance of this question it is an urgent experimental task to search for low energy γ-rays in the decays of both Pb^{199m} and Pb^{197m}. Direct spin measurements of the isomeric states and ground states of Pb^{203}, Pb^{201}, Pb^{199} and Pb^{197} seem highly desirable and should be possible in some of the cases.

${}^{-13}_{0}\mathrm{Pb}^{195}$.—Since no γ-emission has been observed from the isomeric state it is impossible to say anything about the ground state spin. The isomeric state has been assigned $i_{13/2}$ because electron capture leads to a state in Tl^{195} which is supposed to be an $h_{11/2}$ state [3A57, 3A57a].

${}^{-1}_{-2}\mathrm{Hg}^{205}$.—Decays by the emissicn of 1750 keV beta-rays [6K54] (log $ft = 5.5$) to Tl^{205}. The 205 keV γ-ray emitted between the first excited state $(3/2+)$ and the ground state $(1/2+)$ of Tl^{205} has been observed in this decay [18B53]. The failure to observe the 410 and 615 keV γ-rays emitted from the second excited state $(5/2+)$ (see 2.32) can be understood if the ground state spin of Hg^{205} is $1/2-$ (another case of low log ft-value for a first forbidden beta transition). However, more convincing proofs of the absence of the 410 and 615 keV γ-rays in the decay of Hg^{205} are needed before such a statement can be made. No excited levels are known in Hg^{205}.

${}^{-3}_{-2}\mathrm{Hg}^{203}$.—The non-observation of beta transitions between the ground states of Hg^{203} and Tl^{203} may indicate a ground state spin of $5/2-$ in Hg^{203} $(1/2+$ in $Tl^{203})$. Recent measurements on the angular distribution of polarized γ-rays by Wapstra and Boehm [8B57a] indicate a ground state spin of 3/2 though they do not completely exclude 5/2. A 690 keV γ-ray has been observed in the decay of 55 s Au^{203} [17B52]. Nothing is known about the multipolarity of this γ-ray or about the assignment of the 690 keV level. There are experimental indications that in Hg^{203} as well as in Hg^{201} the metastability of the $i_{13/2}$ level for the emission of $M4$ γ-rays is destroyed by complex levels (cf. 3.2).

${}^{-5}_{-2}\mathrm{Hg}^{201}$.—The ground state spin 3/2 has been measured spectroscopically [3K52]. The presence of "anomalous" low-lying states in Hg^{201} is discussed in section 3.25. No $i_{13/2}$ state has been observed so far (cf. Hg^{203}).

${}^{-7}_{-2}\mathrm{Hg}^{199}$.—The ground state spin 1/2 has been measured spectroscopically [3K52]. In the isomeric decay an $M4$ and an $E2$ γ-ray are observed in cascade [2B53]. The isomeric state has therefore the spin 13/2 and the intermediate state the spin 5/2. In the β^--decay of Au^{199} and in the electron capture decay of Tl^{199} a $3/2-$ level is observed at 208 keV. In addition there are two other levels of energies 455 and 491 keV observed in the electron capture decay of Tl^{199} [2B53]. These levels are not single particle levels and are discussed more in detail in section 3.25.

${}^{-9}_{-2}\mathrm{Hg}^{197}$.—If it is assumed that the isomeric state is $i_{13/2}$, the 165 keV $M4$ and 134 keV $E2$ γ-rays emitted in cascade [6M53] suggest an $f_{5/2}$ excited state and a $p_{1/2}$ ground state. In the decay of Tl^{197} an 152 keV $M1$ γ-ray is observed in addition to the 134 keV $E2$ γ-ray [3A57]. Its intensity and multipolarity suggests that it is emitted from a $3/2-$ state (assuming that the ground state is $1/2-$). No more excited states are known. Zeldes [1Z56] refers to a direct spin measurement of the ground state confirming the value 1/2.

${}^{-11}_{-2}\mathrm{Hg}^{195}$.—The isomeric state which is assumed to be an $i_{13/2}$ state (no direct experimental proof) is de-excited by the emission in cascade of two γ-rays of energies 123 keV ($M4$) and 37 keV ($M1$) [2J55]. This suggests a $5/2-$ intermediate state and a $3/2-$ or $5/2-$ ground state. $3/2-$ has been accepted because of the shell model predictions.

${}^{-13}_{-2}\mathrm{Hg}^{193}$.—The observation of a 101 keV $M4$ γ-ray and a 39 keV $M1$ γ-ray emitted in cascade from an isomeric state has led to the same level assignments as in Hg^{195} [2G54]. Again there is no direct experimental proof that the isomeric state is $i_{13/2}$.

${}^{-7}_{-4}\mathrm{Pt}^{197}$.—Assuming that the 337 keV $M4$ γ-ray [4H49] is emitted from an $i_{13/2}$ state (no direct experimental proof) and considering the fact that only this γ-ray has been observed, one is led to the conclusion that the ground state is $5/2-$. However, a more careful search for low energy γ-rays is recommended.

$^{-9}_{-4}\mathrm{Pt}^{195}$.—The ground state spin 1/2 has been spectroscopically measured [3K52]. The emission in cascade from the isomeric state of the 130 keV $M4$, 31 keV $M1$ and 99 keV $M1$ γ-rays suggests the level sequence $i_{13/2}$–$f_{5/2}$–$p_{3/2}$–$p_{1/2}$ [2C54, 2G54]. Coulomb excitation [6B55] supports the 5/2 − and 3/2 − assignments.

$^{-11}_{-4}\mathrm{Pt}^{193}$.—Only a 136 keV $M4$ γ-ray has been observed in the isomeric decay. The ground state spin is 5/2 − if the isomeric state is $i_{13/2}$ and no more γ-ray is emitted. Since this isomeric decay as yet only has been observed by one group of investigators [2C54] it should be remeasured. Zeldes [1Z56] suggests a $p_{3/2}$ ground state.

2.23. *Validity of assignments*

The discussion of low-lying states in odd isotopes of lead, mercury and platinum has shown that unfortunately many assignments are unsatisfactory. In most cases the level assignments are based on the knowledge of multipolarities and the assumption that the $M4$ transitions are emitted from the $i_{13/2}$ state. Only in a few cases (Pb^{207}, Hg^{199}, Hg^{197} and Pt^{195}) is there a complete experimental proof that this is correct. It seems possible to measure the spin of several of the isomeric states (cf. the work by the Berkeley group [12B57]) in Pb, Hg and Pt with the atomic-beam resonance method. This would no doubt give a much more solid background to the discussion of low-lying levels in the odd isotopes of these elements. However, it should be emphasized that the assumption that the isomeric states are $i_{13/2}$ leads to assignments of other levels which are also in agreement with the shell model and with experiments, forming a convincing internal consistency.

When experimentally observed levels are compared with the predictions of the shell model it must be kept in mind that excited states can be obtained either by promoting the last particle to a higher shell or by exciting a particle from an inner shell to a vacancy in a higher shell.

Before we discuss the occurrence of $M4$ transitions in the next section it should be remarked that even if the search for isomers is very carefully performed, such experiments may fail for several reasons, the most promint ones being the following:

(1) There may be no simple way of directly producing the expected metastable state (for example Pt^{201} and Pt^{203}).

(2) In beta or alpha decay it may be energetically possible to populate the isomeric states. Quite often, however, selection rules make such transitions prohibitively improbable.

(3) The metastability of the single-particle level $i_{13/2}$ may be destroyed because of intermediate spin levels of "many-particle" origin (cf. Pb^{205}, Hg^{201} and Hg^{203}).

(4) The isomeric states may be excited but no isomeric gamma-ray observed because of the competition with beta or alpha decay (for instance Pb^{195}).

The above will also apply, *mutatis mutandis*, to the discussion of proton levels (2.3).

2.24. *Level separations* $i_{13/2}$–$f_{5/2}$

As can be seen from Table 7 (p. 447) there are 12 $M4$ transitions known in the odd isotopes of Pb, Hg and Pt. In addition there is a state in Pb^{195} which most probably is an $i_{13/2}$ state. It decays predominantly to the $h_{11/2}$ state in T^{195}. The $M4$ assignments are mostly based on the values of the transition probabilities (see 4.2), relative conversion coefficients and in a few cases on absolute conversion coefficients. It seems possible to determine the K conversion coefficients for these transitions to a much higher degree of accuracy than has been done so far. Perhaps the beautiful constancy of the

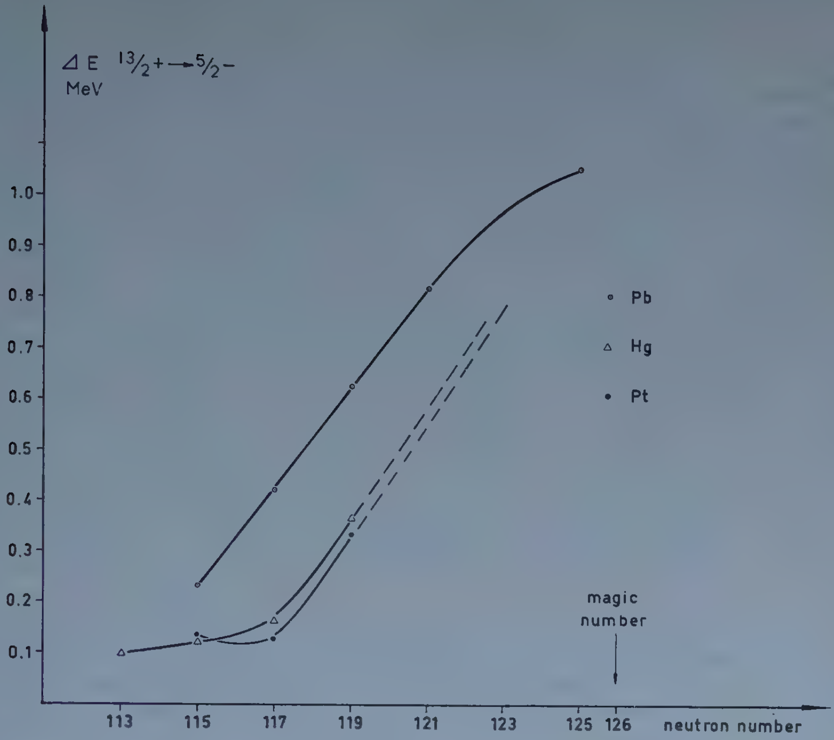

Fig. 2. The level spacing $i_{13/2}$–$f_{5/2}$ in odd mass isotopes of Pb, Hg and Pt as a function of neutron number. Note that no $M4$ transitions have been found in Pb^{205}, Hg^{205}, Hg^{203}, Hg^{201}, Pt^{203}, Pt^{201} and Pt^{199}. Extrapolation and interpolation show the expected energies of these transitions. (The figure is reproduced with slight changes from ref. 5S56.)

matrix elements and the fair agreement with theoretical values are the most convincing proofs that all these transitions are of multipolarity $M4$.

The $i_{13/2}$–$f_{5/2}$ separation is plotted in Figs. 2 and 3 as a function of neutron and proton number respectively. The most striking feature of these curves is the increase of energy towards the magic numbers. Especially interesting is the variation with neutron number. The curves of Bleuler and Terreaux [15B57] indicate that only a small part of this effect should be due to the change of the nuclear radius. Pryce [5P56a] has shown that a much larger effect results from the interaction of neutron holes. Some level spacings in lead isotopes as calculated by Pryce are reproduced in Fig. 5. It is seen that the theoretical estimates agree qualitatively with the experimental results of Fig. 2. Another apparent feature of Fig. 2 is the absence of points representing Pb^{205}, Hg^{201}, Hg^{203}, Hg^{205}, Pt^{199}, Pt^{201} and Pt^{203}. Especially the "missing" $M4$ transition in Pb^{205} caused much trouble before the decay scheme of Bi^{205} was satisfactorily known. This case will be discussed somewhat further, because it may explain the non-observation of $M4$ transitions also in other cases.

In Pb^{206} (d,t) reactions Harvey [9H53] found a level at 0.84 MeV which he assigned $i_{13/2}$ because of its low cross section. Since, in contrast to Bi^{203} and Bi^{207}, no $M4$ transition was observed in the decay of Bi^{205}, it was assumed [5S56] that the $i_{13/2}$ level

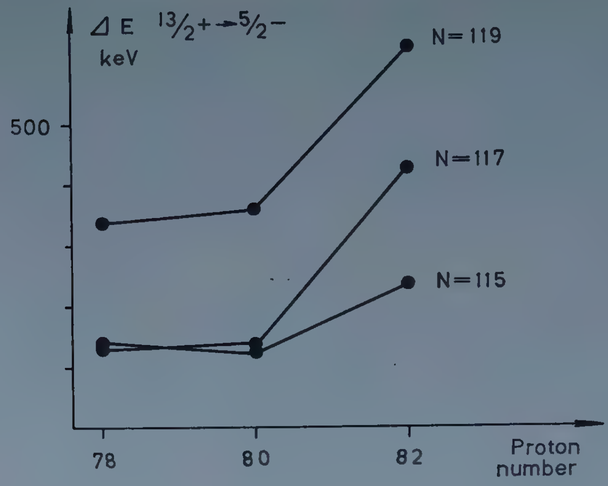

Fig. 3. The level spacing $i_{13/2}$–$f_{5/2}$ in odd mass isotopes of Pb, Hg and Pt as a function of proton number.

for some reason was not populated in the decay of Bi^{205}. However, even before the levels in Pb^{205} were known in more detail there were reasons to believe that the metastability of the $i_{13/2}$ state must be destroyed by an intermediate spin level. So for example is the $M4$ transition in Pb^{207} observed in (γ, n) reactions on natural lead [1B55], which, however, is not the case for the expected $M4$ transition in Pb^{205}. The investigation of the levels in Pb^{205} [3S56] later showed that in fact there is a level at 703 keV of spin 7/2 or 9/2. The calculations of Pryce [5P56] suggested a $(p_{1/2} f_{5/2}{}^2)_{7/2-}$ level at 0.7 MeV which was identified with the experimentally found level. It is thus both experimentally and theoretically established that the metastability of an $i_{13/2}$ level must be destroyed by an intermediate level, which from Pryce's calculations should be a three-hole level. If the energy of the $i_{13/2}$ level is 0.84 MeV as suggested from Harvey's experiments it would be possible to see a 0.14 MeV $M2$ or $E3$ transition to the 703 keV state depending on the assignment of this level (9/2 − or 7/2 −). An $E3$ transition would have a half-life in the $m\mu$s–μs region. Vegors and Axel [1V56] did not observe any such half-life in Pb (γ, n) experiments but the well known 130 μs half-life of the isomeric state in Pb^{206}. This speaks in favour of a 9/2 − assignment to the intermediate level. Pryce's lowest 9/2 − level $(p_{1/2} f_{5/2} p_{3/2})_{9/2-}$ comes at 1.2 MeV. However, when Vegors and Axel performed their experiments they did not know of this problem and may for some reason have missed the transitions from the $i_{13/2}$ state. Experiments of this type are associated with many difficulties. It seems worth while to repeat the experiments of Vegors and Axel or to make other similar experiments. This may give a definite answer to the question discussed above. The main thing, however, is that both experiment and theory have shown that in Pb^{205} there may be levels at rather low energies, which are not single particle levels, and that such levels may be the reason why the $M4$ transition is not observed in Pb^{205}. The same situation may also arise in other nuclei in this region.

Pb^{207} has only one neutron hole and it is an important experimental fact that in

Pb^{207} it has been possible to give single-particle assignments to all observed levels below 2.4 MeV.

It may, however, be questioned why $M4$ transitions are found in Pb^{203} and other Pb isotopes of lower mass number. In Fig. 5 Pryce's approximate calculations show how the position of the lowest complex $7/2-$ and $9/2-$ levels varies with the neutron number. As can be seen the energies relative to the $5/2-$ level are constant or tend to increase with decreasing neutron number. Thus in Pb^{203} the levels destroying the metastability in Pb^{205} have crossed the $i_{13/2}$ level, which explains the fact that the $M4$ transition is again observed.

Considering now the missing $M4$ transitions in Hg and Pt, it is obvious that the addition of two and four proton holes may give rise to still more low-lying levels. The trend of the energies of the first excited states $(2+)$ in the even-even nuclei indeed indicates that low-lying complex states may be expected at much lower energies in the odd isotopes of Hg and Pt (cf. Fig. 9 p 442).

Bergström *et al.* [2B53] showed by (γ, n) reactions on enriched Hg isotopes that there are no $M4$ transitions in Hg^{201} and Hg^{203} (however, the $M4$ transition in Hg^{199} was observed) of the energies indicated by the extrapolated curves of Fig. 2. Already when these experiments were performed in 1953 it was guessed that the negative result of the experiments was due to intermediate levels, which were not predicted by the simple shell model. Nothing definite can of course be said about the origin of the intermediate levels. They may be of "many-particle" character or of collective nature.

The Pb^{205} case illustrates how three neutron holes may couple their angular momenta in complex levels below 1 MeV. In Hg^{205} low-lying complex levels should be due to the coupling of one neutron hole and two proton holes. The authors do not know of any attempts to observe the $i_{13/2}$ state in Hg^{205}. This state may be produced in Hg^{204} (d,p) reactions. If the influence of the two proton holes can be neglected an $M4$ transition of about 800 keV should be observed (cf. Pb^{207}). Most probably, however, the presence of the two proton holes results in low-lying levels of intermediate spins. It may be worth while to search for a half-life in the mμs and μs regions.

Also in the case of Pt^{199} there exists experimental support that the metastability of the $i_{13/2}$ level is destroyed. Pt^{197m} for example is obtained in Pt (d,p) reactions but not Pt^{199m} [2A56]. The $M4$ transition in Pt^{199} is expected to have a half-life of about 1 minute and a gamma-ray energy about 500 keV. Such an activity is produced when Pt is irradiated with deuterons. However, it can be shown that this activity is due to the annihilation radiation from the decay of 72 s O^{14} produced from N^{14}, which to a large extent is present in the platinum metal.

Unfortunately there does not seem to be a simple way to produce excited states in Pt^{201} and Pt^{203}. For still lower values of Z there should be a larger possibility to destroy the metastability of the $i_{13/2}$ levels by low-lying complex levels (cf. the energies of the first excited states in even-even isotopes of Os, Fig. 9).

It is remarkable that no $M4$ transitions have been reported in polonium. The reason may be that the isomeric states are predominantly de-excited by alpha decay. The appearance of low-lying complex levels seems less probable than in Hg because of the fairly high energies of the first excited states in the even-even nuclei of Po. It must be emphasized, however, that no systematic search for short-lived $M4$ transitions in Po has been reported. This could be done for instance in the external beam of a machine giving high energy particles.

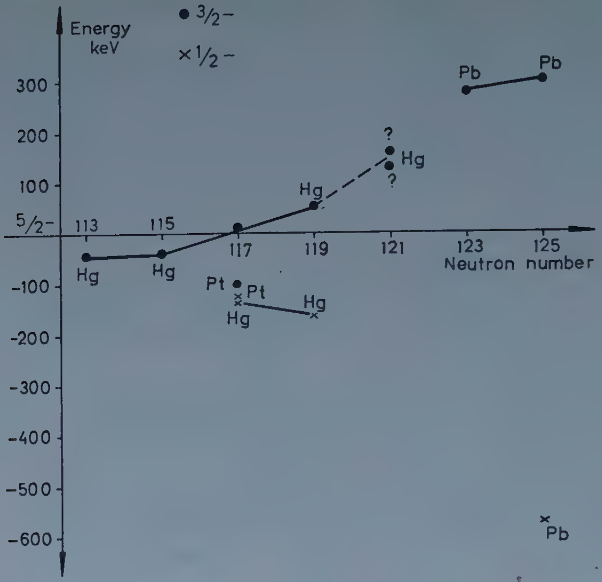

Fig. 4. Experimentally found level spacings $p_{3/2}$–$p_{1/2}$–$f_{5/2}$ in odd mass isotopes of Pb, Hg and Pt as functions of neutron number.

2.25. *Level separations* $f_{5/2}$–$p_{3/2}$–$p_{1/2}$

In Fig. 4 the energies of the $p_{1/2}$ and $p_{3/2}$ levels relative to the $f_{5/2}$ level are plotted as functions of neutron number. Only for Hg experimental information is available to such an extent that it is possible to speak of a systematic behaviour. However, it is perhaps justified to neglect the influence of the protons and connect points representing corresponding levels in Pb, Hg and Pt, because the levels are due to neutron holes. (The lowest levels in the odd Tl isotopes, for instance, are proton hole levels and their spacings are in general not very sensitive to a change in the neutron number.) The trend of the level spacing thus obtained may be compared with the calculations of Pryce (Fig. 5). It is then observed that Pryce's calculation of the level movements in the lead isotopes qualitatively agrees fairly well with the experiments. The spin orbit doublet spacing, for instance, increases towards the magic number $N = 126$. The $p_{3/2}$ level lies above the $f_{5/2}$ level for N close to 126 but these levels cross for lower values of N. It is of course not surprising that the crossing is not correctly predicted. The calculations are rough and the method of connecting the experimental points may be discussed. However, it seems plausible to conclude that also in these cases the change in the level spacing with neutron number is due to the change in interaction between the "valence nucleons".

An extrapolation of the $p_{3/2}$ curve in Fig. 4 indicates that in Hg^{201} the $f_{5/2}$ level is situated about 150 keV above the $p_{3/2}$ ground state. This information may be of some help in the interpretation of the "anomalous" level scheme of Hg^{201} (3.25).

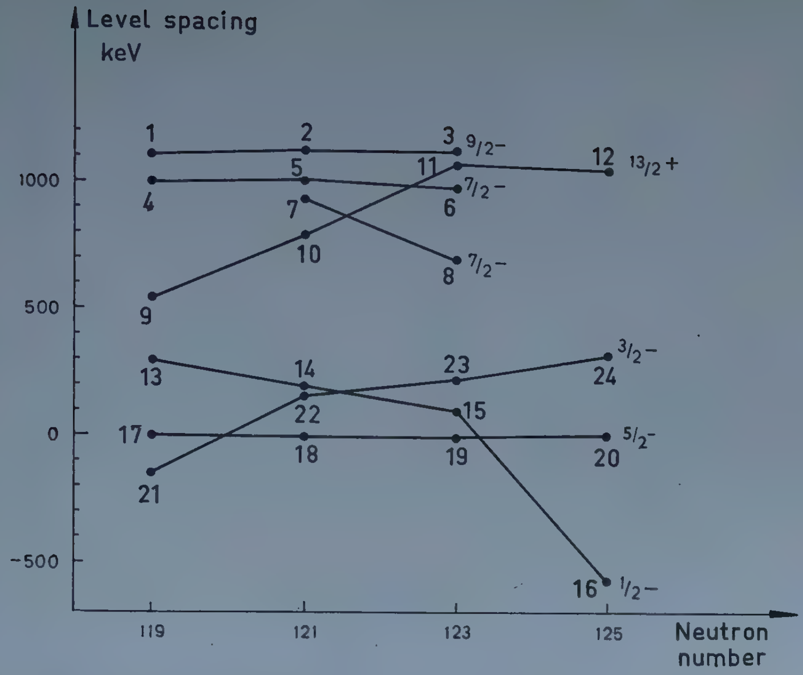

Fig. 5. Energies of single-particle states 1/2 −, 3/2 −, 5/2 − and 13/2 + and low-lying complex states 7/2 − and 9/2 − in Pb isotopes as calculated by M. H. L. Pryce [5P56a]. The method of calculation of the first three levels was based on the simple assumption that all paired neutrons couple to a zero resultant angular momentum. The interaction parameters were taken as in the Pb^{205} calculations [5P56]. A rather arbitrary value was assumed for the mixing matrix elements which makes the calculations so crude that one can scarcely hope to predict correctly, for instance, the crossing of the 3/2 − and 5/2 − levels.

The lowest 7/2 − level in Pb^{203} and Pb^{205} arises from a configuration containing 2 or 4 $f_{5/2}$ neutrons coupled among themselves to give a resultant angular momentum 4; this cannot happen with the closed subshell $f_{5/2}^{-0}$ or the empty subshell $f_{5/2}^{-6}$. Hence the isolated position of this level.

Configuration key:

$1 = p_{1/2}^{-1} f_{5/2}^{-5} p_{3/2}^{-1}$,
$2 = p_{1/2}^{-1} f_{5/2}^{-3} p_{3/2}^{-1}$,
$3 = p_{1/2}^{-1} f_{5/2}^{-1} p_{3/2}^{-1}$,
$4 = p_{1/2}^{-1} f_{5/2}^{-5} p_{3/2}^{-1}$,
$5 = p_{1/1}^{-1} f_{5/2}^{-3} p_{3/2}^{-1}$,
$6 = p_{1/2}^{-1} f_{5/2}^{-3} p_{3/2}^{-1}$,
$7 = p_{1/2}^{-1} f_{5/2}^{-4}$,
$8 = p_{1/2}^{-1} f_{5/2}^{-2}$,
$9 = p_{1/2}^{-2} f_{5/2}^{-4} i_{13/2}^{-1}$,
$10 = p_{1/2}^{-2} f_{5/2}^{-2} i_{13/2}^{-1}$,
$11 = p_{1/2}^{-2} i_{13/2}^{-1}$,
$12 = i_{13/2}^{-1}$,
$13 = p_{1/2}^{-1} f_{5/2}^{-6}$,
$14 = p_{1/2}^{-1} f_{5/2}^{-4}$,
$15 = p_{1/2}^{-1} f_{5/2}^{-2}$,
$16 = p_{1/2}^{-1}$,
$17 = p_{1/2}^{-2} f_{5/2}^{-5}$,
$18 = p_{1/2}^{-2} f_{5/2}^{-3}$,
$19 = p_{1/2}^{-2} f_{5/2}^{-1}$,
$20 = f_{5/2}^{-1}$,
$21 = p_{1/2}^{-2} f_{5/2}^{-4} p_{3/2}^{-1}$,
$22 = p_{1/2}^{-2} f_{5/2}^{-2} p_{3/2}^{-1}$,
$23 = p_{1/2}^{-2} p_{3/2}^{-1}$,
$24 = p_{3/2}^{-1}$.

2.3. *Proton levels*

2.31. *Introductory remarks*

According to Klinkenberg's nuclear shell schemes [3K52] the last two protons of the 82 shell are $s_{1/2}$ protons (cf. Fig. 1). This prediction is borne out by all experimental evidence available on the ground states of odd mass Tl isotopes (Table 3). In the same way the $d_{3/2}$ assignment of the protons 77 through 80 receives support from

Table 3. Ground state assignments of odd mass isotopes of Tl, Au and Ir (cf. 2.32).

Z \ N	114	116	118	120	122	124	126
81	1/2+?	1/2+	1/2+	1/2+?	1/2+	1/2+	1/2+, 3/2+
79	3/2+?	3/2+?	3/2+	3/2+			
77	3/2+	3/2+					

measured ground state spins of odd Au and Ir isotopes. This does not mean, of course, that the spherical picture of the nucleus underlying Klinkenberg's scheme is unique in leading to valid predictions of ground state properties. Mottelson and Nilsson [12M55], for instance, have shown that the 3/2+ assignment of the Ir^{191} and Ir^{193} ground states conforms also with calculations based on deformed nuclear potentials.

Beside the $s_{1/2}$ and $d_{3/2}$ shells there are other proton shells expected to create levels of low excitation in the odd isotopes of Tl, Au, and Ir, notably $d_{5/2}$ and $h_{11/2}$. Thus in Tl low-lying levels may be obtained as hole states by exciting a proton from the $d_{3/2}$, $d_{5/2}$, or $h_{11/2}$ shell to the $s_{1/2}$ shell and in Au and Ir proton holes may correspondingly occur in the $s_{1/2}$, $d_{5/2}$, and $h_{11/2}$ shells by transitions to the $d_{3/2}$ shell (though a proton transition $d_{3/2} \rightarrow h_{11/2}$ is possible too). Excited levels with the appropriate spins and parities have been identified from experiments in several cases. Already in Au, however, there is some ambiguity as to the nature of a 5/2+ level. It has been commonly accepted as the $d_{5/2}$ single proton state (or rather the hole state obtained by raising a $d_{5/2}$ proton to the $d_{3/2}$ shell) but may be interpreted as the first member of the ground state rotational band [8B57]. Similarly a 3/2+ level in Au, which does not fit into the single particle picture, should be of rotational character. In connection with Figs. 6 and 7, however, we are going to discuss the systematics of level spacings in the nuclei concerned mainly from the single-particle point of view. We start with an examination of the experimental data on which the spin assignments are based.

2.32. *Assignment of levels*

The information pertaining to the more or less definite single-proton levels discussed below has been collected in Table 4.

${}^{0}_{-1}\mathrm{Tl}^{207}$.—The ground state decays by an allowed or first forbidden β-transition to the $p_{1/2}$ ground state of Pb^{207}, indicating the spin 1/2 or 3/2 [3F52]. The former assignment is preferred in analogy with the neighbouring Tl^{205} and Tl^{203} ground states with measured spin 1/2. Levels in Tl^{207} are populated by the α-decay of Bi^{211}. A 350 keV γ-ray [1C38] is interpreted as $d_{3/2} \rightarrow s_{1/2}$ from its mixed $E2 + M1$ character and the assumed ground state spin [3F52]. Indications of a weak 85 keV γ-ray in the decay of Bi^{211} have been reported [7C32, 1C38], but no assignment is possible.

${}^{-2}_{-1}\mathrm{Tl}^{205}$.—Spectroscopic measurements have verified the ground state spin 1/2 [3K52]. Two levels at 205 keV and 615 keV are reached in Coulomb excitation [3B55]. The lower level is de-excited by an $E2 + M1$ transition to the ground state which leads to the assignment $d_{3/2} \rightarrow s_{1/2}$. In analogy with the conditions in Tl^{203} (see below) the 615 keV level is tentatively given as $d_{5/2}$.

Table 4. Energies of single-particle states in Tl, Au and Ir isotopes.

Nucleus	Energy (keV) above ground state			
	$s_{1/2}$	$d_{3/2}$	$d_{5/2}$	$h_{11/2}$
Tl^{207}	0	350	—	—
Tl^{205}	0	205	615	—
Tl^{203}	0	279	679	—
Tl^{201}	0	330	692	—
Tl^{199}	0	367	720	—
Tl^{197}	0	387	772	994
Tl^{195}	0	394	777	876
Au^{199}	—	0	—	—
Au^{197}	77	0	279	410
Au^{195}	61	0	261	318
Au^{193}	38	0	258	290
Ir^{193}	73	0	143	80
Ir^{191}	82	0	130	172

$^{-4}_{-1}$Tl^{203}.—The first excited state at 279 keV, reached from Pb^{203}, decays by an $E2 + M1$ transition [1W54] to the $s_{1/2}$ ground state [3K52]. From the second excited state (679 keV) a strong $E2 + M1$ branch goes to the first excited state and a weaker $E2$ branch to the ground state [1W54]. This is in agreement with the level sequence $d_{5/2}$–$d_{3/2}$–$s_{1/2}$ as predicted by the shell model. Both levels are also found in Coulomb excitation [3B55].

$^{-6}_{-1}$Tl^{201}.—In the decay of Pb^{201} two γ-rays of 330 keV (E2 + $M1$) and 361 keV (predominantly $M1$) are interpreted for intensity reasons to be emitted from the first and second excited states, respectively, of Tl^{201} [4B55]. The level assignments $d_{5/2}$–$d_{3/2}$–$s_{1/2}$ are based on systematics.

$^{-8}_{-1}$Tl^{199}.—The ground state spin has been measured as 1/2 by the atomic-beam magnetic resonance method [12B57]. In the decay of Pb^{199} two mixed $E2 + M1$ transitions (367 and 353 keV) have been shown to follow in coincidence [3A57] (the relative intensities determining their order) in agreement with the predicted level sequence $d_{5/2}$–$d_{3/2}$–$s_{1/2}$.

$^{-10}_{-1}$Tl^{197}.—The measured ground state spin 1/2 [12B57] and two cascade γ-rays as in Tl^{199} establish the three lowest levels. Here, however, an $E3$ transition (222.5 keV) has been found in coincidence with the two $E2 + M1$ transitions (387 and 385 keV) [3A57]. Its level of origin, fed from a level in Pb^{197} interpreted as $i_{13/2}$, should thus be $h_{11/2}$ in single-particle notation. The order of the two mixed transitions is not unambiguously determined from the total intensities in this case, because the $d_{3/2}$ and $d_{5/2}$ levels are populated both from the Pb^{197} ground state and (predominantly) via the $E3$ transition. An amplifying argument is obtained, however, from the fact that $d_{3/2} \to s_{1/2}$ is l-forbidden for $M1$ decay, while $d_{5/2} \to d_{3/2}$ is not. Thus the transition showing from its conversion ratios the larger admixture of $M1$ (385 keV) is most probably $d_{5/2} \to d_{3/2}$.

$^{-12}_{-1}$Tl^{195}.—The same set of transitions is found as in Tl^{197} [3A57], but the plausible assumption of an $s_{1/2}$ ground state has not been experimentally confirmed in this case. A 99 keV $E3$ transition follows the decay of a 17 min Pb activity, which for this reason is identified as the $i_{13/2}$ isomeric state of Pb^{195}. The internal transition branch via the Pb^{195} ground state has not been observed and is probably well below 1 %. The total intensities of the two mixed $E2 + M1$ transitions in Tl^{195} should then be equal (neglecting the possible weak $h_{11/2} \to d_{3/2}$ transition) and the l-forbiddenness of $d_{3/2} \to s_{1/2}$ may be expected to show up directly in the relative conversion intensities. In this way a 393.5 keV γ-ray is interpreted as $d_{3/2} \rightarrow s_{1/2}$ and a 383 keV γ-ray,[1] more strongly converted in the K-shell, as $d_{5/2} \rightarrow d_{3/2}$ [3A57b]. (The respective $M1$ admixtures were not possible to determine with sufficient accuracy.)

$^{-6}_{-3}\mathrm{Au}^{199}$.—The ground state spin has been measured as 3/2 with the atomic-beam method [8C56]. Excited levels are populated by the β-decay of Pt^{199} [2L56], but the information is too incomplete to allow any level assignments to be made. The presence of an isomeric level of 2 μs half-life, proposed as an explanation of anomalous β^{-}–γ coincidence intensities [2L56], has not been possible to confirm [1T57a].

$^{-8}_{-3}\mathrm{Au}^{197}$.—Spectroscopic measurements agree with the ground state assignment $d_{3/2}$ [3K52]. An excited level at 409.5 keV, reached from the $i_{13/2}$ isomeric state of Hg^{197}, is interpreted as $h_{11/2}$ because it decays to the ground state by an $E3$ and an $M1$ transition in cascade, the intermediate level being assigned $d_{5/2}$. There are also indications of an $M4$ cross over [6M53]. A cascade of a 192 keV $M1$ transition and a 77 keV $E2 + M1$ transition follows the electron capture decay of the Hg^{197} ground state. The lower energy γ-ray should connect the $s_{1/2}$ state with the $d_{3/2}$ ground state but the $3/2+$ origin of the 192 keV γ-ray cannot be identified with a single particle level. Boehm and Marmier [8B57] recently pointed out that this level as well as the $5/2+$ level in the isomeric branch (denoted $d_{5/2}$ above) may be interpreted as belonging to rotational bands. (This would apply also to the corresponding levels in Au^{195} and Au^{193}). Complementary information on levels in Au^{197} is obtained from Coulomb excitation [6B55], leading finally to the plausible level sequence $d_{3/2}$ (0 keV), $s_{1/2}$ (77 keV), $3/2+$ (268 keV), $d_{5/2}$ (or $5/2+$) (279 keV), $h_{11/2}$ (409.5 keV), and $7/2+$ (550 keV).

$^{-10}_{-3}\mathrm{Au}^{195}$.—A considerable number of levels is known from the electron capture decay of the $i_{13/2}$ state and the ground state of Hg^{195} [2J55]. The main structure of the level scheme is similar to that of Au^{197} which forms the basis of the assignments $d_{3/2}$ (0 keV), $s_{1/2}$ (61 keV), $3/2+$ (240 keV), $d_{5/2}$ (or $5/2+$) (261 keV), and $h_{11/2}$ (318 keV) for the levels of present interest.

$^{-12}_{-3}\mathrm{Au}^{193}$.—Also in this case the level assignments are based on analogies with the odd isotopes of higher mass, the proposed level sequence being $d_{3/2}$ (0 keV), $s_{1/2}$ (38 keV), $3/2+$ (224 keV), $d_{5/2}$ (or $5/2+$) (258 keV), and $h_{11/2}$ (290 keV) [cf. 2G54].

$^{-10}_{-5}\mathrm{Ir}^{193}$.—The ground state assignment $d_{3/2}$ has been confirmed by measurements [3K52, cf. 1Z56]. By the recent discovery of an $M4$ transition to the ground state [8B57] the $h_{11/2}$ level at 80 keV seems to be firmly established. As to other excited levels, several of them fed from Os^{193}, there is some ambiguity. The most reasonable sequence of the low-lying levels seems to be $d_{3/2}$ (0 keV), $s_{1/2}$ (73 keV), $h_{11/2}$ (80 keV), $d_{5/2}$ (or rotational $5/2+$) (143 keV), and $7/2+$ (368 keV). The last two levels have been observed in Coulomb excitation [2D56]. De Waard [2W54] gives the assignment $g_{7/2}$ to the 73 keV level, but this is not consistent with the later found $M4$ transition from the 80 keV state.

$^{-12}_{-5}\mathrm{Ir}^{191}$.—Also in this stable isotope the ground state is known as $d_{3/2}$ [3K52, cf. 1Z56]. A 42 keV $E3$ transition [6M54a] followed by a 130 keV mixed $E2 + M1$ transition [3D57] in the β-decay of Os^{191} indicate an $h_{11/2}$ level at 172 keV and a $d_{5/2}$ (or rotational $5/2+$) level at 130 keV. An 82 keV level, de-exciting to the ground state via an $E2 + M1$ transition, is probably $s_{1/2}$ in analogy with the 73 keV level in Ir^{193}. Boehm and Marmier [8B57] place a rotational $3/2+$ level at 179 keV, and a probable $7/2+$ level at 356 keV has been observed in Coulomb excitation (as well as the 130 keV level) [2D56].

---

[1] Earlier erroneously given as 448 keV [3A57, 3A57a].

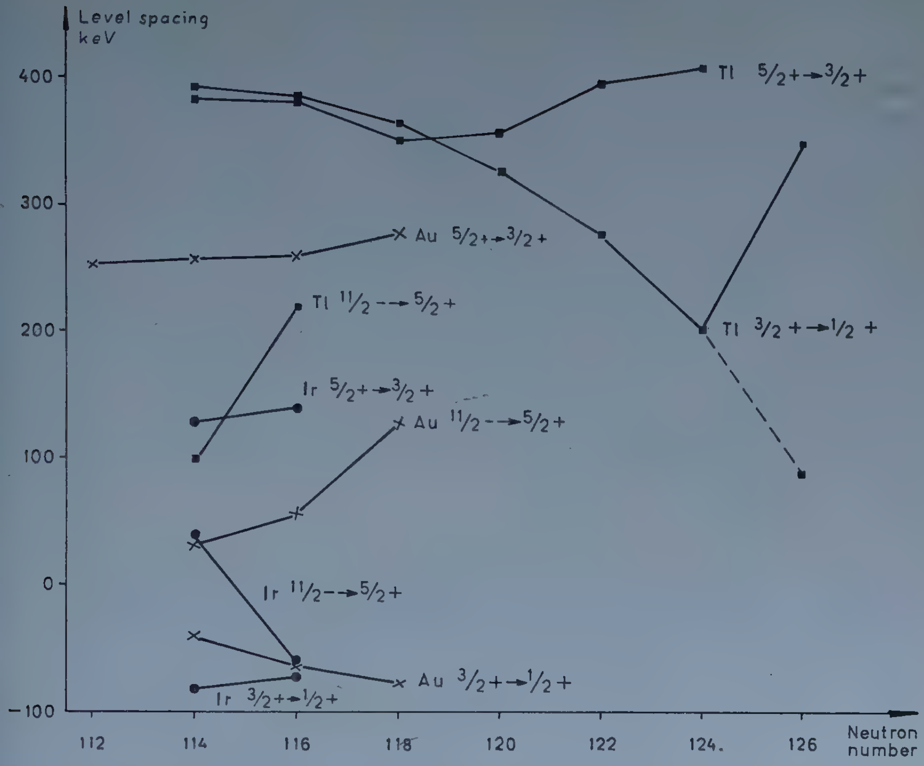

Fig. 6. Level separations in odd mass isotopes of Tl, Au and Ir as functions of neutron number. The lower point for $N = 126$ refers to an anassigned weak gamma-ray in the alpha-decay of Bi^{211} (cf. the text).

2.33. *Level separation* $h_{11/2}$–$d_{5/2}$

It may be asked why so few $h_{11/2}$ levels have been discovered in Tl. One reason is certainly that from Tl^{199} and upwards they are not fed to any appreciable extent from the corresponding $i_{13/2}$ levels in Pb. It would perhaps be possible to excite additional $h_{11/2}$ states by for instance proton bombardment of enriched Hg isotopes. Because of the tendency of a steep rise of the $h_{11/2}$–$d_{5/2}$ separation with neutron number (see Fig. 6) the lifetimes of these isomeric states must be expected to be considerably less than that of the $E3$ transition in Tl^{197} (half-life 0.55 s). They evidently did not show up in the experiments of Vegors and Axel [1V56], who looked for half-lives in the region 10^{-5}–10^{-1} seconds after 22 MeV betatron irradiation of natural Tl, but this may be due to low excitation cross sections. There is, however, also a tendency for the $h_{11/2}$–$s_{1/2}$ distance to increase with neutron number, that means an increasing probability for complex intermediate levels to destroy the metastability.

In Au as in Tl the $h_{11/2}$–$d_{5/2}$ separation increases towards the closed neutron shell, but in Ir the trend is opposite. Here a sharp level crossing takes place from $N = 114$ to $N = 116$, resulting in an $M4$ transition from $h_{11/2}$ to the $d_{3/2}$ ground state in Ir^{193} instead of the $E3$ transitions to $d_{5/2}$ found in the other nuclei concerned.

With the exception of the Ir^{191} point the available data indicate a rise in separation energy also with proton number towards the closed shell (Fig. 7).

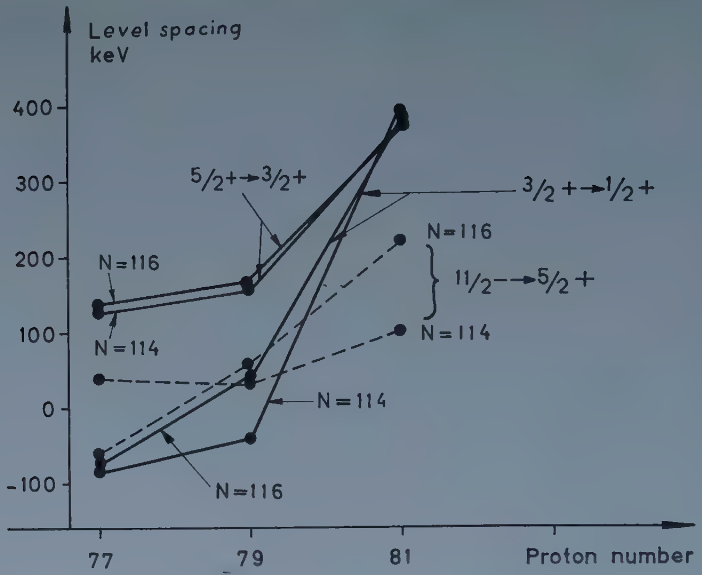

Fig. 7. Level separations in odd mass isotopes of Tl, Au, and Ir as functions of proton number.

2.34. *Level separations* $d_{5/2}$–$d_{3/2}$–$s_{1/2}$

The spin-orbit doublet splitting $d_{5/2}$–$d_{3/2}$ in Au (and Ir) as a function of neutron number (Fig. 6) is surprisingly constant. This is true of the general trend in Tl too, though the slight deviation from a smooth curve shown by two of the points may reflect an influence of the neutron configuration. From this point of view the outstanding smoothness of the $d_{3/2}$–$s_{1/2}$ curve for Tl is the more remarkable. Only the filling in of the two last neutrons in the 126 shell brings about a typical "shell effect". (The continuity in the curve provided by the suspicious 85 keV level in Tl^{207} as indicated in the figure is most probably a mere coincidence.)

A marked increase of the separation energies with proton number is illustrated in Fig. 7, the major steps occurring from 79 to 81 protons. This should be compared with the N-dependence of the $f_{5/2}$–$p_{3/2}$–$p_{1/2}$ separations (Fig. 4); in these cases of neutron transitions the proton number has less influence.

3. Complex levels

3.1. *Theoretical and experimental background*

The systematics of even-odd and odd-even nuclei in the lead region shows that low-lying levels to a large extent can be identified with the single-particle levels of the shell model. A more serious check of the shell model would be to investigate to what extent several particles, each assigned a one-particle state, couple their angular momenta to a resultant nuclear spin other than that of the odd particle. This can for obvious reasons be done only in simple cases, where the number of particles is limited. Therefore calculations have been performed only in the immediate neighbourhood of the double-magic numbers, where it is possible at low excitation energies to consider the nucleus as a hard, spherical core, i.e. it does not contribute to the total angular momentum. The double-magic nuclei which offer such calculations are ${}^{8}_{8}\mathrm{O}^{16}$, ${}^{20}_{20}\mathrm{Ca}^{40}$, ${}^{28}_{20}\mathrm{Ca}^{48}$, (${}^{82}_{50}\mathrm{Sn}^{132}$) and ${}^{126}_{82}\mathrm{Pb}^{208}$. Pryce [5P52] was the first to make such calculations in the lead region, where the approximations used should be best valid. Quite a considerable work has also been successfully performed in the O^{16} [2E55] and Ca regions [3L55]. Sn^{132} is unfortunately situated in a region where practically no information but half-lives of ground states is available [8P53].

It is not the purpose of this experimental survey to describe in detail the methods used in the theoretical calculations. The reader is referred to the papers by Pryce [5P52, 5P56, 1A54], Brink [16B54], True [2T56], Wahlborn [4W57], and Kearsly [5K57]. A few words may be mentioned, however, in order to emphasize the importance of certain experiments and in order to have as complete a reference list as possible.

The calculations of the levels of nuclei which differ from Pb^{208} only with a few particles are similar to the perturbation calculation of the atomic levels in helium. As is well known, in a two-particle case the total energy is given by:

$$E_{\mathrm{tot}} = E_1 + E_2 + E_{\mathrm{int}}. \tag{1}$$

In the zero-order approximation the energy of a certain two-particle configuration is the sum of the energies of the individual particle energies E_1 and E_2. The levels thus obtained are in general considerably degenerated. This degeneracy is, however, removed if the interaction E_{int} of the particles is taken into account. In the helium case this is, in principle, simple because the interaction between the electrons as well as between the nucleus and the electrons is the well known Coulomb interaction. The one-particle levels (hydrogen levels) and the interaction energy can in this case be accurately calculated.

In the Pb^{208} region the situation is much worse. First of all, because of the insufficient knowledge of the nuclear mean potential it is not possible to calculate accurately the one-particle or one-hole cases. An idea of the absolute value of the level spacing of the one-nucleon levels can be obtained from the scheme of Bleuler and Terreaux [15B57]. Though this scheme gives good agreement with experiments in the region of the stable nuclei, it is at present too approximate to be used for the calculation of zero-order energies. Therefore these energies in cases of several particles must be obtained from the experimentally observed one-nucleon levels. This requires that in the one-nucleon cases the correspondence between the observed levels and the predicted shell model levels is unambiguous. In Fig. 8 those cases are included where the excess $|\Delta Z| + |\Delta N|$ of holes and particles from Pb^{208} is smaller than 4. For a complete knowledge of all the zero order levels in this region it is necessary to know accurately the excited states in Pb^{207}, Tl^{207}, Pb^{209}, and Bi^{209} (see Fig. 8). This is unfortunately not the case. Sufficient experimental information and satisfactory identification with shell model levels exist only for Pb^{207}. For this reason most of the calculations made so far have concerned nuclei where a knowledge of the levels in Pb^{207} is required. It is fortunate that the conditions for studying the nuclei Pb^{206}, Pb^{205} and Pb^{204} are such that considerable information has already been accumulated, and still more will be obtained in the near future.

The second difficulty in calculating the energy levels in the above-mentioned way is associated with the poor knowledge of the perturbation energy, i.e. the (n,p), (n,n) and (p,p) interaction. For simplicity Pryce assumed that this interaction could

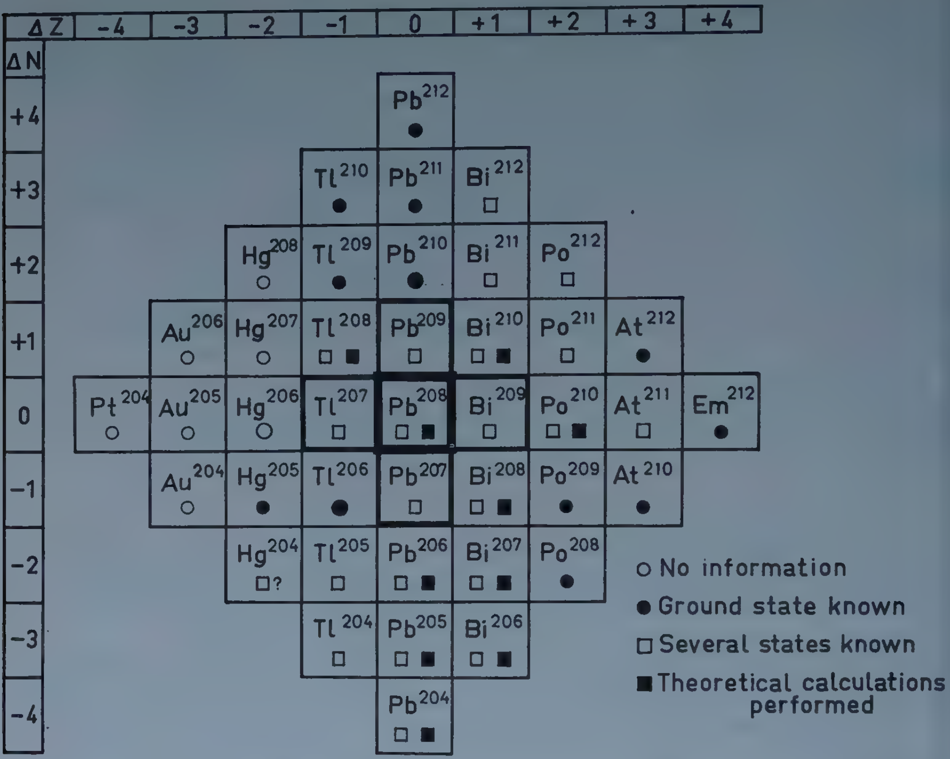

Fig. 8. Nuclei in the Pb^{208} region for which calculations of levels based on the shell model have been performed or may be performed, when more experimental information is available. A filled circle means that only the ground state has been observed. An unfilled square means that in addition to the ground state at least one excited state is known.

be described with a delta function. If configurational mixing is neglected the interaction between a neutron and a proton, for instance, is written [5P52].

$$E_{np} = a_s A_s R + a_t A_t R = R A_s (a_s + 1.5 a_t), \tag{2}$$

where s and t refer to singlet and triplet states. a_s and a_t are calculable constants depending on the configuration of the two particles and of the total spin. A_s and A_t are the strength of the singlet and triplet interaction respectively. From scattering experiments $A_t/A_s \approx 1.5$ is known. R, an integral involving the total radial wave function, is depending on the quantum numbers (nlj) of the two particles and is thus a configuration-dependent quantity. In the works of Pryce R has not been theoretically calculated. The value of RA_s was obtained by comparison with certain experimentally known levels in the two-hole (or two-particle) nuclei.

The calculations of Pryce thus are depending on several parameters which are adjusted to the experiments. In his first paper Pryce discussed the two-nucleon cases [5P52]. However, his original calculations on levels in Bi^{210} (see also the work of Brink [16B54]), Pb^{206} and Tl^{208} suffer from the poor experimental information. For this reason several of the adjustable parameters are arbitrarily chosen. Improved measurements on Pb^{207} [1A55] and Pb^{206} made more detailed calculations on levels in Pb^{206} possible [1A54]. The great success of these calculations was that they were able to predict the decay mode of the isomeric 7 − level in an excellent way. Later more accurate experiments on levels in Pb^{205} allowed Pryce to make similar calculations for this nucleus [5P56]. Also in this case the calculations were able to give the main features of the levels populated from the decay of Bi^{205}. Before making more detailed comparisons, however, it is necessary to have better coincidence information and measurements of conversion coefficients. Such work is in progress at the Nobel Institute [5S57].

An increased number of holes makes the above calculations complicated. Furthermore the comparison between theory and experiment may be highly doubtful because of the neglection of configurational interaction. It therefore seems surprising that the calculations by True [2T56] on levels in Pb^{204} are able to explain so well the decay of the 9 − isomeric state. True suggests two very close-lying 4 + levels which must be populated from the 9 − state. Experimentally the level distance between two low-lying 4 + levels was found to be 289 keV. This may give an idea of the configurational mixing interaction in this special case [2H56].

Bi^{206} and Bi^{207} differ from Pb^{205} and Pb^{206} by the addition of one proton. Since the comparison between experiments and calculations no doubt has had some success in the lead isotopes, it seems worth while to extend the calculations to Bi^{207} and Bi^{206}, where recently accurate measurements have been performed [4A57]. Wahlborn [4W57] has investigated these cases with the same method as used by Pryce. It is then necessary to know at least a few excited states in Bi^{209}. Wahlborn assumed that the ground state is an $h_{9/2}$ state and that the experimentally found excited states at 0.90 and 1.56 MeV are $f_{7/2}$ and $i_{13/2}$ states. The calculation is made possible by the fact that the 83rd proton occupies the same range of levels as the neutron holes. The parameters used in Pryce's work could therefore be taken. The most significant result of Wahlborn's calculations on Bi^{206} is the assignment of 6 + and 4 + to the ground state and first excited state, respectively, for which the level spacing was found to be of the order of 0.1 MeV. This agrees well with the experimental observation of a 60 keV gamma-ray from the first excited state to the ground state. An experimental determination of the ground state spin in Bi^{206} seems possible[1] and would be of very great importance for the comparison between experimentally observed and theoretically predicted level energies and assignments. The first excited state has a half-life of 7.8 μs [4A57a]. This is about 60 times larger than expected from a transition due to a single proton. According to Wahlborn, however, the two lowest states belong to the same configuration, and the $E2$ transition should therefore be due to a reorientation of spins within this configuration. Using the configuration suggested from the above-mentioned treatment Wahlborn calculated a half-life which deviates only 10% from the experimental value [4W57a]. This surprisingly good agreement may be fortuitous, especially when the fact is taken into account that the radial integral appearing in the matrix element was approximated by $3/(L+3)=\frac{3}{5}$, but, nevertheless, it seems to be a support for the level assignments.

If the radial wave functions were completely known the interaction between holes and particles would depend only on one parameter which is independent of the particle configuration. The success which no doubt was obtained in Pryce's pioneer work encouraged other investigators to make more detailed assumptions about the wave functions and the shape of the nucleon interaction. Recently True [2T57] reported that in the case of Pb^{206} (two neutron holes) a considerable improvement is obtained in the calculated values of level energies if harmonic oscillator wave functions are used to represent the neutron holes and the two-body forces are given by a singlet Gaussian potential. Independently Kearsly [5K57] also used oscillator wave functions, but the nucleon interaction was represented by a Yukawa potential. All observed levels below 2.9 MeV were predicted with correct assignment and with an energy accuracy better than 0.1 MeV for a certain value of the single adjustable parameter present. In both the latter two calculations configurational interaction was taken into account. Calculations of this type are of course much more tedious than the simple computations made by Pryce.

---

[1] Note added in proof: Preliminary results of atomic-beam resonance measurements by I. Lindgren, Physics Department, University of Uppsala, support the spin assignment 6.

The improvement of the theoretical calculations now seems to have reached a stage, where there is every reason to be critical and to refine the experimental information. Though extensive experimental work has already been performed for instance on the level schemes of Pb^{205} and Pb^{206}, more detailed experimental information is needed. The level assignments in Pb^{206} given by Alburger and Pryce [1A54] were obtained by combining theoretical and experimental information. A level assignment solely based on experiments requires tremendous work but is perhaps not impossible. Recently, for instance, Lindqvist [4L57] showed by angular correlation measurements that the three $5-$ levels in Pb^{206} had been given the correct spin assignment. Novakov and Hultberg [3N57a] have measured the photoelectron intensities of about 20 gamma-rays in Pb^{206} (resolution $\approx 0.5\,\%$). The relative gamma-ray intensities were obtained with a method developed by Hultberg [10H55]. By comparison of the gamma-ray and electron intensities it was possible to calculate the corresponding K conversion coefficients. All the resulting multipolarity assignments except those of three gamma-rays were found to fit the level scheme suggested by Alburger and Pryce. The 314 and 657 keV gamma-rays, however, both emitted from the 1998 keV $4+$ level, agree better with $E2$ than with the proposed multipolarities $M1$ and $M1$ $(+E2)$ respectively. Furthermore, the 754 keV gamma-ray going between the 3280 keV 5- and the doubtful 2526 keV levels must be ascribed to an $E1$ transition instead of $E2$ as suggested by the level scheme. It is too early to conclude if these deviations may significantly change the level scheme. In addition more satisfactory coincidence measurements are required for both Pb^{205} and Pb^{206}.

We have mentioned these recent investigations in order to emphasize the necessity of combining different kinds of measurements so that the level assignments as much as possible may be unambiguously based on experiments. Theorists should be very careful when comparing their calculations with experimental data, because in spite of the fact that an enormous lot of work has been performed by nuclear spectroscopists there exist in fact only a few level schemes where the given assignments have been checked in a satisfactory way.

It must also always be kept in mind that due to selection rules several levels may not be seen in beta-decay experiments. It is evident that high resolution measurements of particles emitted in nuclear reactions would be a useful complement to beta- and gamma-spectroscopy. The measurements by Harvey [9H53] have been mentioned (see 1.23 and 2.22). His results, though interesting, suffer from a poor resolution. Quite recently a group at the Indiana University [14M57] has analyzed the protons in Pb^{206} (d,p) reactions with a double focusing spectrometer and has found 8 proton groups corresponding to 7 excited states. The accuracy in energy differences was about 0.02 MeV. It is hoped that similar experiments in the future will contribute to a better knowledge of the level schemes discussed.

We finish this section by referring the reader to Fig. 8. Obviously most of the experimental and theoretical information is concentrated in the lower right part of the figure. This is due to the "position" of the stable isotopes of Tl, Pb and Bi, and to the fact that Pb^{207} is so far the only one-nucleon case which from the experimental point of view is satsifactorily known. Pryce's calculations are in addition depending on the knowledge of levels in the two-nucleon case. In calculations where the radial wave functions are explicitly given, however, one is only dependent on the knowledge of the one-nucleon cases. For this reason experimentalists are urgently suggested to investigate further especially the levels in Bi^{209} and Pb^{209}. In these two cases some information [3D57] is already available, though it is not so complete that one could suggest detailed calculations of levels in Bi^{212}, Bi^{211}, Bi^{210}, Pb^{212}, Po^{211}, Po^{210} and At^{211}. For these last nuclei a considerable number of excited states is known, but in many cases no level assignments at all have been given. It is, however, probably only a question of a few years' work before the levels of the several nuclei mentioned above are known to the same degree of accuracy as for example levels in Pb^{206}. In this way the central and right part of Fig. 8 would be experimentally well covered.

It does not seem hopeful to obtain more extensive experimental information on nuclei in the left part of Fig. 8. This is due to the fact that many of these nuclei have not yet been discovered. Because they are expected to be shortlived, beta-spectroscopical investigations will be difficult. Some information may be obtained from particle reactions, but in many cases the measurements would involve neutron energy determinations. For instance, the important one-nucleon case in this region is Tl^{207}, where only one excited state is known from alpha-decay of Bi^{211} [1C38]. Levels in Tl^{207} may be reached in Pb^{207} (n,p) reactions. We here meet with the difficulty of producing neutrons of well defined energies and of sufficiently large intensities to permit high resolution analysis of the protons.

3.2. *Level systematics*

3.21. *Introductory remarks*

In this section we discuss the systematics of levels which are supposed not to be of single-particle character. Somewhat arbitrarily we call these levels complex levels. Among these are obviously the levels in odd-odd and even-even nuclei. Some of the nuclei discussed here are situated quite far from Pb^{208} and will probably never be the subject of calculations of the type discussed in the preceding section. Nevertheless they are included because their properties emphasize those of nuclei more close to the double-magic number.

Another type of complex levels has already been discussed in connection with the missing $M4$ transition in Pb^{205}. The levels concerned arise in odd-even or even-odd nuclei when the nucleons deviating from Pb^{208} orientate their angular momenta in a general way. This gives rise to a much larger number of levels than suggested by the extreme single-particle shell model. The reader is referred to Pryce's paper on Pb^{205} [5P56] and to the discussion in section 2.24 of the present paper.

3.22. *First excited states in even-even nuclei*

The regular behaviour of the first excited states in even-even nuclei was first discussed by G. Scharff-Goldhaber [11S53] and by Preiswerk and Stähelin [7P53].

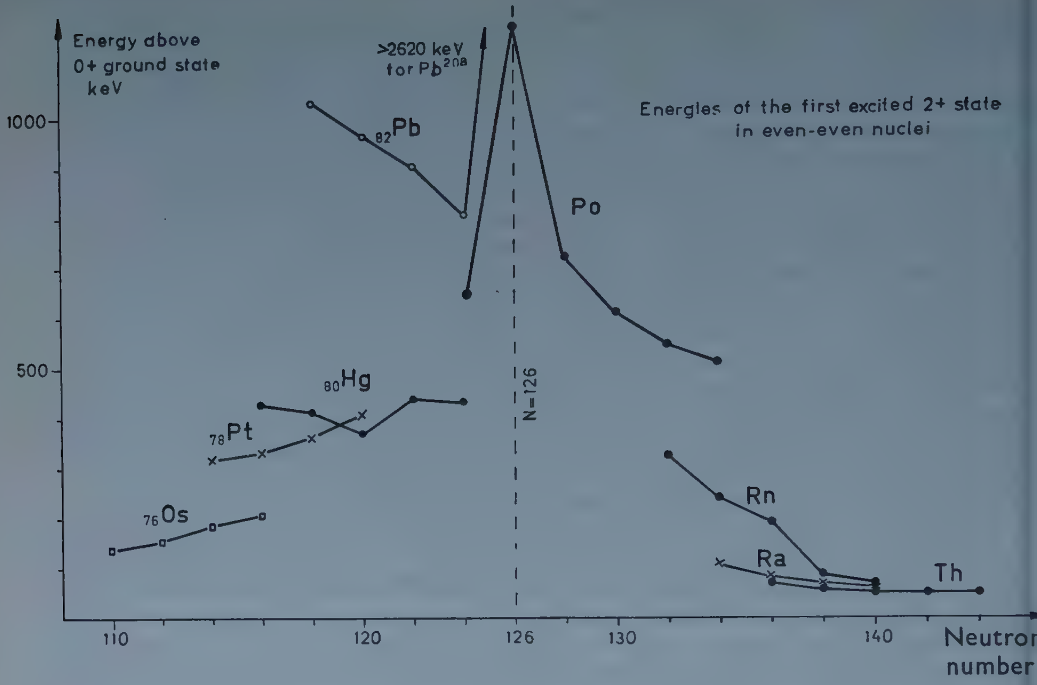

Fig. 9. The first excited state (2 +) in even-even nuclei as a function of neutron number. It may not be relevant from the point of view of the shell model to connect points representing different isotopes of a certain element, because the 2 + states may originate from different configurations.

It was found that the excitation energy is especially high at closed shells (magic numbers). In several works the points reperesenting the energies (versus A) have been approximated with a smooth function. As already Preiswerk and Stähelin pointed out, however, the atomic number is also a relevant parameter (see Figs. 9 and 10). This is especially evident in the Pb case. Previously insufficient information gave the impression that the energies of the first excited states in Pb isotopes increased drastically with A. Later it was shown, however, that the first excited state in Pb^{208} is not a 2+ state [1E54] and that the order of emission of the gamma-rays in Pb^{204} was another than was first believed [4K55, 2H56]. In addition there is also new information about the energies of the 2+ states in Pb^{202} [1M57] and Pb^{200} [1J57]. Thus, in the case of Pb isotopes it is now established that the energy of the first excited 2+ states decreases instead of increases towards $N = 126$. An exception is of course Pb^{208} where no 2+ state has been found as yet, but where it seems plausible to assume that the first excited 2+ state anyhow is larger than 2.62 MeV. In the case of lead it is observed that the change in excitation energy of the first 2+ state is very large when two neutrons are removed from the shell $N = 126$, while the changes for removing still more neutrons are rather small. (Qualitatively the same thing applies to protons.) Approximately the 2+ states for nuclei with the same neutron number have the same energies. The change in energy from ${}_{82}Pb$ to ${}_{80}Hg$ is much larger than from ${}_{80}Hg$ to ${}_{78}Pt$ etc.

From the point of view of the nuclear shell model it is of course not relevant to

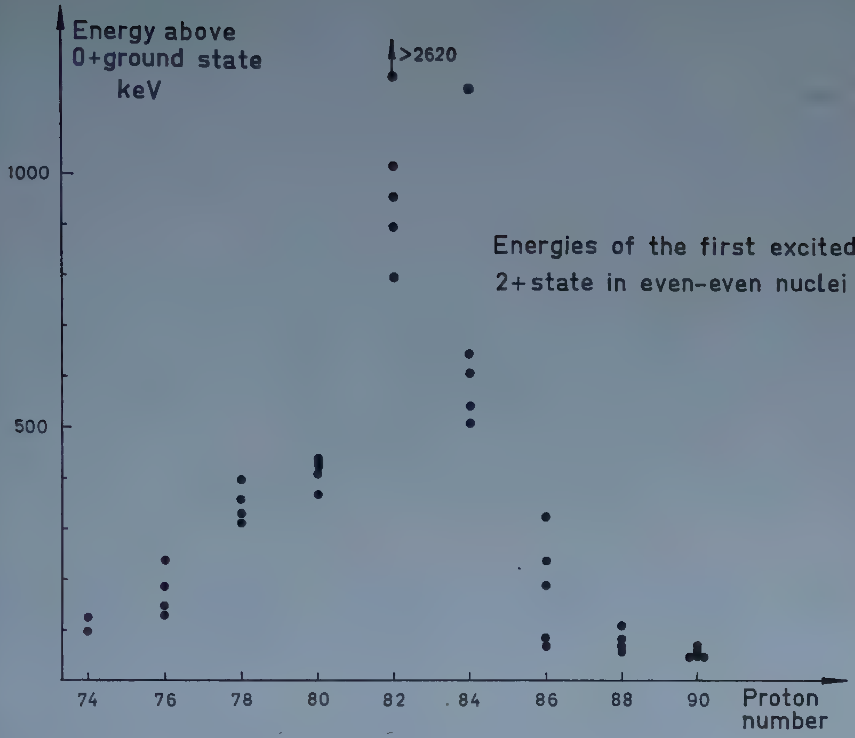

Fig. 10. The first excited state (2 +) in even-even nuclei as a function of proton number.

connect points representing the lowest 2 + states in isotopes of a certain element, since the 2 + states may originate from different configurations. Especially the extrapolation to an unknown point in Pb^{208}, which has no extra holes or particles, is of little interest.

3.23. *Excited states in even lead isotopes*

In Fig. 11 the experimentally known 2 +, 4 +, 5 −, 7 − and 9 − states have been plotted. T is the theoretical value of the position of the $(p_{1/2}{}^2 f_{5/2} i_{13/2})_{7-}$ level in Pb^{204} calculated by True [2T56] and P the value of the $(f_{5/2} i_{13/2})_{9-}$ in Pb^{206} calculated by Pryce [1A54]. The smooth behaviour of the first excited states in Pb has already been discussed. However, also the 4 + and 5 − states seem to behave very regularly. An interesting question is the appearance of isomeric transitions. Two $E3$ transitions have been observed in Pb^{206} and two pairs of $E5$ transitions in Pb^{202} and Pb^{204}, respectively. The pair of isomeric transitions in each nucleus is emitted from the same state. No isomeric transition at all has yet been observed in Pb^{200} and Pb^{198}. It also seemed puzzling that $E3$ transitions were observed from a 7 − state in Pb^{206}, while $E5$ transitions in Pb^{202} and Pb^{204} were emitted from 9 − states. This can be understood from the calculated values of the 7 − state in Pb^{204} (True) and the 9 − state in Pb^{206} included in Fig. 11. Connection of theoretical and experimental points indicates that the 7 − and 9 − levels cross in such a way that the metastability of the

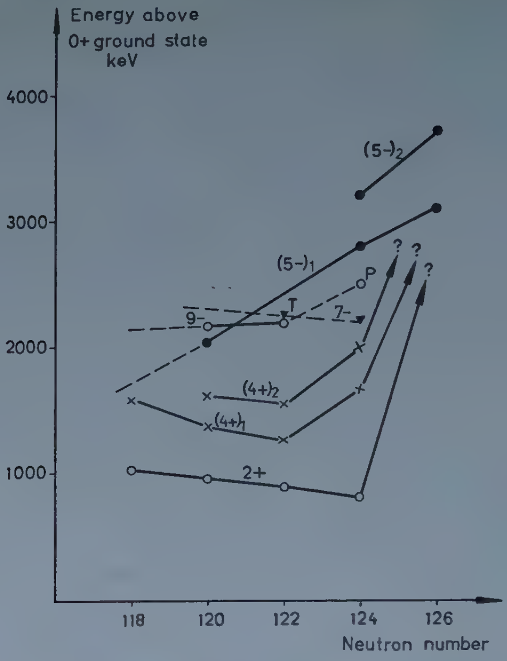

Fig. 11. Excited states in the lead isotopes. From the point of view of the shell model it may not be relevant to connect all the points representing the same assignment, because they may in some cases arise from different configurations.

9 − level is destroyed by the 7 − level in Pb^{206}. This 9 − level decays to two 4 + levels in both Pb^{204} and Pb^{202}. In addition the 9 − level in Pb^{202} also decays to a 5 − level which has crossed the 9 − level. Extrapolation of the $(5-)_1$ line indicates that in Pb^{200} the half-life of the 9 − state would be determined by a 400 keV $E4$ $(9- \rightarrow (5-)_1)$ gamma-ray. The gamma half-life of such a transition would be about 2×10^4 times less than for the 129 keV $E4$ transition in Pb^{202}. The trends of the levels in Pb thus suggest that the 9 − state in Pb^{200} should have a half-life of the order of a few minutes. This would explain why it has not been observed in Tl (p,xn) experiments [1J57]. By rapid milking of Pb from Bi^{200} it may be possible to follow the decay of the 9 − state as in the case of Pb^{204} [2H56]. Such an experiment may fail, however, because of the increasing probability of electron capture from the isomeric state towards lower mass numbers.

The extrapolations used are certainly questionable because the 9 − and 7 − states may arise from different configurations, but nevertheless agreement with the experiments is obtained.

3.24. *Levels in odd-odd nuclei*

Low-lying levels in odd-odd nuclei of Bi, Tl and Au should in several cases have predictable spins and parities. The 79 and 81 proton levels $(s_{1/2}, d_{3/2}, d_{5/2})$ for example have positive parity, while the parity is negative for low-lying states of the 125,

Table 5. Assignments of ground states in odd-odd isotopes of Tl and Au.

N Z	115	117	119	121	123	125
81		2 −[a]	2 −[b]	2 −[c]	2 −[d]	0 −[e]
79	2 − (1 −)[f]	2 −[g]	2 −[h]			

[a] Spin 7 of the isomeric state is measured with the atomic-beam resonance method [12B57]. Thus the ground state spin 2 is uniquely determined by the $M4$–$M1$ cascade from the isomeric state to the ground state [3A57c].

[b] Assignment 2 − suggested because of the three positron branches from the Tl^{200} ground state to the 0 + ground state and 2 + and 4 + excited states in Hg^{200} [2H57].

[c] 2 − suggested from the decay Pb ^{202m}–Tl^{202m} [1M57].

[d] Spin 2 measured with the atomic-beam resonance method [12B57]. Assignment 2 − consistent with the shape of the spectrum of beta particles emitted between the ground state of of Tl^{204} and the 0 + ground state of Pb^{204} [15M52].

[e] Assignment 0 − suggested from the beta-decay ($E_{\max} = 1510$ keV) between the ground state of Tl^{206} and that of Pb^{206} [6K54]. No beta transition has been observed to the 803 keV 2 + state in Pb^{206}.

[f] 2 − or 1 − is consistent with the decay of Au^{194} [3D57].

[g] 2 − suggested from the mode of decay of Au^{196} [9S49, 6S52].

[h] Spin 2 determined with the atomic-beam resonance method [8C56] and supported by studies of the angular distribution of circularly polarized gamma-rays [8B57a]. Negative parity suggested from the shape of beta spectra between the ground state of Au^{198} and the ground state and 2 + state of Hg^{198} [1E55].

123, 121 etc. neutrons ($p_{1/2}, p_{3/2}$ and $f_{5/2}$). For this reason the ground states of odd-odd nuclei should have negative parity. As can be seen from Table 5 there is no exception from this rule.

Posititve parity of low-lying excited states in Tl and Au can result from the

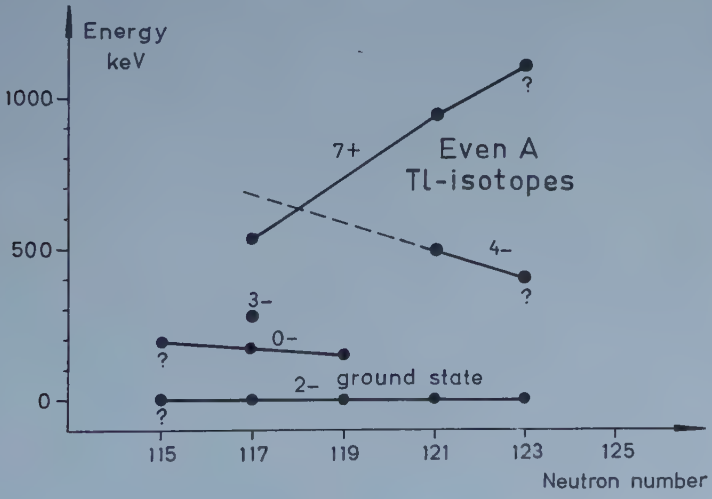

Fig. 12. Levels in the odd-odd isotopes of Tl as functions of neutron number.

Table 6. Comparison between the level spacings $i_{13/2}$–$f_{5/2}$ in odd Pb isotopes and $7+-2-$ in even Tl isotopes.

N	Level spacings, keV	
	$i_{13/2}$–$f_{5/2}$ Pb	$7+-2-$ Tl
117	424	543
121	825	820
123	980[a]	1116

[a] From extrapolation in Fig. 2.

coupling between an odd neutron of negative parity ($p_{1/2}$, $p_{3/2}$ or $f_{5/2}$) and a proton in an $11/2-$ state or between an odd proton in a positive parity state ($s_{1/2}$, $d_{3/2}$ or $d_{5/2}$) and a neutron in a $13/2+$ state. In this way high spin levels of positive parity may arise. The lowest levels of this kind are probably due to $(s_{1/2})_P(i_{13/2})_N$ or $(f_{5/2})_N$ $(h_{11/2})_P$ configurations. Suppose that the $7+$ states observed in Tl^{198}, Tl^{202} and Tl^{204} are due to the configuration $[(s_{1/2})_P(i_{13/2})_N]_{7+}$. The $2-$ ground states in Tl are most probably due to the configuration $[(s_{1/2})_P(f_{5/2})_N]_{2-}$. If this were the case, the level spacing $7+-2-$ should vary with energy in the same way as the $i_{13/2}$–$f_{5/2}$ spacing in the odd lead isotopes. This is admittedly very speculative especially since the $7+$ state in Tl^{204} is not satisfactorily ascertained. Nevertheless it can be seen from Fig. 12 that the level spacing $7+-2-$ increases with N as the $i_{13/2}$–$f_{5/2}$ spacing in the odd lead isotopes (Fig. 2). It should also be noted that the energy spacings are almost equal for the same number of neutrons, which supports the assumptions made as to the configurations (Table 6).

If our assumptions are correct the 117th neutron should be in an $f_{5/2}$ ground state. In ${}^{117}_{82}Pb^{199}$, in fact, the ground state has been given the assignment $5/2-$ [5S56, 3A57], which at first seemed puzzling because it would mean an irregular filling of the $f_{5/2}$ shell (see 2.2). It is possible that the $3-$ level at 282 keV observed in Tl^{198} [2B53] is due to the configuration $[(s_{1/2})_P(f_{5/2})_N]_{3-}$. If this were the case the $M4$ transition between the $7+$ and $3-$ states should be of the $i_{13/2} \rightarrow f_{5/2}$ type and therefore the matrix element of this transition should fit into the systematics. As can be seen from Fig. 18 (p. 461) this is indeed the case, which is another fact supporting the assumptions about the configurations made above.

3.25. *"Anomalous" levels in Hg^{199} and Hg^{201}*

We have repeatedly mentioned the possibility of destruction of metastable states because of the presence of complex levels. The coupling between possible spins of the excited states of the even-even core and the spin of an odd particle is of considerable interest. In Hg^{198} and Hg^{200} the first excited $2+$ states have energies 412 and 368 keV respectively. In Hg^{199} the low-lying levels identified with shell model predictions are $p_{1/2}$ (0), $p_{3/2}$ (158) and $f_{5/2}$ (208). However, at 491 and 455 keV there are levels of the assignments $1/2-$ and $1/2-$ or $3/2-$, respectively [2B53]. These levels should not be single-particle levels. It seems plausible to assume that they arise from the coupling between the 412 keV $2+$ state of the core of Hg^{198} and single-particle states. This possibility seems so interesting that it could be worth while making more detailed measurements on the decay of Tl^{199} than have been made so far. For the same reason further investigations of the levels in Hg^{197} seem desirable. The number of low energy gamma-rays emitted in the decay of Tl^{197} indicates that a similar state of affairs may exist also in this case.

The decay of Tl^{201} seems to be quite a puzzle. 4 $M1$ gamma-rays of energies 31, 32, 135 and 167 keV have been observed [4B55]. The 32 and 135 keV gamma-rays are probably emitted in cascade from the same level as the 167 keV gamma-ray. With present coincidence information it seems impossible to fit in the 31 keV gamma-ray without making the extreme assumption that there exists a state only about 1 keV above the ground state. Even if more refined coincidence measurements would revise this level scheme, the fact remains that with the 4 $M1$ gamma-rays it is impossible to construct a sequence of levels including only the single-particle levels $p_{3/2}$, $p_{1/2}$ and $f_{5/2}$. At least another $1/2-$, $3/2-$, or $5/2-$ level is required. It is possible that this additional level is of the same origin as the "anomalous" levels in Hg^{199}.

4. Multipole transitions

4.1. *Distribution of transitions from metastable states*

In their survey article on nuclear isomerism of 1955, Goldhaber and Sunyar [3G55] were able to record the comparative lifetimes of about 30 transitions in the Z-region 77–83. It is characteristic of the rapid development in this field that at present, two years later, the number of known cases has redoubled as evident from Table 7.

Only transitions originating in levels of definitely stated lifetime are included in this table. There are, however, additional transitions for which an upper limit to the decay rate has been determined and still others which from the proposed level schemes and multipole systematics can be judged to have a measurable half-life. Even such cases have been considered in Table 8, where some further data on transitions from metastable states are given in order of atomic number and mass number.

We have attempted to list in these tables the most accurate values of gamma-ray energy and level half-life available. This necessarily means a quite subjective choice and may in some cases exclude references of considerable interest. As a rule, however,

Table 7. Distribution of multipole transitions from states with measured half-life.

Z	Multipolarity								Total
	$E1$	$E2$	$E3$	$E4$	$E5$	$M1$	$M4$	$E2+M1$	
83		1							1
82	1	4	2	1	4		5		17
81		2	4			1	1	2	10
80		5					4	1	10
79			3				3	1	7
78		4					3		7
77		3	2				1	3	9
Total	1	19	11	1	4	1	17	7	61

Table 8. Multipole transitions from states with measurable half-life.

Z	A	Multi-pole	E_γ keV	Ref.	$T_{1/2}$	Ref.	Remarks
83	210	$M1$	46.503	6F57			$T_{1/2}$ measurable?
	206	$E2$	59.93	4A57	7.8 μs	4A57a	
82	209	$E1$	120	1S56	3.1×10^{-9} s	1S56	
	208	$M1+$ $+E2$	510.85	1L52	$< 10^{-10}$ s	1E54	
		$E2$	583	1E54	2.4×10^{-10} s	1E54	
		$E3$	2614.25	1L52a	$< 10^{-10}$ s	1E54	
	207	$E2$	569	1A55	0.9×10^{-10} s	1G56	
					1.0×10^{-10} s	2S55	Coulomb excitation
		$M4$	1063.9	1A53	0.799 s	1B55	
	206	$E3$	202.5	1A54	123 μs	1T57	
		$E3$	516.1	1A54	123 μs	1T57	
		$E2$	803.3	1A54	7.70×10^{-12} s	2S55	Coulomb excitation
	205						Expected $M4$ not observed [3S56, 1H56], cf. section 2.24
	204	$E2$	374.7	2H56	2.6×10^{-7} s	4S55	
		$E5$	622.2	2H56	67.5 min	2H56	
		$E2$	899.3	2H56	$< 6 \times 10^{-10}$ s	4S55	
		$E5$	911.7	2H56	67.5 min	2H56	
	203	$M4$	825.2	5S56	6.09 s	2A57	
	202	$E4$	129.3	1M57	3.62 h	2A57	
		$E2$	422.1	1M57	$< 10^{-9}$ s	3W56	
		$E5$	547.2	1M57	3.62 h	2A57	
		$E5$	787.2	1M57	3.62 h	2A57	
	201	$M4$	629	5S56	61 s	5S56	
	200	$E2$	462	1J57			$T_{1/2}$ measurable? Possible $E4$ [2B55] not observed with $T_{1/2} > 1$ h [4B55]
	199	$M4$	424.1	3A57	12.2 min	3A57	
	198						Possible $E4$ [2B55] has $T_{1/2} \leqslant 25$ min [3A55]
	197	$M4$	234.0	3A57	42 min	3A57	
	195	$M4$?	—	—	17 min	3A57	Only E.C. branch from high spin level observed
81	208	$M1$	40	3H56	$< 7 \times 10^{-11}$ s	4G53	1.0×10^{-12} s [19B56] probably too low [19B57]
	207	$E2+$ $+M1$	350.1	1C38	$\leq 3 \times 10^{-7}$ s	3F52	
	205	$E2+$ $+M1$	205	3B55	2.48×10^{-10} s	2S55	Coulomb excitation
					4.4×10^{-9} s	3B55	$T_{1/2}$ (γ, $E2$) from Coulomb excitation
	204	$E3$	706	1V56	65 μs	1V56	Assignment according to 1M57
	203	$E2+$ $+M1$	279.17	1W56	1.2×10^{-10} s	2W56	
					3.25×10^{-10} s	2S55	Coulomb excitation
		$E2$	679	1W54	1.12×10^{-12} s	2S55	Coulomb excitation

Table 8 *(continued)*

Z	A	Multipole	E_γ keV	Ref.	$T_{1/2}$	Ref.	Remarks
81	202	$E3$	459.8	1M57	475 μs	1T57a	
	201	$E2+$ $+M1$	330.3	4B55			$T_{1/2}$ measurable? (l-forbidden $M1$ transition)
	200	$E2$	148.0	4B55	8.0×10^{-9} s	2A57a	
	199	$E2+$ $+M1$	367.0	3A57			$T_{1/2}$ measurable? (l-forbidden $M1$ transition)
	198	$E2$	173.4	3A57			$T_{1/2}$ may be measurable
		$M4$	260.7	2B53	1.75 h	2M54	
	197	$E3$	222.45	3A57a	0.55 s	3A57a	
	196	$E2$	191	3A57b			$T_{1/2}$ may be measurable
	195	$E3$	99.1	3A57a	3.5 s	3A57a	
80	204	$E2$	430	3B56a			$T_{1/2}$ may be measurable
	203						Expected $M4$ not observed. Cf. section 2.24
	202	$E2$	439.1	2B53	2.4×10^{-11} s	3M55	Resonance fluorescence
					3.0×10^{-11} s	3B56	$T_{1/2}$ $(\gamma, E2)$ from Coulomb excitation
	201						Cf. $A=203$
	200	$E2$	367.8	2B53	4.7×10^{-11} s	3B56	$T_{1/2}$ $(\gamma, E2)$ from Coulomb excitation
	199	$E2$	158.4	2B53	2.35×10^{-9} s	5B52	
					5.3×10^{-9} s	3B56	$T_{1/2}$ $(\gamma, E2)$ from Coulomb excitation
		$E2+$ $+M1$	208.5	5H50	2.1×10^{-10} s	3M54	Resonance fluorescence
					2.4×10^{-9} s	3B56	$T_{1/2}$ $(\gamma, E2)$ from Coulomb excitation
		$M4$	368	4H49	44.4 min	4M48	
	198	$E2$	47.7	3A57c			$T_{1/2}$: no evidence 5×10^{-9} s–5×10^{-8} s [2A57a]; no evidence 5×10^{-8}–10^{-4} s [3A57d]
		$E2$	411.77	5M52	2.1×10^{-11} s	3B56	$T_{1/2}$ $(\gamma, E2)$ from Coulomb excitation
					2.18×10^{-11} s	3M54a	Resonance fluorescence
	197	$E2$	134.0	6M53	0.8×10^{-8} s	1D50	
		$M4$	165.3	6M53	23 h	6H51	
	196	$E2$	426	6S52			$T_{1/2}$ may be measurable
	195	$M1$	37.1	2J55			$T_{1/2}$ measurable? (l-forbidden $M1$ transition)
		$M4$	122.7	2J55	40 h	2J55	
	193	$M1$	39.2	2G54			$T_{1/2}$ measurable? (l-forbidden $M1$ transition)
		$M4$	101.2	2G54	12 h	2G54	

Table 8 *(continued)*

Z	A	Multipole	E_γ keV	Ref.	$T_{1/2}$	Ref.	Remarks
79	197	$E2+$ $+M1$	77.4	6M53	1.9×10^{-9} s	4S55	
		$E3$	130.2	6M53	7.23 s	2F55	
		$M4$	409.5	6M53	7.23 s	2F55	
	195	$E3$	56.9	2J55	30.6 s	2F55	
		$E2+$ $+M1$	61.4	2J55			$T_{1/2}$ may be measurable
		$M4$	318.4	2J55	30.6 s	2F55	
	193	$E3$	31.9	2G54	3.88 s	2F55	
		$E2+$ $+M1$	37.9	2G54			$T_{1/2}$ may be measurable
		$M4$	289.8	2G54	3.88 s	2F55	
78	199						Expected ≈ 1 min $M4$ not observed after Pt + d [2A57]
	198	$E2$	403	2S55	1.88×10^{-11} s	2S55	Coulomb excitation
	197	$M4$	337	4H49	78 min	4H49	
	196	$E2$	354	6S52	3.49×10^{-11} s	2S55	Coulomb excitation
	195	$M4$	129.9	2C54	3.45 d	4H49	
		$E2$	130.2	2C54	4.2×10^{-9} s		$T_{1/2}$ calculated from 6B55, Coulomb excitation
		$E2$	240	6B55			$T_{1/2}$ may be measurable
	194	$E2$	329.07	2R55	3.85×10^{-11} s	2S55	Coulomb excitation
	193	$M4$	135.5	2C54	3.35 d	2C54	
	192	$E2$	295.94	7B55			$T_{1/2}$ may be measurable
		$E2$	316.46				$T_{1/2}$ may be measurable. Another 5–6 strong $E2$ transitions [7B55]
77	193	$E2$	73.1	2C53	6.0×10^{-9} s	2W54	
		$M4$	80.19	8B57	11.9 d	8B57	
		$E2+$ $+M1$	143	2D56	2.8×10^{-9} s	2D56	$T_{1/2}$ $(\gamma, E2)$ from Coulomb excitation
		$E2$	368	2D56	5.2×10^{-11} s	2D56	$T_{1/2}$ $(\gamma, E2)$ from Coulomb excitation
	192	$E3$	58.0	7M54	1.42 min	4H49	
	191	$E3$	41.7	8S52	4.91 s	2F55	
		$E2+$ $+M1$	82.3	4S55	3.85×10^{-9} s	4S55	
		$E2+$ $+M1$	129.6	3D57	4.0×10^{-9} s	2D56	$T_{1/2}$ $(\gamma, E2)$ from Coulomb excitation
		$E2$	356	2D56	2.5×10^{-11} s	2D56	$T_{1/2}$ $(\gamma, E2)$ from Coulomb excitation

the papers referred to are of recent date and give further references to previous work. When a half-life has been measured by different methods, representative results of each method are given. If no remark is made it is understood that the decay rate was directly measured (cf. 1.24).

4.2. *Transition probabilities*

4.21. *Treatment of data*

The great number of newly discovered isomers in nuclei of $Z = 77$–83 forms a good reason for reexamining the systematics of gamma-ray transition probabilities in this region of the periodic table. In addition, improved measurements on earlier known transitions have been reported in several cases. To some extent the comparison between experimental and theoretical transition probabilities may also be influenced by the recent development in the field of internal conversion coefficients (see 4.3).

If we denote by G the fraction of all decays from the level of observed lifetime τ that goes via the multipole transition of interest (that is, G includes internal conversion as well as radiative decay), the experimental gamma-ray transition probability is given by

$$P_{\exp} = \frac{G}{\tau(1+\alpha)}, \tag{3}$$

where α is the total internal conversion coefficient of the transition.

Accurate measurements of conversion coefficients are relatively rare. Throughout this work we have therefore chosen to calculate α from theoretical values of the partial coefficients α_K etc. For reasons that will be made clear in the next section the most reliable computations available at present are those of Sliv and Band [13S56] for α_K and those of Rose *et al.* [3R54] as far as the ratios between K and L coefficients are concerned. Thus we write

$$\alpha = \alpha_K + \alpha_L + \alpha_M + \cdots = \alpha_K \left(1 + \frac{\alpha_L}{\alpha_K} + \frac{\alpha_{M+N+\cdots}}{\alpha_K}\right) = \alpha_K \left(1 + \frac{1.3\,\alpha_L}{\alpha_K}\right), \tag{4}$$

where the last stage is a result of the empirical "thumb rule" approximation $\alpha_{M+N+\cdots} = 0.3\ \alpha_L$. This approximation may certainly lead to significant errors when α_K is small relative to α_L. In particular this is so at transition energies below the K electron binding energy, where the absolute L conversion coefficients of Rose *et al.* [3R54] have to be used in calculating α. (It may be remarked that Rose *et al.* have calculated M conversion coefficients, but these can be used only for comparisons between the various subshells because the effect of screening was not included.)

Besides appearing in the denominator of Eq. (3), the conversion coefficients may enter into the experimental transition probabilities through the factor G. If, for instance, a level is de-excited by an electron capture branch in addition to the multipole transition, G can be determined by measuring in an electron spectrometer the intensity of the K conversion line of the latter relative to that of a multipole transition following the electron capture decay. Denoting these intensities I_K and I'_K, respectively, we have

$$I_{L+M+N+\cdots} = I_K \frac{\alpha_{L+M+N+\cdots}}{\alpha_K}; \qquad I_\gamma = \frac{I_K}{\alpha_K} \text{ etc.} \tag{5}$$

and
$$G = \frac{I_K\left(1+\dfrac{\alpha_{L+M+N+\cdots}}{\alpha_K}+\dfrac{1}{\alpha_K}\right)}{I_K\left(1+\dfrac{\alpha_{L+M+N+\cdots}}{\alpha_K}+\dfrac{1}{\alpha_K}\right)+I'_K\left(1+\dfrac{\alpha'_{L+M+N\cdots}}{\alpha'_K}+\dfrac{1}{\alpha'_K}\right)}$$

$$= \frac{I_K\dfrac{1+\alpha}{\alpha_K}}{I_K\dfrac{1+\alpha}{\alpha_K}+I'_K\dfrac{1+\alpha'}{\alpha'_K}} \tag{6}$$

where the conversion coefficients are calculated according to the preceding paragraph. Similar discussions apply to other types of branching.

From a quantum theoretical treatment of multipole radiation the gamma-ray transition probabilities are obtained as functions of multipole order L, energy E_γ, nuclear radius a, a statistical factor S and the nuclear matrix element $\mathfrak{M}_{EL}$ or $\mathfrak{M}_{ML}$, referring to electric and magnetic $2L$ pole radiation respectively. The matrix elements contain the dependence of the transition probabilities on specific nuclear properties, which in general are unknown. Under certain simplifying assumptions, however, matrix elements can be evaluated for different nuclear models.

As pointed out already in the introduction, nuclei near the double shell closure $Z=82$, $N=126$ may be expected to show characteristics especially suited for a single-particle shell model treatment. In terms of this model Moszkowski [11M55] gives the gamma-ray transition probabilities as

$$P(E,L) = C(E,L) \times A^{2L/3} \times E_\gamma^{2L+1} \times S, \tag{7 a}$$

$$P(M,L) = C(M,L) \times A^{2(L-1)/3} \times E_\gamma^{2L+1} \times S. \tag{7 b}$$

The constants take on different values for single proton transitions and single neutron transitions. We have chosen to compare the experimental probabilities for $E2$, $E3$, $E4$, and $E5$ transitions with the single proton estimates and those for $M4$ transitions, most frequently occurring in odd neutron nuclei, with the corresponding single neutron values. In all cases we put the statistical factor equal to 1 (from which it deviates by less than a factor 2 in the actual cases where tabulated values are available). The mass number factors in Eq. (7) arise from the introduction of the nuclear radius as $a = a_0 \times A^{1/3}$. Thus the constants contain a_0 to the powers $2L$ for electric and $2(L-1)$ for magnetic transitions. Moszkowski used $a_0 = 1.45 \times 10^{-13}$ cm. We have recalculated the constants with $a_0 = 1.2 \times 10^{-13}$ cm.

As a measure of the agreement between single-particle theory and experiment we define a deviation factor

$$F = P_{\text{exp}}/P_{\text{theor}}. \tag{8}$$

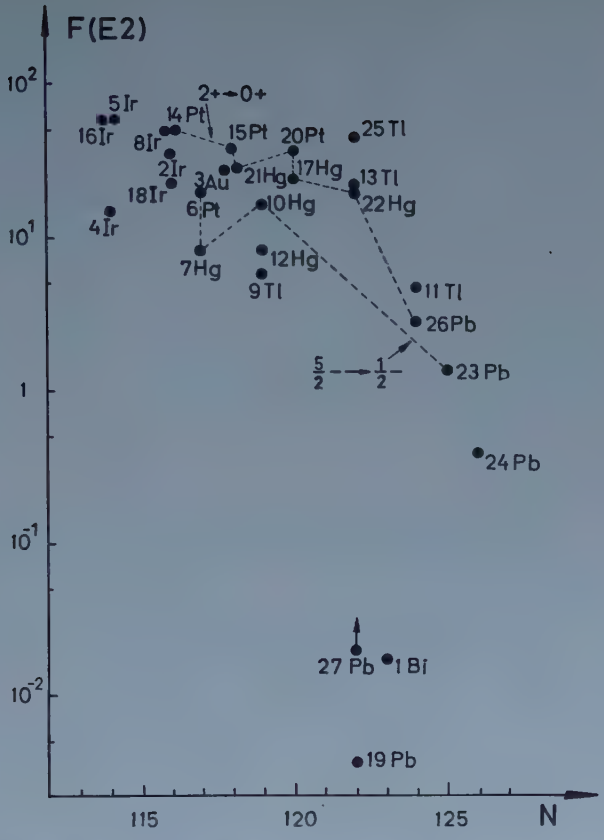

Fig. 13. The deviation factor F of $E2$ transitions as a function of neutron number. The numbering of the points refers to Table 9.

Thus F may be said to represent the departure of the experimental matrix elements from those obtained by the single-particle estimates (including, however, also the influence of the statistical factors).

The relevant data on transition probabilities are collected in Tables 9–12. Note especially that we have here listed the experimental lifetimes of the levels in contrast to Table 8 where the half-lives were given.

A few general remarks concerning the uncertainty of the deviation factors F will be made. From Eqs. (7) and (8) an error in the transition energy is seen to appear magnified to the power $2L+1$ in F. Nevertheless it is found that in almost all the cases where error limits are given for both E_γ and τ, $(2L+1)dE_\gamma/E_\gamma$ is smaller than $d\tau/\tau$. This fact can hardly be explained as due to a more conservative treatment of the lifetime data. (On the contrary it is felt that the possibility of considerable systematic errors is often disregarded in this connection; cf. 1.24.) It should rather be considered significant for the difficulties inherent in these measurements. For reasons discussed above an insufficient knowledge of conversion coefficients may give rise to non-negligible errors in F, especially at low energies, where $\alpha \gg 1$ for the multi-

Table 9. Gamma-transition probabilities for $E2$ transitions.

No.	Nucleus	E_γ MeV	Ref.	$\tau(E2)_{\mathrm{exp}}$ sec	Ref.	α_{total}	P_{exp} sec^{-1}	P_{theor} sec^{-1}	F	Adopted spin change	Remarks
1	$_{83}\mathrm{Bi}_{123}^{206}$	0.05993 ± 0.00006	4A57	$(1.13 \pm 0.04) \times 10^{-5}$	4A57a	74.57	1.17×10^{3}	7.05×10^{4}	$(1.66 \pm 0.08) \times 10^{-2}$	$4+ \to 6+$?	
2	$_{77}\mathrm{Ir}_{116}^{193}$	0.0731	2C53	$(8.7 \pm 0.6) \times 10^{-9}$	2W54	17.18	6.3×10^{6}	1.75×10^{5}	36	$(\frac{1}{2}+) \to \frac{3}{2}+$	
3	$_{79}\mathrm{Au}_{118}^{197}$	0.0774	6M53	1.5×10^{-7}	4S55	[a]	6.7×10^{6}	2.39×10^{5}	28	$\frac{1}{2}+ \to \frac{3}{2}+$	[a] $E2+M1$; $\tau(\gamma, E2)$ according to 4S55
4	$_{77}\mathrm{Ir}_{114}^{191}$	0.0823	4S55	2.1×10^{-7}	4S55	[b]	4.8×10^{6}	3.11×10^{5}	15	$(\frac{1}{2}+) \to \frac{3}{2}+$	[b] $E2+M1$; $\tau(\gamma, E2)$ according to 4S55
5	$_{77}\mathrm{Ir}_{114}^{191}$	0.1296	3D57	5.7×10^{-9}	2D56	[c]	1.8×10^{8}	3.02×10^{6}	60	$\frac{5}{2}+ \to \frac{3}{2}+$	[c] $E2+M1$; $\tau(\gamma, E2)$ from Coulomb excitation
6	$_{78}\mathrm{Pt}_{117}^{195}$	0.1302	2C54	1.6×10^{-8}	6B55	[d]	6.3×10^{7}	3.17×10^{6}	20	$\frac{5}{2}- \to \frac{1}{2}-$	[d] $\tau(\gamma, E2)$ from Coulomb excitation
7	$_{80}\mathrm{Hg}_{117}^{197}$	0.1340	6M53	$(1.2 \pm 0.1) \times 10^{-8}$	1D50	1.72	3.1×10^{7}	3.71×10^{6}	8.4	$\frac{5}{2}- \to \frac{1}{2}-$	
8	$_{77}\mathrm{Ir}_{116}^{193}$	0.143 ± 0.004	2D56	4.0×10^{-9}	2D56	[e]	2.5×10^{8}	5.00×10^{6}	50	$(\frac{5}{2}+) \to \frac{3}{2}+$	[e] $E2+M1$; $\tau(\gamma, E2)$ from Coulomb excitation
9	$_{81}\mathrm{Tl}_{119}^{200}$	0.1480 ± 0.0003	4B55	$(1.2 \pm 0.3) \times 10^{-8}$	2A57a	1.23	3.7×10^{7}	6.23×10^{6}	5.9 ± 1.5	$0- \to 2-$	
10	$_{80}\mathrm{Hg}_{119}^{199}$	0.1584 ± 0.0003	2B53 5H50	$(3.4 \pm 0.3) \times 10^{-9}$ [f]	5B52	0.91	1.5×10^{8}	8.69×10^{6}	17 ± 1.5	$\frac{5}{2}- \to \frac{1}{2}-$	[f] $\tau(\gamma, E2) = 7.7 \times 10^{-9}$ s from Coulomb excitation [3B56, cf. 2D56]
11	$_{81}\mathrm{Tl}_{124}^{205}$	0.205 ± 0.004	3B55	6.3×10^{-9}	3B55	[g]	1.6×10^{8}	3.28×10^{7}	4.9	$\frac{3}{2}+ \to \frac{1}{2}+$	[g] $E2+M1$; $\tau(\gamma, E2)$ from Coulomb excitation
12	$_{80}\mathrm{Hg}_{119}^{199}$	0.2085 ± 0.0003	5H50	3.5×10^{-9}	3B56	[h]	2.9×10^{8}	3.43×10^{7}	8.5	$\frac{3}{2}- \to \frac{1}{2}-$	[h] $E2+M1$; $\tau(\gamma, E2)$ from Coulomb excitation. [Cf. 3M54]
13	$_{81}\mathrm{Tl}_{122}^{203}$	0.27917 ± 0.00005	1W56	2.5×10^{-10}	2W56	0.14	3.5×10^{9}	1.52×10^{8}	23	$\frac{3}{2}+ \to \frac{1}{2}+$	$E2+M1$; $E2/M1 = 2.25 \pm 0.25$ [10M56] used in the

											citation
15	$_{78}Pt^{196}_{118}$	0.354	6S52	5.04×10^{-11}	2S55	0.062	1.87×10^{10}	4.75×10^{8}	39	$2+ \to 0+$	$\tau(E2)$ from Coulomb excitation
16	$_{77}Ir^{191}_{114}$	0.356	2D56	3.6×10^{-11}	2D56	[i]	2.8×10^{10}	4.72×10^{8}	59	$(\frac{7}{2}+) \to \frac{3}{2}+$	[i] $\tau(\gamma, E2)$ from Coulomb excitation
17	$_{80}Hg^{200}_{120}$	0.3678 ± 0.0004	2B53	6.8×10^{-11}	3B56	[j]	1.5×10^{10}	5.90×10^{8}	25	$2+ \to 0+$	[j] $\tau(\gamma, E2)$ from Coulomb excitation
18	$_{77}Ir^{193}_{116}$	0.368 ± 0.008	2D56	7.5×10^{-11}	2D56	[k]	1.3×10^{10}	5.65×10^{8}	23	$(\frac{7}{2}+) \to \frac{3}{2}+$	[k] $\tau(\gamma, E2)$ from Coulomb excitation
19	$_{82}Pb^{204}_{122}$	0.3747 ± 0.0004	2H56	4.0×10^{-7}	4S55	[l]	2.5×10^{6}	6.65×10^{8}	3.7×10^{-3}	$4+ \to 2+$	[l] $\tau(\gamma, E2)$ according to 4S55
20	$_{78}Pt^{198}_{120}$	0.403	2S55	2.71×10^{-11}	2S55	0.044	3.53×10^{10}	9.20×10^{8}	38	$2+ \to 0+$	$\tau(E2)$ from Coulomb excitation
21	$_{80}Hg^{198}_{118}$	$0.411770 \pm$ ± 0.000036	5M52	$(3.3 \pm 0.3) \times 10^{-11}$	3M54a	[m]	3.0×10^{10}	1.02×10^{9}	29 ± 2.6	$2+ \to 0+$	[m] $\tau(\gamma, E2)$ from resonance fluorescence
22	$_{80}Hg^{202}_{122}$	0.4391 ± 0.0004	2B53	$(3.5 \pm 0.7) \times 10^{-11}$	3M55	[n]	2.9×10^{10}	1.45×10^{9}	20 ± 4	$2+ \to 0+$	[n] $\tau(\gamma, E2)$ from resonance fluorescence
23	$_{82}Pb^{207}_{125}$	0.569	1A55	$(1.3 \pm 0.4) \times 10^{-10}$	1G56	0.022	7.5×10^{9}	5.48×10^{9}	1.4	$\frac{5}{2}- \to \frac{1}{2}-$	
24	$_{82}Pb^{208}_{126}$	0.583	1E54	$(3.5 \pm 1.0) \times 10^{-10}$	1E54	0.021	2.8×10^{9}	6.23×10^{9}	0.4	$5- \to 3-$	
25	$_{81}Tl^{203}_{122}$	0.679 ± 0.002	1W54	1.62×10^{-12}	2S55	0.014	6.09×10^{11}	1.29×10^{10}	47	$\frac{5}{2}+ \to \frac{1}{2}+$	$\tau(E2)$ from Coulomb excitation
26	$_{82}Pb^{206}_{124}$	0.8033 ± 0.0004	1A54	1.11×10^{-11}	2S55	0.010	8.92×10^{10}	3.05×10^{10}	2.9	$2+ \to 0+$	$\tau(E2)$ from Coulomb excitation
27	$_{82}Pb^{204}_{122}$	0.8993 ± 0.0003	2H56	$\leq 10^{-9}$	4S55	[o]	$\geq 10^{9}$	5.30×10^{10}	$\geq 2 \times 10^{-2}$	$2+ \to 0+$	[o] $\tau(\gamma, E2)$ according to 4S55

Table 10. Gamma-transition probabilities for $E3$ transitions.

No.	Nucleus	E_γ MeV	Ref.	τ_{exp} sec	Ref.	G %	Ref.	α_{total}	P_{exp} sec^{-1}	P_{theor} sec^{-1}	F	Adopted spin change
1	$_{79}Au^{193}_{114}$	0.0319 (±0.0003)	2G54	5.60 ± 0.36	2F55	96.6	[a]	96370	1.79×10^{-6}	4.41×10^{-5}	4.06×10^{-2}	$\frac{11}{2}- \to \frac{5}{2}+$
2	$_{77}Ir^{191}_{114}$	0.0417	8S52	7.09 ± 0.20	2F55	100 ?		17527	8.05×10^{-6}	2.82×10^{-4}	2.85×10^{-2}	$\frac{11}{2}- \to \frac{5}{2}+$
3	$_{79}Au^{195}_{116}$	0.0569	2J55	$(4.42 \pm 0.03) \times 10$	2F55	99.3	[b]	3317	6.77×10^{-6}	2.59×10^{-3}	2.61×10^{-3}	$\frac{11}{2}- \to \frac{5}{2}+$
4	$_{77}Ir^{192}_{115}$	0.0580 ± 0.0004	7M54	$(1.23 \pm 0.06) \times 10^2$	4H49	100 ?		2342	3.47×10^{-6}	2.87×10^{-3}	$(1.21 \pm 0.09) \times 10^{-3}$	?
5	$_{81}Tl^{195}_{114}$	0.0991 ± 0.0001	3A57a	5.0 ± 0.5	3A57a	100	3A57a	154.5	1.3×10^{-3}	1.26×10^{-1}	$(1.0 \pm 0.1) \times 10^{-2}$	$\frac{11}{2}- \to \frac{5}{2}+$
6	$_{79}Au^{197}_{118}$	0.1302	6M53	1.07×10	4F47	≈99	5C57	29.75	3.0×10^{-3}	8.69×10^{-1}	3.5×10^{-3}	$\frac{11}{2}- \to \frac{5}{2}+$
7	$_{82}Pb^{206}_{124}$	0.2025 ± 0.0003	1A54	$(1.77 \pm 0.06) \times 10^{-4}$	1T57	0.39	[c]	3.861	4.53	2.09×10	2.17×10^{-1}	$7- \to (4+)_2$
8	$_{81}Tl^{197}_{116}$	0.22245 ± 0.00005	3A57a	$(7.9 \pm 1.4) \times 10^{-1}$	3A57a	100 [d]	3A57a	2.261	3.9×10^{-1}	3.69×10	$(1.1 \pm 0.2) \times 10^{-2}$	$\frac{11}{2}- \to \frac{5}{2}+$
9	$_{81}Tl^{202}_{121}$	0.4598 ± 0.0002	1M57	$(6.85 \pm 0.29) \times 10^{-4}$	1T57a	100	1M57	0.124	1.30×10^3	6.26×10^3	$(2.08 \pm 0.08) \times 10^{-1}$	$7+ \to 4-$
10	$_{82}Pb^{206}_{124}$	0.5161 ± 0.0003	1A54	$(1.77 \pm 0.06) \times 10^{-4}$	1T57	99.61	[e]	0.092	5.15×10^3	1.46×10^4	$(3.53 \pm 0.12) \times 10^{-1}$	$7- \to (4+)_1$
11	$_{81}Tl^{204}_{123}$	0.706 ± 0.020 [f]	1V56	$(9.4 \pm 0.7) \times 10^{-5}$ [f]	1V56	100	1M57	0.036	1.0×10^4	1.28×10^5	$(7.9 \pm 1.6) \times 10^{-2}$	$7+ \to 4-$
12	$_{82}Pb^{208}_{126}$	2.61425 ± 0.00050	1L52a	$< 1.04 \times 10^{-10}$	1E54	100	1E54	negl.	$> 7.1 \times 10^9$	1.28×10^9	> 5.5	$3- \to 0+$

[a] Branching calc. from 2G54. [b] Branching calc. from 2J55. [c] Branching calc. from 1A54. [d] Weak indications of $M4$ branch. [e] Branching calc. from 1A54. [f] Assignment according to 1M57.

Table 11. Gamma-transition probabilities for $E4$ and $E5$ transitions.

Nucleus	E_γ MeV	Ref.	τ_{exp} sec	Ref.	G %	Ref.	α_{total}	P_{exp} sec^{-1}	P_{theor} sec^{-1}	F	Adopted spin change
$E4$ $_{82}Pb^{202}_{120}$	0.1293 ± 0.0001	1M57	$(1.88 \pm 0.01) \times 10^4$	1M57	37 ± 3	1M57	477.4	4.11×10^{-8}	1.56×10^{-7}	$(2.63 \pm 0.18) \times 10^{-1}$	$9- \to 5-$
$E5$ $_{82}Pb^{202}_{120}$	0.5472 ± 0.0002	1M57	$(1.88 \pm 0.01) \times 10^4$	1M57	0.21 ± 0.05	1M57	0.697	6.58×10^{-8}	1.53×10^{-7}	$(4.30 \pm 1.03) \times 10^{-1}$	$9- \to (4+)_2$
$_{82}Pb^{204}_{122}$	0.6222 ± 0.0002	2H56	$(5.84 \pm 0.04) \times 10^3$	2H56	0.27 ± 0.03	2H56	0.309	3.53×10^{-7}	6.49×10^{-7}	$(5.44 \pm 0.61) \times 10^{-1}$	$9- \to (4+)_2$
$_{82}Pb^{202}_{120}$	0.7872 ± 0.0003	1M57	$(1.88 \pm 0.01) \times 10^4$	1M57	54 ± 4	1M57	0.203	2.39×10^{-5}	8.35×10^{-6}	2.86 ± 0.21	$9- \to (4+)_1$
$_{82}Pb^{204}_{122}$	0.9117 ± 0.0003	2H56	$(5.84 \pm 0.04) \times 10^3$	2H56	99.73	2H56	0.095	1.56×10^{-4}	4.34×10^{-5}	3.59 ± 0.04	$9- \to (4+)_1$

Table 12. Gamma-transition probabilities for *M*4 transitions.

No.	Nucleus	E_γ MeV	Ref.	τ_{exp} sec	Ref.	G %	Ref.	α_{total}	P_{exp} sec^{-1}	P_{theor} sec^{-1}	F	Adopted spin change
1	$_{77}\mathrm{Ir}_{116}^{193}$	0.08019 ± 0.00005	8B57	$(1.48 \pm 0.06) \times 10^6$	8B57	100	8B57	27210^a	2.48×10^{-11}	1.34×10^{-10}	$(1.85 \pm 0.09) \times 10^{-1}$	$\frac{11}{2} - \rightarrow \frac{3}{2} +$
2	$_{80}\mathrm{Hg}_{113}^{193}$	$0.1012 (\pm 0.0003)$	2G54	6.23×10^4	2G54	13.1	^{b}	5353	3.93×10^{-10}	1.09×10^{-9}	3.61×10^{-1}	$\frac{13}{2} + \rightarrow \frac{5}{2} -$
3	$_{80}\mathrm{Hg}_{115}^{195}$	0.1227	2J55	$(2.08 \pm 0.03) \times 10^5$	2J55	50	2J55	1698	1.41×10^{-9}	6.28×10^{-9}	2.25×10^{-1}	$\frac{13}{2} + \rightarrow \frac{5}{2} -$
4	$_{78}\mathrm{Pt}_{117}^{195}$	0.1299	2C54	$(4.30 \pm 0.19) \times 10^5$	4H49	100	6M54	1001	2.32×10^{-9}	1.05×10^{-8}	2.21×10^{-1}	$\frac{13}{2} + \rightarrow \frac{5}{2} -$
5	$_{78}\mathrm{Pt}_{115}^{193}$	0.1355	2C54	$(4.18 \pm 0.12) \times 10^5$	2C54	100	2C54	793	3.01×10^{-9}	1.50×10^{-8}	2.01×10^{-1}	$\frac{13}{2} + \rightarrow \frac{5}{2} -$
6	$_{80}\mathrm{Hg}_{117}^{197}$	0.1653	6M53	1.19×10^5	6H51	96.6	2J55	300	2.44×10^{-8}	9.37×10^{-8}	2.60×10^{-1}	$\frac{13}{2} + \rightarrow \frac{5}{2} -$
7	$_{82}\mathrm{Pb}_{115}^{197}$	0.2340 ± 0.0004	3A57	$(3.6 \pm 0.2) \times 10^3$	3A57	19.2 ± 1.2	3A57	57.5	9.12×10^{-7}	2.14×10^{-6}	$(4.26 \pm 0.38) \times 10^{-1}$	$\frac{13}{2} + \rightarrow \frac{5}{2} -$
8	$_{81}\mathrm{Tl}_{117}^{198}$	0.2607 ± 0.0005	2B53	9.09×10^3	2M54	52	^{c}	32.0	1.73×10^{-6}	5.71×10^{-6}	3.03×10^{-1}	$7 + \rightarrow 3 -$
9	$_{79}\mathrm{Au}_{114}^{193}$	0.2898 (0.0003)	2G54	5.60 ± 0.36	2F55	3.4	^{d}	17.5	3.28×10^{-4}	1.41×10^{-5}	2.33×10	$\frac{11}{2} - \rightarrow \frac{3}{2} +$
10	$_{79}\mathrm{Au}_{116}^{195}$	0.3184	2J55	$(4.42 \pm 0.03) \times 10$	2F55	0.7	^{e}	11.3	1.29×10^{-4}	3.35×10^{-5}	3.85	$\frac{11}{2} - \rightarrow \frac{3}{2} +$
11	$_{78}\mathrm{Pt}_{119}^{197}$	0.337 ± 0.006	4H49	$(6.75 \pm 0.26) \times 10^3$	4H49	100	6M54	8.30	1.59×10^{-5}	5.70×10^{-5}	$(2.79 \pm 0.46) \times 10^{-1}$	$\frac{13}{2} + \rightarrow \frac{5}{2} -$
12	$_{80}\mathrm{Hg}_{119}^{199}$	0.368 ± 0.007	4H49	$(3.84 \pm 0.04) \times 10^3$	4M48	100	6M54	6.39	3.89×10^{-5}	1.28×10^{-4}	$(3.04 \pm 0.52) \times 10^{-1}$	$\frac{13}{2} + \rightarrow \frac{5}{2} -$
13	$_{79}\mathrm{Au}_{118}^{197}$	0.4095	6M53	$(1.04 \pm 0.04) \times 10$	2F55	≈ 1	5C57	3.80	2×10^{-4}	3.29×10^{-4}	6×10^{-1}	$\frac{11}{2} - \rightarrow \frac{3}{2} +$
14	$_{82}\mathrm{Pb}_{117}^{199}$	0.4241 ± 0.0008	3A57	$(1.06 \pm 0.03) \times 10^3$	3A57	100	3A57	3.94	1.91×10^{-4}	4.61×10^{-4}	$(4.14 \pm 0.15) \times 10^{-1}$	$\frac{13}{2} + \rightarrow \frac{5}{2} -$
15	$_{82}\mathrm{Pb}_{119}^{201}$	0.629 ± 0.001	5S56	$(8.8 \pm 0.3) \times 10$	5S56	100	5S56	0.818	6.3×10^{-3}	1.63×10^{-2}	$(3.87 \pm 0.15) \times 10^{-1}$	$\frac{13}{2} + \rightarrow \frac{5}{2} -$
16	$_{82}\mathrm{Pb}_{121}^{203}$	0.8252 ± 0.0005	5S56	(8.79 ± 0.14)	2A57	100	5S56	0.299	8.76×10^{-2}	1.92×10^{-1}	$(4.56 \pm 0.08) \times 10^{-1}$	$\frac{13}{2} + \rightarrow \frac{5}{2} -$
17	$_{82}\mathrm{Pb}_{125}^{207}$	1.0639 ± 0.0003	1A53	1.15 ± 0.19	1B55	100	1A55	0.127	7.72×10^{-1}	1.96	$(3.94 \pm 0.07) \times 10^{-1}$	$\frac{13}{2} + \rightarrow \frac{5}{2} -$

[a] Calculated as 1.3 $\alpha_{\Sigma L}$. [b] Branching calculated from 2G54. [c] Branching calculated from 1P54 assuming decay scheme proposed by 3A57c.
[d] Branching calculated from 2G54. [e] Branching calculated from 2J55.

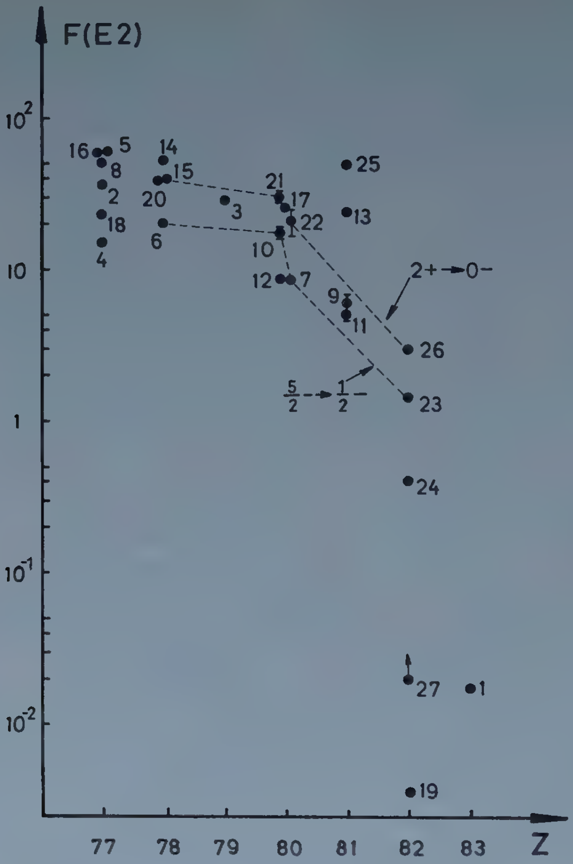

Fig. 14. The deviation factor F of $E2$ transitions as a function of proton number. The numbering of the points refers to Table 9.

polarities concerned. In the relatively few cases where it has been possible to assign r.m.s. error limits to F, a 3 % contribution from α has been assumed. This is intended mainly to cover interpolation uncertainties. The branching fractions G are of a varying accuracy. In general their relative errors must be expected to increase with decreasing G and may exceed 100 % in some of the actual cases.

Summarizing it may be stated that with few exceptions, mainly represented by the transitions for which error limits to F of about 10 % or less are given in the tables, the experimental material pertaining to gamma-ray transition probabilities is far from satisfactory. This should be remembered in looking for regularities and trends in Fig. 13–19, which show the deviation factors as functions of nucleon numbers for the different multipolarities.

4.22. *Discussion of regularities*

Though for reasons just mentioned no attempts to "fine structure" analysis of the figures will in general be made in the following discussion, we have considered it

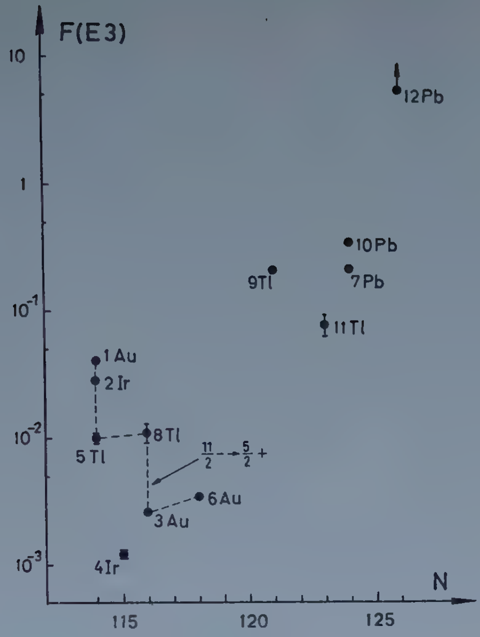

Fig. 15. The deviation factor F of $E3$ transitions as a function of neutron number. The numbering of the points refers to Table 10.

of interest, especially in view of the double shell closure, to illustrate the Z-dependence as well as the N-dependence of F when this is permitted by the experimental material available.

Most of the $E2$ transitions are characterized by high deviation factors, that is, they are more rapid than predicted by the single particle model. F as a function of the neutron number, however, shows a marked and sudden decrease near $N = 126$ (Fig. 13, p. 453, cf. ref. 3G55). This "shell effect" is perhaps even more clearly demonstrated in a plot against Z (Fig. 14). It is certainly of a special interest to follow the behaviour of corresponding transitions in the various nuclei. This possibility has been indicated in the figures for the $2+ \rightarrow 0+$ transitions in even-even nuclei and the $5/2- \rightarrow 1/2-$ transitions appearing in even-odd nuclei. In both these cases the transition probabilities for $Z = 82$ agree fairly well with the single-particle estimates. (It may be worth mentioning that the final spin 1/2 gives a statistical factor $= 1$.) The other $E2$ transitions in lead which involve different spin changes are still slower. It is interesting to note that according to a theoretical treatment [4W57] (cf. 3.1) the similarly hindered quadrupole transition in the odd-odd Bi^{206}, originating in the first excited state, probably proceeds without change of nucleon configuration, which may explain the slowing down [4W57a].

The general trend of the $E3$ transitions in $F-N$ and $F-Z$ plots (Figs. 15 and 16) is quite opposite to that of the $E2$ transitions. F is less than one (with the prominent exception of the ground state transition in Pb^{208}) and increases towards $N = 126$ [cf. 3G55] and $Z = 82$. The most frequent type of spin change, $11/2- \rightarrow 5/2+$, does not give rise to a smooth $F-Z$ curve. It is tempting, however, to pay special atten-

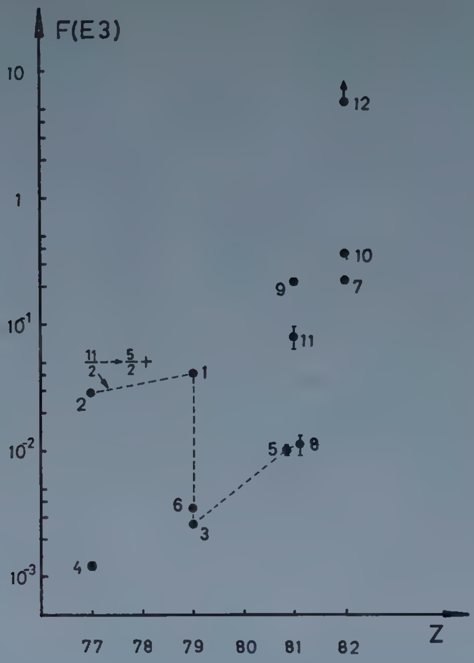

Fig. 16. The deviation factor F of $E3$ transitions as a function of proton number. The numbering of the points refers to Table 10.

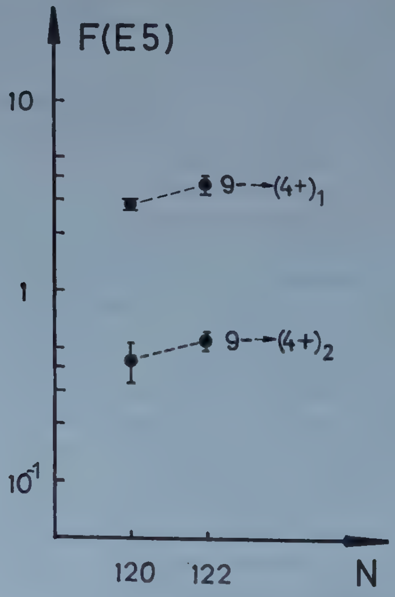

Fig. 17. The deviation factor F of $E5$ transitions as a function of neutron number.

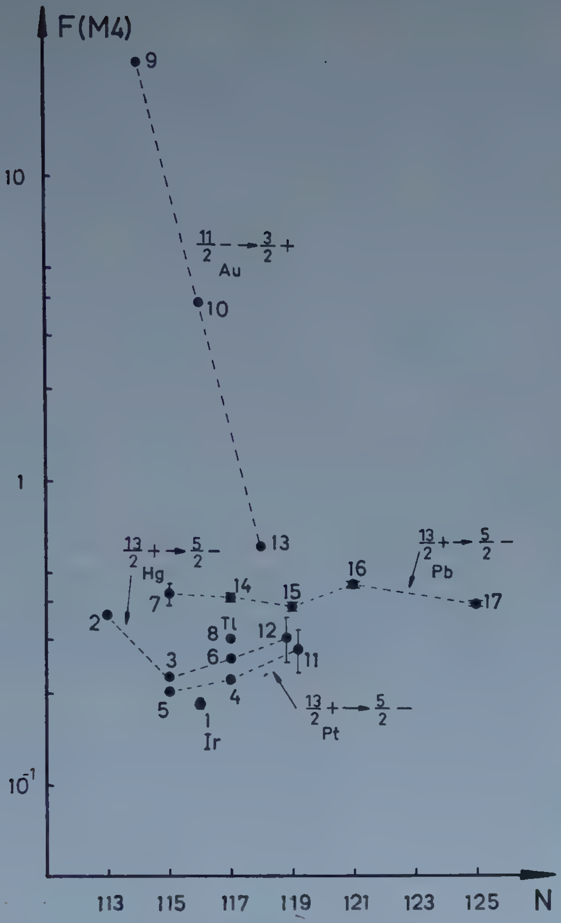

Fig. 18. The deviation factor F of $M4$ transitions as a function of neutron number. The numbering of the points refers to Table 12.

ion to the pairs Au^{195}–Au^{197} and Tl^{195}–Tl^{197} which show good internal agreement (as would be expected of analogous proton transitions in nuclei differing only by wo neutrons) and in addition seem to follow the general trend of the Z-dependence. The deviation of the other points may reflect differences in configuration.

The sparse $E5$ data, which exclusively concern transitions in lead, point to the same rough agreement with theory as shown by $E2$ and $E3$ transitions near the 82 proton shell (Fig. 17). An interesting feature is the pronounced dependence on configuration exhibited by transitions from the $9-$ states to final $4+$ states of different character. If it is at all possible to speak of an N-dependence in this case it indicates again an increase of F with neutron number towards $N = 126$.

$M4$ transition probabilities have long been known to agree surprisingly well with single-particle calculations. In view of this fact the interpretation of Fig. 18 meets with difficulties. Here the behaviour of the "cross over" $M4$ transitions ($11/2- \rightarrow$

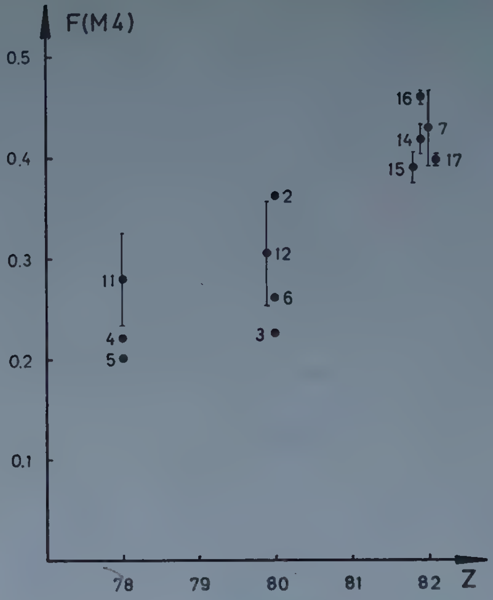

Fig. 19. The deviation factor F of $M4$ transitions in Pt, Hg and Pb as a function of proton number. The numbering of the points refers to Table 12.

$3/2+$) in odd Au isotopes deviates in a striking manner from the approximately N-independent course of the $13/2+ \rightarrow 5/2-$ curves. It will be recalled that the $M4$ deviation factors were calculated for neutron transitions, while the Au transitions concerned are ascribed to protons. Taking this into account improves indeed the general agreement, but the difference by a factor ≈ 30 between the extreme Au points remains. On the other hand the $11/2- \rightarrow 3/2+$ transition in Ir^{193} does not deviate markedly from the bulk of transitions in Fig. 18. It is also worth noticing that Goldhaber and Sunyar [3G55], looking for finer details of the $M4$ systematics over the whole periodic system, could not find any favouring by a factor ≈ 2 of the proton transitions relative to the neutron transitions as demanded by theory [11M55]. A redetermination of the $M4/E3$ branching in the odd Au isotopes seems highly desirable. It would also be interesting to know the corresponding branching in Tl^{195} and Tl^{197}; attempts to study the $M4$ transitions in these nuclei have not been successful so far [3A57b]. As to the odd neutron nuclei, the absence of any shell effect among the lead isomers was pointed out by Stockendal *et al.* [5S56]. For Hg and Pt the experimental data are not as unambiguous, but the deviation factor seems to be constant within the limits of error in both cases. Already in Fig. 18, however, there are indications of a Z-dependence, which is better demonstrated in Fig. 19. (Note the linear F-scale.) A particularly significant feature is that the main increase in F takes place nearest to $Z = 82$. Similar observations have recently been made in the second island of isomers [5A57]. A redetermination of data pertaining to this effect in all three islands with special attention paid to the possible occurrence of earlier unknown branching from the isomeric states is in progress [5A57a].

4.23. *Multipole mixing*

The question of multipole mixing is intimately related to the theory of gamma-emission probability. According to Weisskopf's treatment [14B52] the lowest multipole order allowed by spin and parity selection rules is by far the most probable one. This is conveniently expressed by writing the Moszkowski formulae for single proton transitions (see 4.21) in the following way:

$$\frac{P(E,L)}{P(M,L+1)}=\frac{C(E,L)}{C(M,L+1)\,E_\gamma^2} \tag{9a}$$

$$\frac{P(M,L)}{P(E,L+1)}=\frac{C(M,L)}{C(M,L+1)\,E_\gamma^2 A^{4/3}} \tag{9b}$$

In (9a) the ratio $C(E,L)/C(M,L+1)$ between the constants is about 10^6 for all multipole combinations of practical importance, while the corresponding ratio in (9b) varies from about 10^5 for $M1/E2$ to about 10^7 for $M4/E5$. Thus even in the favourable case of a 1 MeV gamma-ray in a heavy nucleus ($A \approx 200$) the $E2$ admixture into an $M1$ transition should not amount to more than about 1 %. Only when the radiation of the lower multipolarity is considerably hindered or that of the higher enhanced does mixing occur to such an extent that it clearly shows up for instance in angular correlations between the emitted quanta or electrons and in the conversion coefficients. We are going to discuss briefly some multipolarity combinations for which observable mixing ratios or limits of admixture have been reported.

*M*1, *E*2.—The authors have not aimed at a complete review of mixed $M1 + E2$ transitions in the lead region. This is partly due to the fact that relatively few accurate measurements of the mixing ratio exist. On the other hand the number of reported cases is so large that it could no doubt be the subject of a separate survey. Many of these cases, however, are evidently in error, mainly because of the previously insufficient knowledge of conversion coefficients. A typical example is provided by Pb^{206}, in which according to Alburger and Pryce [1A54] 9 of the observed gamma-rays should have mixed $M1$–$E2$ character in order to fit the level scheme and the intensity relations. The conversion coefficients of these transitions have recently been measured by Novakov and Hultberg [3N57a]. Within the experimental errors their results agree with the "finite size" conversion coefficients (cf. 4.31) for either pure $E2$ or pure $M1$ radiation. In other cases the application of the "finite size" correction does not invalidate the conclusion that the $E2$ admixture is appreciable. Such a case is that of the 279 keV transition in Tl^{203}, which is supposed to involve the hole states $s_{1/2}{}^{-1}$ and $d_{3/2}{}^{-1}$ and thus from a strict single-particle point of view is l-forbidden for $M1$ radiation. Transitions of this type have been systematically studied by Graham and Bell [4G53] and by de Waard and Gerholm [2W56]. Recently Gerholm and his collaborators [1G57] started an interesting investigation of the l-forbidden $d_{3/2}\rightarrow s_{1/2}$ transitions in Tl^{201}, Tl^{199}, Tl^{197}, and Tl^{195} using a multichannel goniometer, a double lens coincidence spectrometer, and electromagnetically separated samples.

*M*3, *E*4.—Mihelich and Goldhaber [6M55] investigated the 74 keV transition in the decay of the 14 hr isomeric state of Os^{191} (not listed in the tables of 4.1 and 4.21) and suggested the multipolarity $M3$ with a small admixture of $E4$. This was required to account for the presence of L_{II} conversion electrons. The long half-life no doubt indicates a hindered $M3$ transition. This case seems so interesting that it ought to be carefully remeasured.

*M*4, *E*5.—The constancy of the experimental $M4$ matrix elements (cf. the deviation factors, 4.22) indicates that if there is any multipole mixing it must be of a similar extent in all the cases (with the possible exception of the odd Au transitions). The possibility of $E5$ admixture in the 165 keV $M4$ gamma-ray in Hg^{197} has been discussed by Coburn *et al.* [5C57]. They conclude from both conversion line intensities and angular correlation data that there is no detectable admixture. The decay of Hg^{199m} is analogous to the decay of Hg^{197m}. Bolotin and Wilkinson [13B55], however, measured the K conversion coefficient of the 368 keV isomeric transition in Hg^{199} and obtained a value which together with information from angular correlation experiments suggested a mixing ratio $E5/M4 = 30\,\%$. This result, being in sharp contrast to the insignificant $E5$ admixture in the Hg^{197} $M4$ transition, could not be confirmed by Pound and Wertheim [4P56], who report an $E5$ contribution of only 0.8 %. Even this figure, however, is considered too high by Coburn *et al.*

*E*2, *M*3.—Coburn *et al.* [5C57] have looked for $M3$ admixture in the 134 keV $E2$ transition in Hg^{197}, concluding that if it is at all present it must be very small. From angular correlation measurements in Pb^{204} Krohn and Raboy [4K55] suggest 0.5 % $M3$ radiation together with $E2$ in the 375 keV gamma-ray. Electron intensity measurements by Herrlander *et al.* [2H56] indicate that the $M3$ admixture is less than 0.5 %.

*E*3, *M*4.—$E3$ transitions in the lead region have been shown in general to be considerably hindered (4.22). Thus when it was discovered [3A57e] that their $(L_{\mathrm{I}} + L_{\mathrm{II}})/L_{\mathrm{III}}$ conversion ratios were lower than the theoretical values throughout, multipole mixing was considered as one of the possible explanations. The 1–2 % $M4$ admixture indicated by the $(L_{\mathrm{I}} + L_{\mathrm{II}})/L_{\mathrm{III}}$ ratios, however, was not compatible with the K/L ratios. In view of the later development, when a computing error affecting the theoretical L_{III} coefficients was revealed [3R56], it is still more conclusive that the $M4$ admixture calculated from the $L_{\mathrm{I}}/L_{\mathrm{II}}$ ratio of the 222.5 keV $E3$ transition in Tl^{197} [3A57a] was less than 0.2 % and zero within the limits of error. A reexamination of the experimental material using the corrected L_{III} coefficients shows that even the $(L_{\mathrm{I}} + L_{\mathrm{II}})/L_{\mathrm{III}}$ ratios now agree with a pure $E3$ character of the transitions.

*E*4, *M*5.—The only known $E4$ transition in the region of present interest is the 129 keV gamma-ray in Pb^{202}. The L conversion ratio suggests that a possible $M5$ admixture must be smaller than 5 % [1M57].

*E*5, *M*6.—From angular correlation measurements Krohn and Raboy [4K55] suggested that the 912 keV $E5$ transition in Pb^{204} should have an admixture of 1 % $M6$ radiation. Herrlander *et al.* [2H56], however, showed by electron intensity measurements that the amount must be less than 0.5 %. Later experiments by Krohn and Raboy [8H56] confirm this conclusion.

The above survey of multipole mixing, though admittedly not complete, indicates that in fact there does not exist very many conclusive results. In most cases it has been possible only to put an upper limit to the amount of admixture. With the exception of the $M3$–$E4$ mixing reported in Os^{191} and some $M1 + E2$ transitions the limits of mixing of high multipolarities are in agreement with the Weisskopf theory. This means that the lower multipolarity (E, L or M, L) is seldom hindered to such a degree relative to the competing higher multipolarity ($M, L+1$ or $E, L+1$, respectively) that the latter is detectable with the present experimental methods. It should finally be remarked that erroneous conclusions regarding multipole mixing may result from the neglection of special nuclear matrix elements [6C56] (cf. 4.31) in the theoretical internal conversion coefficients which should influence even angular correlation measurements involving conversion electrons.

4.3. *Internal conversion ratios*

4.31. *Introductory remarks*

Until a few years ago the method of determining multipole orders of gamma-ray transitions by means of internal conversion data suffered from the limitation that reliable theoretical values were available only for isolated sets of multipolarities, electron shells, transition energies, and atomic numbers. In 1954, however, M. E. Rose and his collaborators [3R54] started to distribute the results of an extensive computation scheme, including K-shell and L-subshell conversion coefficients for all multipoles of practical interest, covering a wide range of energies and Z-values, and taking the effect of screening into account. As the work proceeded, an increasing amount of experimental evidence, concerning absolute conversion coefficients as well as K/L and $(L_I + L_{II})/L_{III}$ ratios, pointed to a satisfactory agreement between theory and experiment. That, on the whole, this is true of the conversion ratios of $E2$, $E3$, $E5$, and $M4$ transitions in the Z region of present interest is illustrated by Figs. 20–26. These figures show the variation of conversion ratios with transition

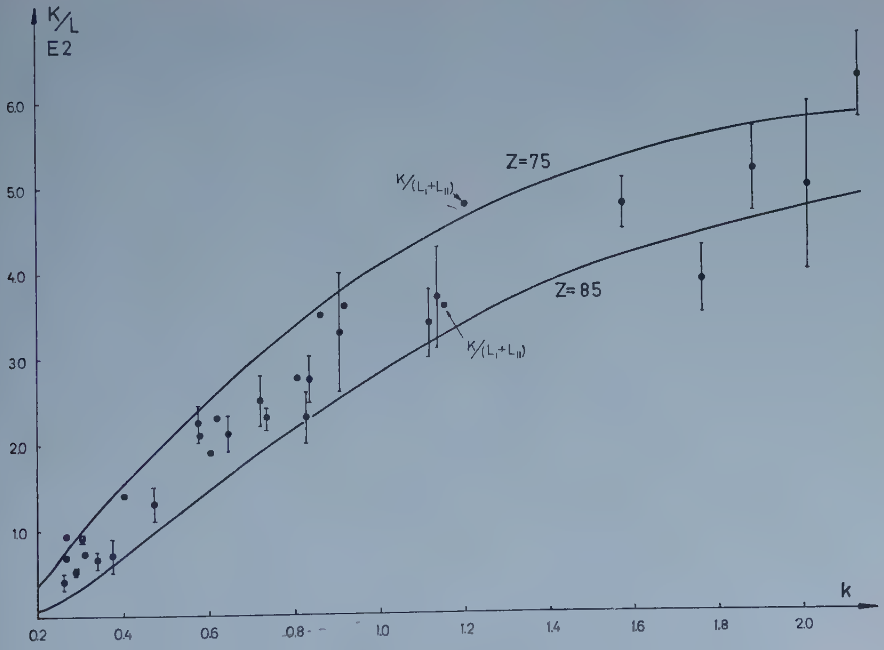

Fig. 20. The K/L conversion ratio of $E2$ transitions as a function of energy in mc² units. In the cases where L is represented by $L_I + L_{II}$ the inclusion of L_{III} would lower the values by about 10 %.

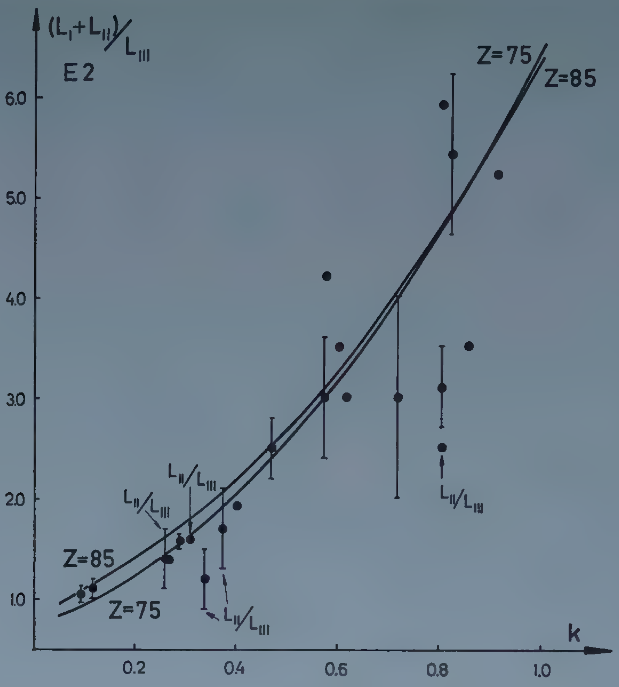

Fig. 21. The $(L_I+L_{II})/L_{III}$ conversion ratio of $E2$ transitions as a function of energy in mc^2 units. In the cases where L_{II}/L_{III} is given the inclusion of L_I would raise the values by about 12 % at $k\approx 0.3$ and by 100 % at $k=0.8$.

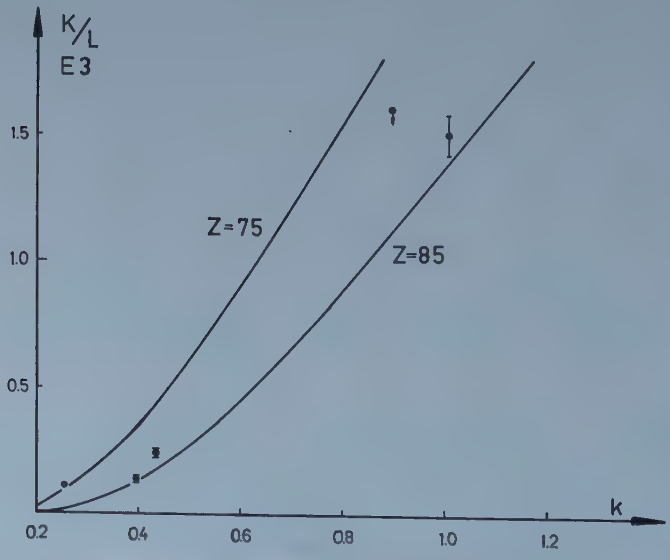

Fig. 22. The K/L conversion ratio of $E3$ transitions as a function of energy in mc^2 units.

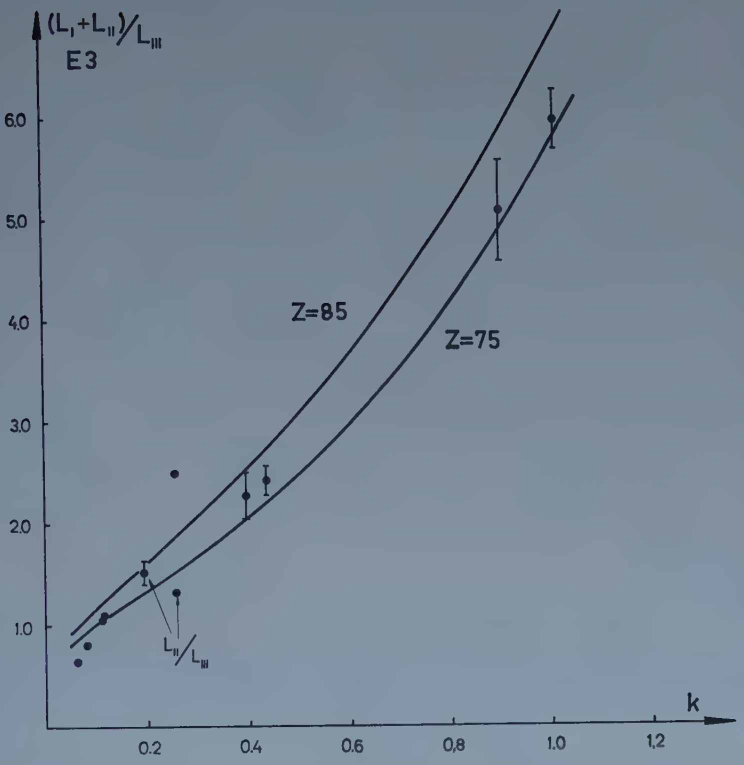

Fig. 23. The $(L_I+L_{II})/L_{III}$ conversion ratio of E3 transitions as a function of energy in mc^2 units. In the cases where L_{II}/L_{III} is given the inclusion of L_I would raise the values by about 4 %.

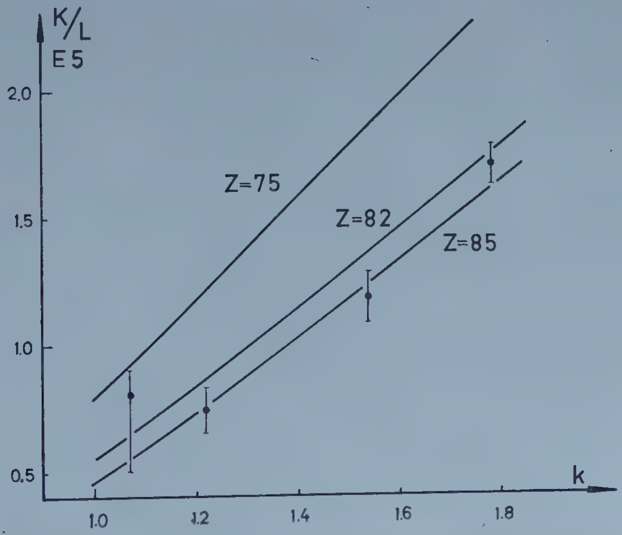

Fig. 24. The K/L conversion ratio of $E5$ transitions as a function of energy in mc^2 units.

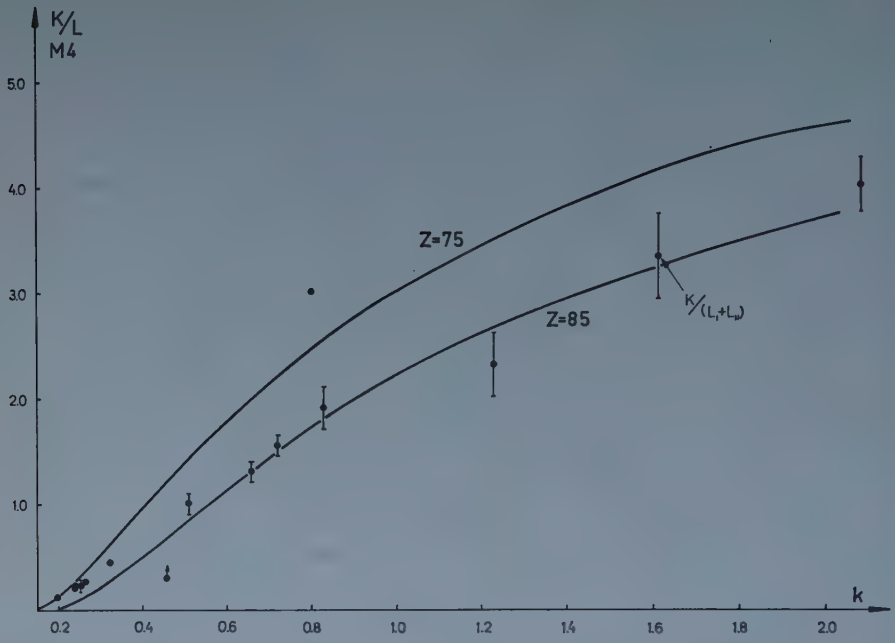

Fig. 25. The K/L conversion ratio of $M4$ transitions as a function of energy in mc² units. In the case where L is represented by $L_{\mathrm{I}}+L_{\mathrm{II}}$ the inclusion of L_{III} would lower the value by about 10 %.

energy k, expressed in mc² units. The experimental material is taken from Tables 13–16.

Careful measurements of K conversion coefficients of $M1$ transitions in heavy nuclei, however, revealed a discrepancy, implying that the theoretical values are as much as 40 % too high [1W56]. This was explained by the fact that the nucleus had been treated as a point charge in the calculations, an approximation that will evidently lose in validity with increasing proton number. In fact, K conversion coefficients calculated by Sliv and Band [13S56] with regard paid to the finite nuclear size, deviate from the point charge values by more than a factor two for high Z, high energy $M1$ transitions. Other types of transition are influenced to an extent that is less for electric than for magnetic transitions and decreases with increasing multipole order. Though full agreement with accurate experimental values is not obtained even with the Sliv–Band tables [1W56, 2N56], they must at present be considered the most reliable set of K conversion coefficients (cf. 4.2).

No finite nuclear size calculations of L conversion have yet been completed. (Such calculations have been started both by the American and the Russian groups.) Experiments indicate, however, that the L_{I} and probably the L_{II} coefficients behave similarly to the K coefficients [1W56, 14S56], while L_{III} is substantially unaffected. There are even theoretical arguments in favour of this interpretation [3R56, 11B55]. Nuclear size effects may, therefore, be expected to show up in the conversion ratios. This was considered to justify a more rigorous comparison between point charge theory and experiment than represented by Figs. 20–26. Such a comparison receives

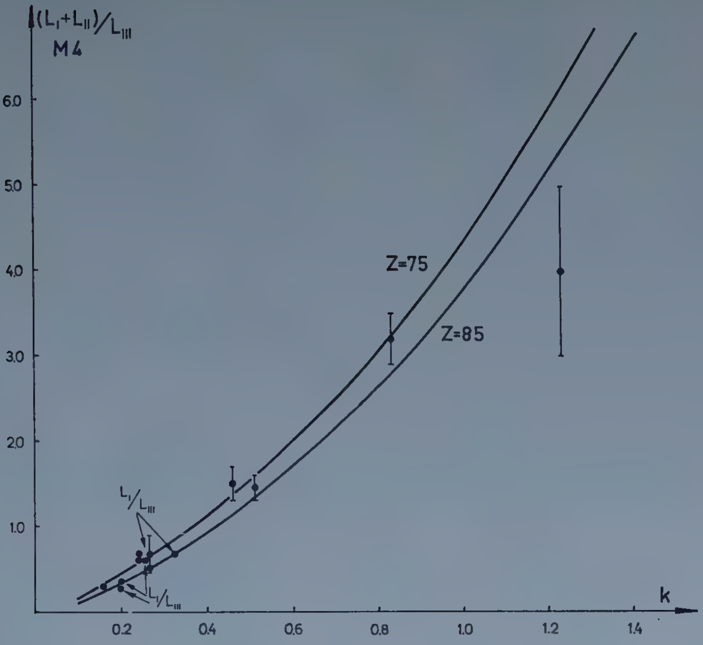

Fig. 26. The $(L_I + L_{II})/L_{III}$ conversion ratio of $M4$ transitions as a function of energy in mc^2 units. Where L_I/L_{III} is given the inclusion of L_{II} would raise the values by about 20 %.

in increased interest by the recent observation by Church and Weneser [6C56] that additional matrix elements, not included in Sliv's and Band's treatment, arise from the interaction of the atomic electrons with the nuclear charge and current distributions. (This is less explicitly expressed in an earlier paper by Kramer [2K56].) Also n this case the corrections are probably most important for $M1$ transitions, but in principle all multipolarities should be influenced. It is pointed out that different electron shells and subshells may be differently affected, that is, conversion ratios may be particularly sensitive to this type of nuclear size effect.

4.32. *Treatment of data*

Rose *et al.* give the theoretical conversion coefficients for $Z = 15$ through 95 in steps of 10 and for a number of transition energies between $k = 0.05$ and $k = 2.0$. In interpolating to interjacent Z-values, a commonly accepted procedure seems to be the connection by straight lines of neighbouring points in a log-lin representation of the coefficients against Z. We have found, however, that in some cases this leads to considerable deviations from a smooth curve joining the given points within a larger range of atomic numbers. Thus, interpolating between $Z = 75$ and $Z = 85$, we have considered also the points corresponding to $Z = 65$ and 95. Sometimes, notably for the L_I coefficients of $E2$ transitions, it was necessary to include even $Z = 45$ and 35.

The interpolation to actual transition energies was performed by plotting the conversion coefficients against energy in a log-log diagram. A difficulty was encountered in connection with the K shell conversion of low energy transitions, where the

Table 13. Internal conversion ratios for $E2$ transitions.

Nucleus	E_γ keV	k	Ref.	K/L				$(L_I+L_{II})/L_{III}$				Remarks
				Exp.	Ref.	Theor.	$\frac{\text{Exp.}}{\text{Theor.}}$	Exp.	Ref.	Theor.	$\frac{\text{Exp.}}{\text{Theor.}}$	
$_{80}$Hg^{198}	47.7	0.093	3A57c					1.05±0.08	3A57c	1.03	1.02±0.08	$L_I/L_{II}=0.025\pm0.008$ $M_{II}/M_{III}=1.01\pm0.10$ [3A57c]
$_{83}$Bi^{206}	59.9	0.117	4A57					1.11±0.10	4A57	1.13	0.98±0.11	$L_I/L_{II}=0.028\pm0.006$ $M_{II}/M_{III}=1.02\pm0.10$ [4A57]
$_{80}$Hg^{197}	134.0	0.262	6M53	0.4±0.1	3A57	0.402	1.00±0.25	1.4±0.3	3A57	1.38	1.01±0.22	L conv. ratios refer to L_{II}/L_{III}
$_{78}$Pt^{192}	136.33	0.267	7B55	0.93	7B55	0.523	1.78	1.4	7B55	1.51	0.93	
$_{76}$Os^{186}	137.19	0.268	2P56	0.68±0.04	1N57	0.663	1.03±0.07					$L/M=4.4$ [3M51]
$_{81}$Tl^{200}	148.0	0.290	4B55	0.52±0.05	2A57a	0.474	1.10±0.12	1.58±0.07	2A57a	1.66	0.95±0.05	$L_I/L_{II}=0.12\pm0.03$ [2A57a]
$_{76}$Os^{188}	155.3	0.304	8M53	0.91±0.05	1N57	0.864	1.05±0.07					
$_{80}$Hg^{199}	158.4	0.310	2B53	0.73	10S51	0.612	1.19	1.6	6M52	1.49	1.07	L conv. ratios refer to L_{II}/L_{III}
$_{81}$Tl^{198}	173.4	0.339	3A57	0.65±0.10	3A57	0.702	0.93±0.15	1.2±0.3	3A57	1.57	0.76±0.19	L conv. ratios refer to L_{II}/L_{III} $L_{II}/M\approx2$; $M/N\approx2$ [3A57]
$_{81}$Tl^{196}	191	0.374	3A57b	0.7±0.2	3A57b	0.859	0.81±0.23	1.7±0.4	3A57b	1.65	1.03±0.24	L conv. ratios refer to L_{II}/L_{III}
$_{76}$Os^{192}	205.75	0.403	5M52	1.4	7B55	1.43	0.98	1.93	7B55	2.08	0.91	
$_{81}$Tl^{202}	241.1	0.472	1M57	1.3±0.2	1M57	1.27	1.02±0.16	2.5±0.3	1M57	2.48	1.01±0.12	
$_{78}$Pt^{192}	295.94	0.579	7B55	2.1	7B55	2.05	1.02	4.2	7B55	3.00	1.40	
$_{78}$Pt^{192}	308.45	0.604	7B55	1.9	7B55	2.16	0.88	3.5	7B55	3.13	1.12	
$_{78}$Pt^{192}	316.5	0.619	7B55	2.3	7B55	2.22	1.04	3.0	7B55	3.27	0.92	
$_{78}$Pt^{194}	329.07	0.644	2R55	2.12±0.21	9B57	2.33	0.91±0.10					
$_{80}$Hg^{200}	367.8	0.720	2B53	2.5±0.3	2H57	2.43	1.03±0.13	3.0±1.0	2B53	3.91	0.77±0.26	
$_{82}$Pb^{204}	374.7	0.733	2H56	1.76±0.1 $(K/(L+M))$	9M54	2.23	1.03±0.07					$L/(M+N)=3.5\pm1$ [9M54] $K/L=1.3\times1.76$ used in the calculations
$_{80}$Hg^{198}	411.77	0.806	5M52	2.77	10B55	2.80	0.99	5.9 2.5 3.1±0.4	10B55 6M52 4C56	4.62 2.36 4.62	1.28 1.06 0.67±0.09	L conv. ratios refer to L_{II}/L_{III} $L_I/L_{II}=0.87\pm0.18$ [4C56]
$_{82}$Pb^{202}	422.1	0.826	1M57	2.3±0.3	1M57	2.62	0.88±0.12	5.4±0.8	1M57	4.88	1.11±0.17	
$_{80}$Hg^{196}	426	0.834	6S52	2.75±0.28	3A57b	2.86	0.96±0.10					$L_{II}>L_I$ [3A57b]
$_{80}$Hg^{202}	439.1	0.859	2B53	2.7 $(K/(L+M))$	1K56	2.96	1.19	3.5	2B53	5.05	0.69	$K/L=1.3\times2.7$ used in the calculations
$_{82}$Pb^{200}	462.3	0.905	1J57	3.3±0.7	1J57	2.88	1.15±0.25					
$_{78}$Pt^{192}	467.98	0.916	7B55	3.6	7B55	3.44	1.05	5.2	7B55	5.56	0.94	
$_{82}$Pb^{207}	569.0	1.114	1A55	3.4±0.4	1A55	3.53	0.96±0.12					
$_{80}$Hg^{200}	579.4	1.134	2H57	3.7±0.6	2H57	3.84	0.96±0.16					
$_{78}$Pt^{192}	588.4	1.151	7B55	3.6	7B55	4.65	0.77					K/L ratios refer to $K/(L_I+L_{II})$
$_{78}$Pt^{192}	612.9	1.199	7B55	4.8	7B55	4.79	1.00					K/L ratios refer to $K/(L_I+L_{II})$
$_{82}$Pb^{206}	803.3	1.572	1A54	4.8±0.3	1A54	4.55	1.05±0.07					$K/(L+M)=4.0\pm0.3$ [1A54]
$_{82}$Pb^{204}	899.3	1.760	2H56	3.9±0.4	2H56	4.80	0.81±0.09					
$_{82}$Pb^{202}	961.4	1.881	1M57	5.2±0.5	1M57	4.96	1.05±0.11	≈15	1M57	17.10	≈0.88	

Table 14. Internal conversion ratios for $E3$ transitions.

Nucleus	E_γ keV	k	Ref.	K/L Exp.	K/L Ref.	K/L Theor.	K/L $\frac{\text{Exp.}}{\text{Theor.}}$	$(L_I+L_{II})/L_{III}$ Exp.	$(L_I+L_{II})/L_{III}$ Ref.	$(L_I+L_{II})/L_{III}$ Theor.	$(L_I+L_{II})/L_{III}$ $\frac{\text{Exp.}}{\text{Theor.}}$	Remarks
$_{79}Au^{193}$	31.9	0.062	2G54					0.65	2G54	0.916	0.71	
$_{77}Ir^{191}$	41.7	0.081	8S52					0.81	8S52	1.00	0.81	$L_I/L_{II} \leq 0.1$ [8S52]
$_{79}Au^{195}$	56.9	0.111	2J55					1.05	2J55	1.16	0.91	$L_I/L_{II} \leq 0.1$ [12S57]
$_{77}Ir^{192}$	58.0	0.114	7M54					1.1	7M54	1.09	1.01	
$_{81}Tl^{195}$	99.1	0.194	3A57a					1.52 ± 0.12	3A57a	1.42	1.07 ± 0.09	L conv. ratios refer to L_{II}/L_{III}
$_{79}Au^{197}$	130.2	0.254	6M53	0.114	2J55	0.0438	2.60	$\left\{ 1.32 \right.$	2J55	1.53	0.86	L conv. ratios refer to L_{II}/L_{III}
								$\left. 2.5 \right\}$	6M53	1.60	1.56	$L_I/L_{II} \leq 0.1$ [2M53]
$_{82}Pb^{206}$	202.5	0.396	1A54	$0.140 \pm$ ± 0.014	1A54	0.169	0.83 ± 0.09	2.28 ± 0.23	1A54	2.41	0.95 ± 0.10	Uncertainty in exp. values estimated from ref. 1A54
$_{81}Tl^{197}$	222.45	0.435	3A57a	$0.242 \pm$ ± 0.018	3A57a	0.246	0.98 ± 0.08	2.43 ± 0.15	3A57a	2.59	0.94 ± 0.06	
$_{81}Tl^{202}$	459.8	0.900	1M57	< 1.6	1M57	1.36	< 1.19	5.1 ± 0.5	1M57	5.36	0.95 ± 0.10	
$_{82}Pb^{206}$	516.1	1.01	1A54	1.50 ± 0.08	1A54 1S56	1.61	0.93 ± 0.06	6.0 ± 0.3	1S56	6.28	0.96 ± 0.06	Exp. K/L from treatment of data in ref. 1A54 and 1S56.

Table 15. Internal conversion ratios for $E4$ and $E5$ transitions.

Nucleus	E_γ keV	k	Ref.	K/L Exp.	K/L Ref.	K/L Theor.	K/L $\frac{\text{Exp.}}{\text{Theor.}}$	$(L_I+L_{II})/L_{III}$ Exp.	$(L_I+L_{II})/L_{III}$ Ref.	$(L_I+L_{II})/L_{III}$ Theor.	$(L_I+L_{II})/L_{III}$ $\frac{\text{Exp.}}{\text{Theor.}}$	Remarks
$E4$												
$_{82}Pb^{202}$	129.3	0.253	1M57	< 0.004	1M57	0.0038	< 1.05	1.97 ± 0.14	1M57	1.93	1.02 ± 0.08	
$E5$												
$_{82}Pb^{202}$	547.2	1.071	1M57	$0.8 {+0.1 \atop -0.3}$	1M57	0.64	$1.25 {+0.16 \atop -0.47}$	6.0 ± 1.5	1M57	6.97	0.86 ± 0.22	
$_{82}Pb^{204}$	622.2	1.218	2H56	0.74 ± 0.09	2H56	0.86	0.86 ± 0.11					
$_{82}Pb^{202}$	787.2	1.541	1M57	1.18 ± 0.10	1M57	1.36	0.87 ± 0.08	≈ 10	1M57	10.9	≈ 0.9	
$_{82}Pb^{204}$	911.7	1.784	2H56	1.70 ± 0.08	2H56	1.75	0.97 ± 0.05	11 ± 2	2H56	13.0	0.85 ± 0.15	

Table 16. Internal conversion ratios for $M4$ transitions.

Nucleus	E_γ keV	k	Ref.	K/L				$(L_I+L_{II})/L_{III}$				Remarks
				Exp.	Ref.	Theor.	$\frac{\text{Exp.}}{\text{Theor.}}$	Exp.	Ref.	Theor.	$\frac{\text{Exp.}}{\text{Theor.}}$	
$_{77}Ir^{193}$	80.19	0.157	8B57					0.289	8B57	0.268	1.08	$L_I:L_{II}:L_{III}=5.5:1:22.5$ [8B57]
$_{80}Hg^{193}$	101.2	0.198	2G54	0.12	6M54	0.04	3.0	0.27 0.36	2G54	0.308	0.88 1.17	L conv. ratios refer to L_I/L_{III} L_{II} weak [2G54]
$_{80}Hg^{195}$	122.7	0.240	2J55	0.23	2J55	0.13	1.77	0.68	2J55	0.484	1.40	$L_I:L_{II}:L_{III}=1.0:0.2:2.0$;
				0.2	2G54		1.5	0.6	2G54		1.2	$L/M=2$ [2G54]
$_{78}Pt^{195}$	129.9	0.254	2C54	0.23 ± 0.06	4H49	0.22	1.05 ± 0.28	0.6	2C54	0.468	1.3	L conv. ratios refer to L_I/L_{III}; $L/M=2.11$ [7S52]
$_{78}Pt^{193}$	135.5	0.265	2C54	0.27	8S53	0.26	1.04	0.67 ± 0.22	2C54	0.486	1.38 ± 0.44	L conv. ratios refer to L_I/L_{III}
								0.51	8S53	0.588	0.87	$K:L_I:L_{III}:(M_I+M_{III}):N_I=100:123:241:132:57$ [8S53]
$_{80}Hg^{197}$	165.3	0.323	6M53	0.45	6H51	0.41	1.10	0.67	6M53	0.611	1.10	L conv. ratios refer to L_I/L_{III}
$_{82}Pb^{197}$	234.0	0.458	3A57	>0.3	3A57	0.81	>0.37	1.5 ± 0.2	3A57	1.43	1.05 ± 0.14	$M/N=3.5$ [3A57]
$_{81}Tl^{198}$	260.7	0.510	2B53	1.0 ± 0.1	1P54	1.08	0.93 ± 0.10	1.46 ± 0.15	1P54	1.36	1.07 ± 0.11	$L/(M+N)=3.68$ [1P54]
$_{78}Pt^{197}$	337	0.659	4H49	1.30 ± 0.10	4H49	1.78	0.73 ± 0.06					
$_{80}Hg^{199}$	368	0.720	4H49	1.55 ± 0.10	4H49	1.82	0.85 ± 0.06					
$_{79}Au^{197}$	409.5	0.801	6M53	2.3 $(K/(L+M))$	2J55	2.15	1.40					$K/L=1.3\times2.3$ used in the calculations
$_{82}Pb^{199}$	424.1	0.830	3A57	1.9 ± 0.2	3A57	1.96	0.97 ± 0.11	3.2 ± 0.3	3A57	2.89	1.11 ± 0.11	
$_{82}Pb^{201}$	629	1.231	5S56	2.3 ± 0.3	5S56	2.82	0.82 ± 0.11	4 ± 1	5S56	5.57	0.72 ± 0.18	
$_{82}Pb^{203}$	825.2	1.615	5S56	3.3 ± 0.4	5S56	3.82	0.86 ± 0.11					K/L ratios refer to $K/(L_I+L_{II})$
$_{82}Pb^{207}$	1063.9	2.082	1A53	3.95 ± 0.25	1A55	3.90	1.01 ± 0.07					$L/M=3.2$ [1A53] Theoretical ratio by extrapolation

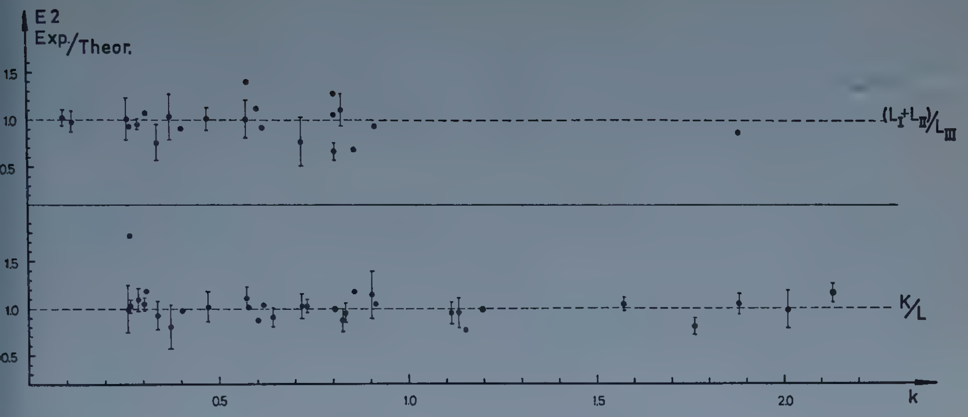

Fig. 27. The ratios between experimental and theoretical values of K/L and $(L_I+L_{II})/L_{III}$ conversion ratios of $E2$ transitions as functions of energy in mc² units.

log-log representation deviates appreciably from straight lines. The absence of points between $k=0.20$ and 0.40 in Rose's tables makes an accurate interpolation unfeasible. Sliv and Band, however, give finite size corrected values for $k=0.20$, 0.25, 0.30, 0.35, and 0.50, which we have used to construct "curve shape standards". The difference between the conversion ratios obtained in this way and the "true" point charge ratios will probably not significantly exceed the interpolation error $\pm 3\%$ which we have assumed throughout the calculations, summarized in Tables 13–16.

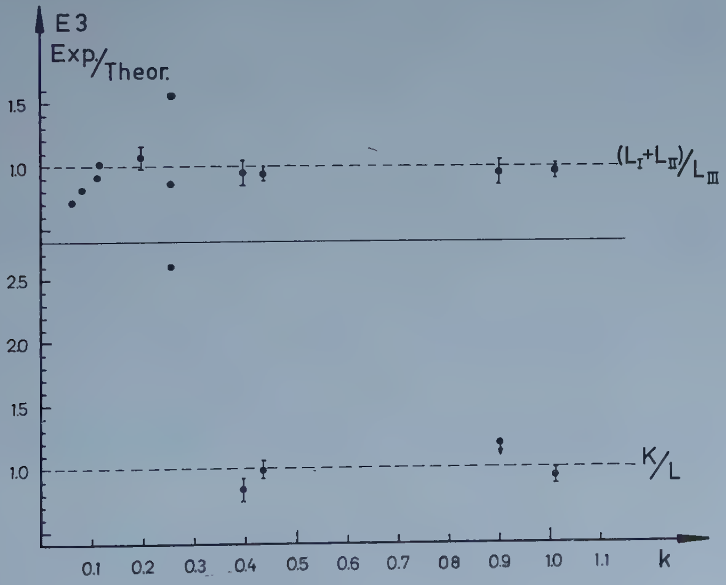

Fig. 28. The ratios between experimental and theoretical values of K/L and $(L_I+L_{II})/L_{III}$ conversion ratios of $E3$ transitions as functions of energy in mc² units.

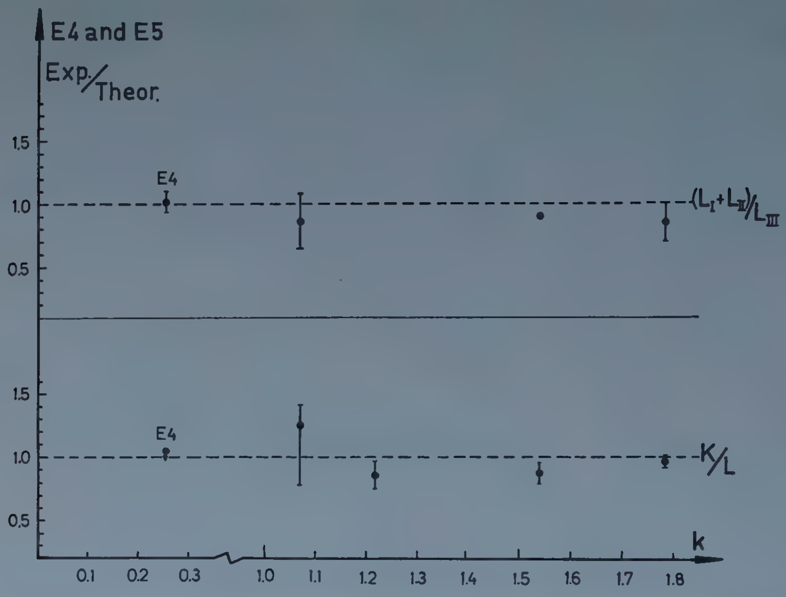

Fig. 29. The ratios between experimental and theoretical values of K/L and $(L_I+L_{II})/L_{III}$ conversion ratios of $E4$ and $E5$ transitions as functions of energy in mc² units.

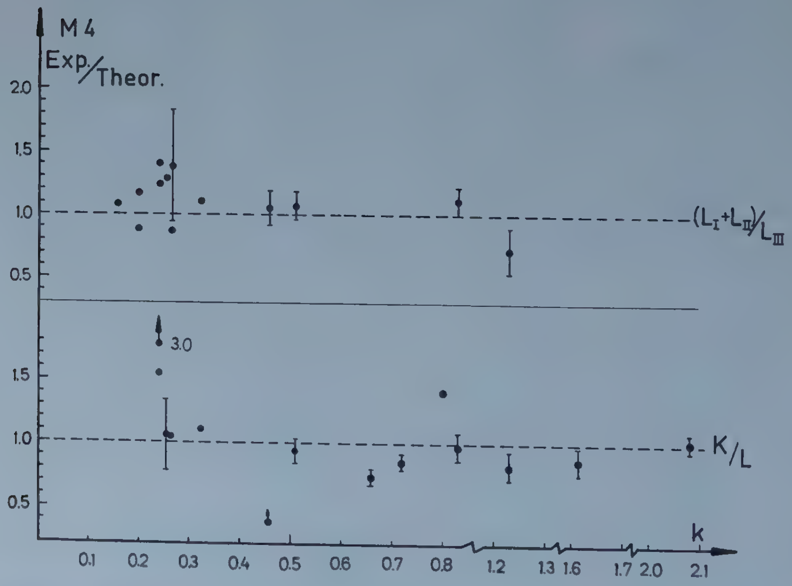

Fig. 30. The ratios between experimental and theoretical values of K/L and $(L_I+L_{II})/L_{III}$ conversion ratios of $M4$ transitions as functions of energy in mc² units.

In these tables only such transitions have been included which for various reasons are believed to be reasonably "pure". The main results of the treatment appear from columns 8 and 12, where the ratios between experimental and theoretical values of K/L and $(L_{\mathrm{I}}+L_{\mathrm{II}})/L_{\mathrm{III}}$, respectively, are given (with r.m.s. errors when possible). Graphical representations of the ratios Exp./Theor. are shown in Figs. 27–30.

4.33. *Discussion*

It is directly apparent from the figures that the general trend for all multipolarities indicates a convincingly good agreement between theory and experiment. In particular no systematic deviations as would result from nuclear size effects in the Sliv–Band sense can be distinguished. It is true that there are isolated points quite far off from the line Exp./Theor. = 1, which could be ascribed to the influence of nuclear structure pointed out by Church and Weneser. As a rule, however, these points correspond to less reliable experimental data. Inversely, the most careful measurements lead to points fitting the line within the limits of error. The conclusion is that in order to confirm any type of nuclear size effect from conversion ratios of the multipolarities concerned the precision of electron intensity measurements must in general be considerably improved. It should be remembered that the values quoted in this paper have been taken from different investigators. An accurate systematic investigation of the conversion ratios of the "pure" multipole transitions listed in Tables 13–16 is strongly suggested.

Finally a few words ought to be said about the $E3$ transitions. In an early phase of the present work a very striking discrepancy, showing a systematic trend with transition energy and amounting to more than 50 % at low energies, was discovered between experimental and theoretical $(L_{\mathrm{I}}+L_{\mathrm{II}})/L_{\mathrm{III}}$ ratios [3A57e]. Different ways of explaining this anomaly were discussed in the paper referred to, but no plausible explanation was found. A recalculation of the L_{III} coefficients [3R56] later turned out to remove the discrepancy. As seen from Fig. 28, however, there is still a slight tendency of the Exp./Theor. ratio to decrease towards low energies, but the deviation of these few points may as well depend on experimental errors.

ACKNOWLEDGEMENTS

We are deeply indebted to the heads of our respective institutes, Prof. M. Siegbahn and Prof. T. Svedberg, for their kind interest in our work and for the wholehearted support they have given us.

Our sincere thanks are due to many collegues at the Nobel Institute of Physics and the Gustaf Werner Institute for Nuclear Chemistry as well as the Physics Department, University of Uppsala, for excellent cooperation in the experimental investigations forming the backbone of this survey and for permission to quote unpublished data.

The stimulating contact with Prof. M. H. L. Pryce has been of basic importance in the preparation of Chapter 3. His readiness to put unpublished material at our disposal is gratefully acknowledged.

Finally we wish to express our gratitude to Prof. K. Bleuler and Civ.ing. S. Wahlborn for many discussions on various theoretical aspects of our work and to Prof. M. E. Rose for private communications concerning internal conversion coefficients.

Nobel Institute of Physics, Stockholm, and The Gustaf Werner Institute for Nuclear Chemistry, Uppsala, June 1957.

REFERENCES[1]

1A53 D. E. Alburger, Phys. Rev. *92*, 1257 (1953).
1A54 D. E. Alburger and M. H. L. Pryce, Phys. Rev. *95*, 1482 (1954).
1A55 D. E. Alburger and A. W. Sunyar, Phys. Rev. *99*, 695 (1955).
2A56 B. Åström, unpublished work.
2A57 B. Åström, Arkiv Fysik *12*, 237 (1957).
2A57a B. Åström, B. Johansson, and I. Bergström, Arkiv Fysik *12*, 205 (1957).
3A55 G. Andersson, E. Arbman, I. Bergström, and A. H. Wapstra, Phil. Mag. *46*, 70 (1955).
3A57 G. Andersson, E. Arbman, and B. Jung, Arkiv Fysik *11*, 297 (1957).
3A57a G. Andersson, P. A. Tove, B. Jung, and I. B. Svensson, Nuclear Physics *3*, 493 (1957).
3A57b G. Andersson, J. O. Burgman, and B. Jung, unpublished work.
3A57c G. Andersson and I. Bergström, Nuclear Physics *3*, 506 (1957).
3A57d G. Andersson, E. Arbman, J. O. Burgman, and P. A. Tove, unpublished work.
3A57e G. Andersson and I. Bergström, Nuclear Physics *3*, 541 (1957).
4A57 E. Arbman, Nuclear Physics *3*, 625 (1957).
4A57a E. Arbman and P. A. Tove, in course of publication (Arkiv Fysik).
5A57 T. Alväger and G. Oelsner, Arkiv Fysik *12*, 319 (1957).
5A57a T. Alväger, work in progress.
6A56 K. Alder, A. Bohr, T. Huus, B. Mottelson, and A. Winther, Revs. Modern Phys. *28*, 432 (1956).

1B55 W. L. Bendel, M. E. Toms, and R. A. Tobin, Phys. Rev. *99*, 672 (A) (1955).
2B53 I. Bergström, R. D. Hill, and G. de Pasquali, Phys. Rev. *92*, 918 (1953).
2B55 I. Bergström and A. H. Wapstra, Phil. Mag. *46*, 61 (1955).
3B55 R. Barloutaud, T. Grjebine, and M. Riou, Compt. Rend. *240*, 1207 (1955).
3B56 R. Barloutaud, T. Grjebine, and M. Riou, Compt. Rend. *242*, 1284 (1956).
3B56a R. Barloutaud, T. Grjebine, and M. Riou, Physica *22*, 1129 (1956).
4B55 K. E. Bergkvist, I. Bergström, C. J. Herrlander, S. Hultberg, H. Slätis, E. Sokolowski, A. H. Wapstra, and T. Wiedling, Phil. Mag. *46*, 65 (1955).
4B57 K. E. Bergkvist, unpublished work.
5B52 R. E. Bell, R. L. Graham, and H. E. Petch, Can. J. Phys. *30*, 35 (1952).
5B55 R. E. Bell, Chapter XVIII (I), Beta- and Gamma-Ray Spectroscopy. Ed. K. Siegbahn. North-Holland Publishing Co., 1955.
6B55 E. M. Bernstein and H. W. Lewis, Phys. Rev. *100*, 1345 (1955).
7B55 L.L. Baggerly, P. Marmier, F. Boehm, and J. W. M. DuMond, Phys. Rev. *100*, 1364 (1955).
8B57 F. Boehm and P. Marmier, Phys. Rev. *105*, 974 (1957).
8B57a F. Boehm and A. H. Wapstra, Phys. Rev. *106*, 1364 (1957).
9B57 G. Bäckström, private communication.
10B55 R. D. Birkhoff, A. W. Smith, H. H. Hubbell, Jr., and J. S. Cheka, Rev. Sci. Instr. *26*, 959 (1955).
11B55 H. Brysk and M. E. Rose, ORNL-1830 (unpublished).
12B57 G. O. Brink, J. C. Hubbs, W. A. Nierenberg, and J. L. Worcester, UCRL-3643 (unpublished).
13B55 H. H. Bolotin and R. G. Wilkinson, Phys. Rev. *99*, 671 (A) (1955).
14B52 J. M. Blatt and V. F. Weisskopf, Theoretical Nuclear Physics. J. Wiley and Sons, New York, 1952.
15B57 K. Bleuler and C. Terreaux, Helv. Phys. Acta *30*, 183 (1957).
16B54 D. M. Brink, Proc. Phys. Soc. *A 67*, 757 (1954).
17B52 F. D. S. Butement and R. Shillito, Proc. Phys. Soc. *A 65*, 945 (1952).
18B53 B. Burson, J. Cork, and W. Jordan, ANL-5140 (unpublished).
19B56 J. Burde and S. G. Cohen, Phys. Rev. *104*, 1093 (1956).
19B57 J. Burde, private communication.

1C38 S. P. Choong and J. Surugue, J. Phys. Radium *9*, 437 (1938).
2C52 J. M. Cork, D. W. Martin, J. M. LeBlanc, and C. E. Branyan, Phys. Rev. *85*, 386 (1952).

---

[1] The system of references employed is the one introduced by Hollander *et.al.*, Revs. Modern Phys. *25*, 469 (1953).

2C53 J. M. Cork, J. M. LeBlanc, W. H. Nester, D. W. Martin, and M. K. Brice, Phys. Rev. *90,* 444 (1953).
2C54 J. M. Cork, M. K. Brice, L. C. Schmid, G. D. Hickman, and H. Nine, Phys. Rev. *94,* 1218 (1954).
3C50 T. C. Chu, Phys. Rev. *79,* 582 (1950).
4C56 D. R. Connors, W. C. Miller, and B. Waldman, Phys. Rev. *102,* 1584 (1956).
5C57 H. H. Coburn, J. V. Kane, and S. Frankel, Phys. Rev. *105,* 1293 (1957).
6C56 E. L. Church and J. Weneser, Phys. Rev. *104,* 1382 (1956).
7C32 M. Curie and S. Rosenblum, Compt. rend. *194,* 1232 (1932).
8C56 R. L. Christensen, D. R. Hamilton, A. Lemonick, F. M. Pipkin, J. B. Reynolds, and H. H. Stroke, Phys. Rev. *101,* 1389 (1956).
9C56 L. Cranberg and J. S. Levin, Phys. Rev. *103,* 343 (1956).

1D50 M. Deutsch and W. E. Wright, Phys. Rev. *77,* 139 (1950).
2D56 R. H. Davis, A. S. Divatia, D. A. Lind, and R. D. Moffat, Phys. Rev. *103,* 1801 (1956).
3D57 B. S. Dzhelepov and L. K. Peker, Decay Schemes of Radioactive Isotopes. Academy of Science U.S.S.R. 1957.
4D53 W. G. Davey and P. B. Moon, Proc. Phys. Soc. *A 66,* 956 (1953).
5D55 J. W. M. DuMond, Chapter IV, Beta- and Gamma-Ray Spectroscopy. Ed. K. Siegbahn. North-Holland Publishing Co., 1955.
6D56 R. B. Day, Phys. Rev. *102,* 767 (1956).

1E54 L. G. Elliott, R. L. Graham, J. Walker, and J. L. Wolfson, Phys. Rev. *93,* 356 (1954).
1E54a L. G. Elliott, M. A. Preston, and J. L. Wolfson, Can. J. Phys. *32,* 153 (1954).
1E55 L. G. Elliott, M. A. Preston, and J. L. Wolfson, Can. J. Phys. *33,* 607 (1955).
2E55 J. P. Elliott and B. H. Flowers, Proc. Roy. Soc. *A 229,* 536 (1955).

1F56 A. R. Fritsch, UCRL-3452 (unpublished).
2F55 V. K. Fischer, Phys. Rev. *99,* 764 (1955).
3F52 P. Falk-Vairant, J. Teillac, and C. Victor, J. Phys. Radium, *13,* 313 (1952).
4F47 H. Frauenfelder, P. C. Gugelot, O. Huber, H. Medicus, P. Preiswerk, P. Scherrer, and R. Steffen, Helv. Phys. Acta *20,* 238 (1947).
5F57 P. O. Fröman, Mat. Fys. Skr. Dan. Vid. Selsk. *1,* No. 3 (1957).
6F57 M. Frilley and M. Valaderes, J. Phys. Radium *18,* 468 (1957).

1G56 T. R. Gerholm, Arkiv Fysik *10,* 523 (1956).
1G57 T. R. Gerholm, E. Karlsson, J. Lindskog, and J. O. Burgman, work in progress.
2G54 L. P. Gillon, K. Gopalakrishnan, A. de-Shalit, and J. W. Mihelich, Phys. Rev. *93,* 124 (1954).
3G52 M. Goldhaber and R. D. Hill, Revs. Modern Phys. *24,* 179 (1952).
3G55 M. Goldhaber and A. W. Sunyar, Chapter XVI (II), Beta- and Gamma-Ray Spectroscopy. Ed. K. Siegbahn. North-Holland Publishing Co., 1955.
4G51 R. L. Graham and R. E. Bell, Phys. Rev. *84,* 380 (1951).
4G53 R. L. Graham and R. E. Bell, Can. J. Phys. *31,* 377 (1953).

1H56 R. H. Herber, T. T. Sugihara, C. D. Coryell, W. E. Bennett, and J. R. Huizenga, Phys. Rev. *103,* 955 (1956).
2H56 C. J. Herrlander, R. Stockendal, J. A. McDonell, and I. Bergström, Nuclear Physics *1,* 643 (1956).
2H57 C. J. Herrlander and T. R. Gerholm, Nuclear Physics *3,* 161 (1957).
3H56 J. W. Horton, Phys. Rev. *101,* 717 (1956).
4H49 N. Hole, Arkiv Mat. Astron. Fys. *36 A,* No. 9 (1949).
5H50 R. D. Hill, Phys. Rev. *79,* 413 (1950).
6H51 O. Huber, F. Humbel, H. Schneider, A. de-Shalit, and W. Zünti, Helv. Phys. Acta *24,* 127 (1951).
6H53 O. Huber, J. Halter, R. Joly, D. Maeder, and J. Brunner, Helv. Phys. Acta *26,* 591 (1953).
7H53 J. M. Hollander, I. Perlman, and G. T. Seaborg, Revs. Modern Phys. *25,* 469 (1953).
8H56 J. R. Huizenga, V. E. Krohn, and S. Raboy, Phys. Rev. *102,* 1063 (1956).

9H53 J. A. Harvey, Can. J. Phys. *31,* 278 (1953).
10H55 S. Hultberg, Arkiv Fysik *9,* 245 (1955).

1J57 B. Jung and G. Andersson, unpublished work.
2J55 R. Joly, J. Brunner, J. Halter, and O. Huber, Helv. Phys. Acta *28,* 403 (1955).

1K56 P. Kramer, H. C. Hamers, and G. Meijer, Physica *22,* 208 (1956).
2K56 G. Kramer, Z. Physik *146,* 187 (1956).
3K52 P. F. A. Klinkenberg, Revs. Modern Phys. *24,* 63 (1952).
4K55 V. E. Krohn and S. Raboy, Phys. Rev. *97,* 1017 (1955).
5K57 M. J. Kearsley, Nuclear Physics *4,* 157 (1957).
6K54 R. W. King, Revs. Modern Phys. *26,* 327 (1954).

1L52 G. Lindström, Arkiv Fysik *4,* 1 (1952).
1L52a G. Lindström, Phys. Rev. *87,* 678 (1952).
2L56 J. M. LeBlanc, J. M. Cork, and S. B. Burson, Phys. Rev. *104,* 1670 (1956).
3L55 C. Levinson and K. W. Ford, Phys. Rev. *100,* 13 (1955).
4L57 T. Lindqvist, Arkiv Fysik in press.

1M57 J. A. McDonell, R. Stockendal, C. J. Herrlander, and I. Bergström, Nuclear Physics *3,* 513 (1957).
2M54 M. C. Michel and D. H. Templeton, Phys. Rev. *93,* 1422 (1954).
3M51 F. R. Metzger and R. D. Hill, Phys. Rev. *82,* 646 (1951).
3M54 F. R. Metzger and W. B. Todd, Phys. Rev. *94,* 794 (A) (1954).
3M54a F. R. Metzger and W. B. Todd, Phys. Rev. *95,* 853 (1954).
3M55 F. R. Metzger, Phys. Rev. *98,* 200 (1955).
4M48 D. L. Mock, R. C. Waddel, L. W. Fagg, and R. A. Tobin, Phys. Rev. *74,* 1536 (1948).
5M52 D. E. Muller, H. C. Hoyt, D. J. Klein, and J. W. M. DuMond, Phys. Rev. *88,* 775 (1952).
6M52 J. W. Mihelich, Phys. Rev. *87,* 646 (1952).
6M53 J. W. Mihelich and A. de-Shalit, Phys. Rev. *91,* 78 (1953).
6M54 J. W. Mihelich and A. de-Shalit, Phys. Rev. *93,* 135 (1954).
6M54a J. W. Mihelich, M. McKeown, and M. Goldhaber, Phys. Rev. *96,* 1450 (1954).
6M55 J. W. Mihelich and M. Goldhaber, Phys. Rev. *98,* 1185 (A) (1955).
7M54 J. D. Mize, M. E. Bunker, and J. W. Starner, Phys. Rev. *96,* 444 (1954).
8M53 C.C. McMullen and M. W. Johns, Phys. Rev. *91,* 418 (1953).
9M54 D. Maeder, A. H. Wapstra, G. J. Nijgh, and L. T. M. Ornstein, Physica *20,* 521 (1954).
10M56 F. K. McGowan and P. H. Stelson, Phys. Rev. *103,* 1133 (1956).
11M55 S. A. Moszkowski, Chapter XIII, Beta- and Gamma-Ray Spectroscopy. Ed. K. Siegbahn. North-Holland Publishing Co., 1955.
12M55 B. R. Mottelson and S. G. Nilsson, Phys. Rev. *99,* 1615 (1955).
13M55 K. G. Malmfors, Chapter XVIII (II), Beta- and Gamma-Ray Spectroscopy. Ed. K. Siegbahn, North-Holland Publishing Co., 1955.
14M57 M. T. McEllistrem, H. J. Martin, D. W. Miller, and M. B. Sampson, Bull. Am. Phys. Soc. *2,* 208 (1957).
15M52 E. der Mateosian and A. Smith, Phys. Rev. *88,* 1186 (1952).

1N57 O. B. Nielsen, private communication.
2N56 K. O. Nielsen, O. B. Nielsen, and M. A. Waggoner, Nuclear Physics *2,* 476 (1956/57).
3N57 T. Novakov, R. Stockendal, B. Johansson, and M. Schmorak, in course of publication (Arkiv Fysik).
3N57a T. Novakov, S. Hultberg, and B. Andersson, in course of publication (Arkiv Fysik).

1P54 T. O. Passell, M. C. Michel, and I. Bergström, Phys. Rev. *95,* 999 (1954).
2P56 F. T. Porter, M. S. Freedman, T. B. Novey, and F. Wagner, Jr., Phys. Rev. *103,* 921 (1956).
3P56 I. Perlman and J. O. Rasmussen, UCRL-3424 (unpublished).
4P56 R. V. Pound and G. K. Wertheim, Phys. Rev. *102,* 396 (1956).
5P52 M. H. L. Pryce, Proc. Phys. Soc. *A 65,* 773 (1952).
5P56 M. H. L. Pryce, Nuclear Physics *2,* 226 (1956/57).
5P56a M. H. L. Pryce, private communication.
6P54 J. R. Prescott, Proc. Phys. Soc. *A 67,* 254 (1954).

P53 P. Preiswerk and P. Stähelin, Nuovo Cimento *10,* 1219 (1953).
P53 A. C. Pappas, M. I. T. Lab. for Nuclear Science, Technical Report No. 63 (unpublished).

R56 M. Riou, private communcation.
R55 N. Ryde and B. Andersson, Proc. Phys. Soc. *B 68,* 1117 (1955).
R54 M. E. Rose *et al.,* privately distributed tables (1954–1956).
R56 M. E. Rose, private communcations (1956–1957).

S56 D. Strominger, F. S. Stephens, Jr., and J. O. Rasmussen, Phys. Rev. *103,* 748 (1956).
S55 P. H. Stelson and F. K. McGowan, Phys. Rev. *99,* 112 (1955).
S56 M. Schmorak, R. Stockendal, J. A. McDonell, I. Bergström, and T. R. Gerholm, Nuclear Physics *2,* 193 (1956/57).
S55 A. W. Sunyar, Phys. Rev. *98,* 653 (1955).
S56 R. Stockendal, J. A. McDonell, M. Schmorak, and I. Bergström, Arkiv Fysik *11,* 165 (1956).
S57 R. Stockendal and S. Hultberg, work in progress.
S52 P. Stähelin, Phys. Rev. *87,* 374 (1952).
S52 A. de-Shalit, O. Huber, and H. Schneider, Helv. Phys. Acta *25,* 279 (1952).
S52 J. B. Swan and R. D. Hill, Phys. Rev. *88,* 831 (1952).
S53 J. B. Swan, W. M. Portnoy, and R. D. Hill, Phys. Rev. *90,* 257 (1953).
S49 R. M. Steffen, O. Huber, and F. Humbel, Helv. Phys. Acta *22,* 167 (1949).
0S51 K. Siegbahn, Manne Siegbahn 1886 3/12 1951. Uppsala 1951, p. 199.
1S53 G. Scharff-Goldhaber, Phys. Rev. *90,* 587 (1953).
1S57 G. Scharff-Goldhaber, D. E. Alburger, G. Harbottle, and M. McKeown, Bull. Am. Phys. Soc. *2,* 25 (1957).
2S57 H. Slätis, private communication.
3S56 L. A. Sliv and I. M. Band, privately distributed tables.
4S56 E. Sokolowski, K. Edvarson, and K. Siegbahn, Nuclear Physics *1,* 160 (1956).

1T57 P. A. Tove, Nuclear Instruments *1,* 95 (1957).
1T57a P. A. Tove, private communication.
2T56 W. W. True, Phys. Rev. *101,* 1342 (1956).
2T57 W. W. True, Bull. Am. Phys. Soc. *2,* 228 (1957).

1V56 S. H. Vegors, Jr. and P. Axel, Phys. Rev. *101,* 1067 (1956).
2V56 J. Volpe and G. Hinman, Phys. Rev. *104,* 753 (1956).

1W54 A. H. Wapstra, D. Maeder, G. J. Nijgh, and L. T. M. Ornstein, Physica *20,* 169 (1954).
1W56 A. H. Wapstra and G. J. Nijgh, Nuclear Physics *1,* 245 (1956).
2W54 H. de Waard, Physica *20,* 41 (1954).
2W56 H. de Waard and T. R. Gerholm, Nuclear Physics *1,* 281 (1956).
3W56 G. K. Wertheim and R. V. Pound, Phys. Rev. *102,* 185 (1956).
4W57 S. Wahlborn, Nuclear Physics *3,* 644 (1957).
4W57a S. Wahlborn, private communication.

1Z56 N. Zeldes, Nuclear Physics *2,* 1 (1956/57).

Tryckt den 30 augusti 1957

Uppsala 1957. Almqvist & Wiksells Boktryckeri AB